UNIVERSITY OF OKLAHOMA

GRADUATE COLLEGE

DEVELOPMENT LENGTH OF 0.6 IN. PRESTRESSING STRANDS IN PRECAST, PRESTRESSED CALCIUM SULFOALUMINATE CEMENT CONCRETE

A THESIS

SUBMITTED TO THE GRADUATE FACULTY

in partial fulfillment of the requirements for the

Degree of

MASTER OF SCIENCE

By

TROY MICHAEL BOWSER
Norman, Oklahoma
2016

DEVELOPMENT LENGTH OF 0.6 IN. PRESTRESSING STRANDS IN PRECAST, PRESTRESSED CALCIUM SULFOALUMINATE CEMENT CONCRETE

A THESIS APPROVED FOR THE
SCHOOL OF CIVIL ENGINEERING AND ENVIRONMENTAL SCIENCE

BY

_____
Dr. Royce Floyd, Chair

_____
Dr. Jeffery Volz

_____
Dr. Christopher Ramseyer

Acknowledgements

I would like to thank the CEES Department at the University of Oklahoma, specifically my thesis committee. I would like to thank Mike Schmitz for his guidance, assistance, and work. I have learned as much from Mike as I have from most of my engineering classes. I would like to Dr. Royce Floyd. He took a chance on me early in my academic career when I had very little to offer as a student and as a person. I do not think that I would be in the position I am today if not for his unwavering support and guidance. He is one of the most influential people that I have had in my life and is one of the best men I have known.

I would like to thank Cameron Murray for his role in all of my graduate studies. He has been instrumental in the completion of my studies and research program despite having no obligation to do so. I have learned a lot from his commitment to his studies and research work and I value his friendship immensely. I would also like to thank Connor Casey, Chandler Funderberg, Stephen Tanksley for all of their help with trial batches, beam construction, measurements, and testing. I would also like to thank Alexandria Stumps for her help in the early part of research.

I must thank my sister, Deanna, who first instilled in me the idea of going to graduate school. Her and her husband, John have since been my biggest fans and my sources of support and encouragement during the tough times that never seemed like they would end. Their contribution to my life is unmatched and I will forever be grateful to them. Finally, I would like to thank my parents, my brother Greg, and his wife Katie for their love and assurance over the years.

Table of Contents

Acknowledgements iv

Table of Contents v

List of Tables viii

List of Figures ix

Abstract xiii

Chapter 1: Introduction 1

Chapter 2: Literature Review 1

2.1 Calcium Sulfoaluminate Cement 1

2.2 Prestressed Calcium Sulfoaluminate Cement Concrete 3

2.3 Transfer and Development Length in Prestressing Strands 4

Chapter 3: Objectives 11

Chapter 4: Methodology 12

4.1 Beam Specimens 12

4.2 Mix Design 13

4.2.1 CSA Cement Concrete 13

4.2.2 Portland Cement Concrete 14

4.3 Beam Construction 15

4.3.1 Overview 15

4.3.2 Prestressing Strands 16

4.3.3 Formwork 16

4.3.4 Reinforcement 16

4.3.5 Strand Tensioning 17

4.3.6 Concrete Mixing and Placement 18
4.3.7 Transfer Length Measurements 20
4.3.8 Prestress Loss Measurements 24
4.4 Beam Testing 25
Chapter 5: Beam Concrete Results 27
5.1 CSA Trial Batches 27
5.2 Portland Cement (PC) Beams 31
5.3 24-Hour Release CSA (24RS) Beams 32
5.4 2-Hour Release CSA (RS) Beams 34
Chapter 6: Transfer Length Results 35
6.1 Introduction 35
6.2 DEMEC Transfer Lengths 36
6.2.1 Introduction 36
6.2.2 Portland Cement (PC) Beams 36
6.2.3 24-hr Release CSA (24RS) Beams 39
6.2.4 2-hr Release CSA (RS) Beams 42
6.3 End Slip Transfer Lengths 47
6.3.1 Introduction 47
6.3.2 Portland Cement (PC) Beams 47
6.3.3 24-hr Release CSA (24RS) Beams 48
6.3.4 2-hr Release CSA (RS) Beams 48
6.4 Summary and Discussion 50
Chapter 7: Development Length Results 55

7.1 Introduction 55
7.2 Portland Cement (PC) Beams 55
7.3 24-hr Release CSA (24RS) Beams 60
7.4 2-hr Release CSA (RS) Beams 61
7.5 Summary and Discussion 62
Chapter 8: Prestress Losses 63
Chapter 9: Summary, Conclusions, and Recommendations 65
9.1 Summary 65
9.2 Conclusions 66
9.3 Recommendations 67
References 68
Appendix A: Beam Analysis 75
Appendix B: Trial Batches 77
Appendix C: Concrete Compressive Strengths 79
Appendix D: DEMEC Strain Profiles 83
Appendix E: Flexural Test Crack Patterns 89

List of Tables

Table 1: Specimen Groups 13

Table 2: Final Mix Design for CSA Specimens 14

Table 3: Mix Design for PC Specimens 15

Table 4: ASTM Standards 20

Table 5: Temperatures on a 70-Degree Day 28

Table 6: Temperatures on an 80-Degree Day 29

Table 7: Concrete Properties of PC Batches 31

Table 8: Concrete Properties of 24RS Batches 33

Table 9: Concrete Properties of RS Batches 35

Table 10: DEMEC Transfer Lengths over Time for PC Specimens 37

Table 11: DEMEC Transfer Lengths Over Time for 24RS Specimens 39

Table 12: DEMEC Transfer Lengths Over Time for RS Specimens 43

Table 13: Flexural Testing Results of PC Specimens 57

Table 14: Results of Flexural Tests for 24RS Specimens 60

Table 15: Results of Flexural Tests for RS Specimens 62

Table 16: Measure Prestress Compared to Estimated Prestress after 28 Days 65

Table 17: Calculated Development Lengths and Nominal Flexural Capacities 76

Table 18: Summary of CSA Trial Batches 78

List of Figures

Figure 1: Beam Reinforcing Detail 13

Figure 2: Steel Abutment at Dead End of Prestressing Bed 17

Figure 3: Steel Abutment at Live End of Prestressing Bed 17

Figure 4: 50-kip Load Cell 18

Figure 5: Depth Micrometer to Measure End Slip 21

Figure 6: Plexiglas and Steel Clamps for End Slip 21

Figure 7: British Cement Association Gage for DEMEC Measurements 22

Figure 8: 95% Average Maximum Strain Method 22

Figure 9: Brass Inserts used for DEMEC Points 23

Figure 10: Special Formwork for Brass Insert Installation 23

Figure 11: DEMEC Point Layout 24

Figure 12: DEMEC Point 24

Figure 13: VWSG Attachment to Strands 25

Figure 14: Load Application Set-up 26

Figure 15: Wire Pot Set-up at Load Point 26

Figure 16: LVDTs Mounted on Strands 27

Figure 17: Strength Gain vs. Time on a 70-Degree Day 28

Figure 18: Strength Gain vs. Time on an 80-Degree Day 30

Figure 19: Loss of Paste at Bottom of Specimen 32

Figure 20: (Left) Bottom of Cylinder. (Right) Top of Cylinder 32

Figure 21: Bugholes in Specimen 24RS1 33

Figure 22: Large Bughole in 24RS1 34

Figure 23: Unusable Brass Insert on 24RS1 34
Figure 24:DEMEC Strain Profiles at 28 Days for PC Specimens 38
Figure 25: Comparison of Transfer Lengths for PC Specimens at 28 Days 39
Figure 26: DEMEC Strain Profile at 36 Days for 24RS Specimens 41
Figure 27: Comparison of Transfer Lengths for 24RS Specimens at 36 Days 42
Figure 28: DEMEC Strain Profile at 36 Days for RS Specimens 44
Figure 29: Comparison of Transfer Lengths at 36 Days for RS Specimens 45
Figure 300: DEMEC Transfer Lengths Over Time for the PC Group 45
Figure 311: DEMEC Transfer Lengths Over Time for the 24RS Group 46
Figure 322: DEMEC Transfer Lengths Over Time for the RS Group 46
Figure 33: Transfer Lengths of PC Specimens from End Slip and DEMEC 47
Figure 34: Transfer Lengths of 24RS Specimens from End Slip and DEMEC 48
Figure 35: Transfer Lengths of RS Specimens from End Slip and DEMEC 50
Figure 36: Average DEMEC Transfer Lengths of Specimens Over Time 51
Figure 37: Average Normalized DEMEC Transfer Lengths of Specimens Over Time. 52
Figure 38: Average Normalized Transfer Lengths for Each Group 52
Figure 39: Raw Average Transfer Lengths of Each Group with Error Bars 54
Figure 40: Comparison to Previous Research 55
Figure 41: Load vs. Deflection Curves for PC Specimens 56
Figure 42: Typical Crushing and Crack Distribution for Flexural Failure 58
Figure 43: Longitudinal Cracks Appear when Strands Slip 58
Figure 44: Load vs. Strand Slip Plot for South PC1 Strands 59
Figure 45: Load vs. Strand Slip Plot for South PC2 Strands 59

Figure 46: Load vs. Deflection Curves for 24RS Specimens 60
Figure 47: Load vs. Deflection Curves for RS Specimens 61
Figure 48: Prestress in Strands vs. Time for 24RS3 and 24RS4 64
Figure 49: Prestress in Strands vs. Time for RS3 and RS4 64
Figure 50: Strength Gain vs. Concrete Age for PC1 and PC2 79
Figure 51: Strength Gain vs. Concrete Age for PC3 and PC4 80
Figure 52: Strength Gain vs. Concrete Age for 24RS1 and 24RS2 80
Figure 53: Strength Gain vs. Concrete Age for 24RS3 and 24RS4 81
Figure 54: Strength Gain vs. Concrete Age for RS1 and RS2 81
Figure 55: Strength Gain vs. Concrete Age for RS3 and RS4 82
Figure 56: PC1 DEMEC Strain Profiles 83
Figure 57: PC2 DEMEC Strain Profiles 84
Figure 58: PC3 DEMEC Strain Profiles 84
Figure 59: PC4 DEMEC Strain Profiles 85
Figure 60: 24RS1 Strain Profiles 85
Figure 61: 24RS2 DEMEC Strain Profiles 86
Figure 62: 24RS3 DEMEC Strain Profiles 86
Figure 63: 24RS4 DEMEC Strain Profiles 87
Figure 64: RS1 DEMEC Strain Profiles 87
Figure 65: RS2 DEMEC Strain Profiles 88
Figure 66: RS3 DEMEC Strain Profiles 88
Figure 67: RS4 DEMEC Strain Profiles 89
Figure 68: PC1 at Failure 89

Figure 69: PC2 at Failure 90
Figure 70: PC3 at Failure 90
Figure 71: PC4 at Failure 90
Figure 72: 24RS1 at Failure 91
Figure 73: 24RS2 at Failure 91
Figure 74: 24RS3 at Failure 91
Figure 75: 24RS4 at Failure 92
Figure 76: RS1 at Failure 92
Figure 77: RS2 at Failure 92
Figure 78: RS3 at Failure 93
Figure 79: RS4 at Failure 93

Abstract

Calcium sulfoaluminate cement is a very rapid setting, hydraulic cement that releases approximately half as much carbon dioxide during production as conventional portland cement. Calcium sulfoaluminate cement produces concrete with high early strength, excellent durability, and limited shrinkage. These properties have the potential to substantially improve the speed of production and performance of precast products. The compressive strength typically required for prestress release at an age of 18-24 hours can be reached in just a few hours, without the need for heat curing. Three series of 6.5 in. by 12 in. by 18 ft long rectangular beams prestressed with 0.6 in. prestressing strands were cast to evaluate the effect of calcium sulfoaluminate cement concrete age at the time of prestress release on bond behavior and prestress losses. One series of calcium sulfoaluminate beams was cast with prestress release targeted for a compressive strength of 3500 psi at approximately 2 hours of age and a second set with prestress release at 24 hours of age, at which time the compressive strength was significantly higher. A series of conventional concrete beams with a similar compressive strength at release was also cast for comparison. Surface strain and strand end slip were measured to evaluate transfer length and vibrating wire strain gages were embedded to evaluate prestress losses. The CSA specimens with vibrating wire strain gages yielded reduced prestress losses compared to conventional concrete. The specimens also showed no significant detrimental effects of early age prestress transfer and similar transfer lengths for rapid setting and conventional concrete. Code predicted transfer and development lengths proved reasonable for the CSA specimens.

Chapter 1: Introduction

Calcium sulfoaluminate (CSA) cement is an alternative to conventional portland cement that yields concrete with high strength at an early age. CSA cement concrete reaches the compressive strength necessary for prestress release in less than one-third of the time of portland cement concrete (Floyd & Ramseyer, 2016). Since production of precast, prestressed concrete is limited by the time the concrete takes to gain strength, CSA cement can substantially improve the efficiency of the production process to meet increasing demand. In addition to its rapid setting capabilities, CSA cement also boasts relatively low CO_2 emissions and potentially increased durability compared to portland cement. CSA cement has been studied since the late-1960s (ACI committee 223, 1970). However, there are limited studies on its acceptability for use in prestressed concrete (Floyd & Sadhasivam, 2013;Floyd & Ramseyer, 2016) and there are still questions regarding the material's effect on transfer and development length of prestressing strands. This study looks further into whether the development length of 0.6 in. prestressing strands in precast, prestressed CSA cement concrete beams deviates from the code defined boundaries for structural concrete. Additionally, prestress release times of two hours and 24 hours are examined to look at the effects of release time on the transfer and development length of the strands.

Chapter 2: Literature Review

2.1 Calcium Sulfoaluminate Cement

Amid concerns of global warming due to greenhouse gas emissions, engineers have become increasingly involved in the evolution of how materials are to be produced moving forward. This has become a major area of concern for the construction industry

since conventional portland cement production accounts for approximately 5% of manmade CO_2 emissions and 3% of annual global energy consumption (Damtoft et al., 2008; Hicks et al., 2015). With global demand of cement projected to increase by roughly 400% by the year 2050 (Damtoft et al., 2008), calcium sulfoaluminate cement (CSA) presents an alternative to portland cement to help mitigate the greenhouse gases emitted from the construction industry. CSA cement clinker is produced at a temperature nearly 200ºC lower than portland cement, produces less than half of the CO_2, and is easier to grind into cement powder for use in concrete (Sharp et al., 1999). In addition to the environmental benefits, CSA cement can yield high early age compressive strengths, tremendous durability (Bescher et al., 2012.), and minimal shrinkage (Quillin, 2001). The rapid curing of CSA cement concrete can help make up for the relatively high material costs by reducing the labor and time of construction. Although CSA cements are not commonly used as a construction material in the U.S. and Europe, China has been producing and using the material for nearly 35 years (Juenger et al., 2011).

Similar to portland cement clinker, limestone and calcium sulfate (gypsum) are utilized to produce CSA cement clinker, but bauxite or another source of alumina is required. The composition of CSA cements consists of calcium sulfoaluminate, or ye'elimite (C_4A_3S), and belite (C_2S). CSA cement clinkers can also include minor amounts of calcium aluminate ferrate, anhydrite, gehlenite, or mayenite. Depending on the desired properties of the cement, the clinker is mixed with appropriate amounts of gypsum to produce cements ranging from rapid setting to expansive. During the hydration process, ye'elimite reacts rapidly to form the initial products ettringite and

monosulfate (Winnefeld & Lothenbach, 2010). The formation of ettringite generates the high compressive strength at early ages for CSA cement concretes as the reactions happen much faster than in conventional concretes (Sharp et al., 1999). Typically, the initial setting time for CSA cement concretes is between 30 minutes and four hours, depending on the exact composition of the cement (Juenger et al., 2011). After about seven days, the ye'elimite is consumed and the belite is free to react and form calcium silicate hydrate which aids in the long-term strength gain of the concrete (Quillin, 2001;Winnefeld & Lothenbach, 2010;Chen et al., 2012).

2.2 Prestressed Calcium Sulfoaluminate Cement Concrete

The accelerated curing time of CSA cement concrete makes it beneficial for use in the construction of precast, prestressed concrete members. CSA cement concrete can reach the required compressive strength for prestressed concrete in less than one-third of the time required for conventional concrete mixtures. This is an optimum characteristic for prestressed members since production time is often limited by how long the member needs to cure before the tension in the prestressing strands can be released and absorbed by the concrete. Moreover, research has shown that the early age high strength of the material may lead to reduced creep over time (Floyd & Ramseyer, 2016). Reduced values of creep and shrinkage can lessen the prestress losses over the lifetime of the member.

In a 2013 study done by Floyd and Sadhasivam, it was determined that the fresh properties, strength gain, and elastic modulus of CSA cement concrete mixtures adhered to the mandatory specifications for prestressed bridge girders in the state of Oklahoma. Considering the limited research done on CSA cement concrete relative to prestresed

concrete, this study paved the way for further examination of the performance of CSA cement concrete in prestressed applications.

2.3 Transfer and Development Length in Prestressing Strands

Prestressing strand bond behavior in prestressed concrete is typically quantified using the development length and transfer length of the prestressing strands. Prestress transfer length is the distance from the end of the beam to the point where the effective prestress is fully transferred from the steel to the concrete. The development length is the summation of the transfer length and flexural bond length for a given strand and is the embedment length necessary for the tensile strength of the steel to be fully developed. Transfer length is a common area of interest in research due to its role in shear design and concrete stresses at release at beam ends. Overestimations in transfer length can lead to inefficient shear design and higher than predicted stresses at release, while underestimations in transfer length can lead to inadequate shear design and lower than predicted stresses at release (Morcous et al., 2013).

Numerous mechanisms are used to transfer the prestress from the strands into the concrete. The three primary mechanisms that contribute to the bond between concrete and steel are adhesion, friction, and mechanical resistance. Adhesion is the "glue" between the strand and the concrete and typically does not contribute significantly once there is movement between the strand and concrete, such as occurs in the transfer length during prestress release since the strand is not fully anchored in this region. Friction forces are thought to be the chief factor in the transfer of prestress between the concrete and the steel. Due to Poisson's ratio, a reduction in strand diameter occurs during tensioning. After prestress release however, the strand diameter

increases creating a wedging action in the concrete. This action is believed to increase the frictional resistance between the steel and the concrete. Mechanical resistance occurs due to the helical shape of the prestressing strands. The concrete that fills the gaps between individual wires resists pull-out of the strand (Hanson, 1959).

Many research programs have been conducted concerning the bond between prestressing strands and concrete beginning with Janney's work in the 1950s. The majority of this work has used conventional concrete, but things such as lightweight concrete, various strand diameters, high-performance concrete, and self-consolidating concrete have been studied in the last few decades. Some factors that have been shown to influence transfer length include strand size, strand stress, concrete strength at release, time dependent effects (losses), type of release (gradual or sudden), consolidation and consistency of concrete around strand, surface condition of strand, confinement, cover and spacing, type of strand, and type of loading (Janney, 1954; Nilson, 1987; Staton et al., 2009; Hanson and Kaar, 1959).

Increasing strand diameter has been seen to increase the transfer and development length. Kaar, LaFraugh, and Mass (1963) were the first to identify this characteristic. Transfer length was analyzed for 0.25 in., 0.375 in., 0.5 in., and 0.6 in. diameter strands and found to be longer in larger diameter strands. During this experiment, it was also noted that the relationship between strand diameter and transfer length at release was approximately linear (Kaar et al., 1963). The direct relationship between strand diameter and transfer length found in this research was adopted into current code equations for transfer and development length.

When the initial stress in a strand increases, the surface area that is necessary to transfer the stress to the concrete also increases, resulting in longer transfer lengths. Current equations for transfer and development lengths are based on the effective stress in the strands after all losses, f_{se}. Although this is sensible for flexural bond length, the use of the effective prestress does not necessarily seem applicable to transfer length at release. Instead, the stress in the strand immediately after release, f_{si}, should be applied to the calculation of transfer length (Buckner, 1995). This approach results in longer, more conservative transfer length calculations. Some researchers have proposed equations for transfer length expressed as a function of f_{si} instead of f_{se} (Zia et al., 1979; Buckner, 1995), but research regarding this matter is still inconsistent.

Although the experiment performed by Kaar, LaFraugh, and Mass in 1963 showed that concrete strength had little effect on transfer length, many studies since have shown a correlation between high concrete strengths and decreased transfer lengths. According to Barnes et al. (2003), the frictional resistance in strand bond depends on how well the concrete surrounding the strand reacts to the outward pressure of the strands. The release results in radial cracking in the concrete surrounding the strand, which softens the concrete. Therefore, a higher tensile strength and stiffness means the concrete can respond better to the radial expansion, resulting in better friction and shorter transfer lengths. Since the ACI 318-11 Sections 8.5.1 and 9.5.2.3 show that the modulus of elasticity and modulus of rupture are directly related to the square root of concrete strength, it makes sense that transfer length should also be related to the square root of concrete strength at release (Barnes et al., 2003). While Kaar, LaFraugh, and Mass only looked at concrete release strengths up to 5,000, release strengths today

can range to over 10,000 psi. Many researchers, including Mitchell et al. (1993), Lane (1998), and Ramirez and Russell (2008), have since published studies relating increased concrete strengths to decreased transfer lengths. The studies have also resulted in a number of proposed, revised equations for transfer length and development length (Zia et al., 1979, Mitchell et al., 1993, Lane, 1998, Ramirez and Russell, 2008), almost all of which relate transfer length to the square root of concrete compressive strength. However, much debate still exists over the exact effect of concrete compressive strength on transfer and development lengths.

In some research, transfer lengths have been seen to increase over time. The increases in transfer length are likely due to propagation of radial cracking and the resulting softening of the concrete grip (Barnes et al., 2003).

Sudden release methods, such as flame cutting, have been seen to result in longer transfer lengths than more gradual release methods. Similarly, transfer lengths have also been shown to be longer at live ends, or locations where the strand is first cut to relieve tension, as opposed to dead ends, or ends not directly adjacent to the first release point in the strand. Kaar, LaFraugh, and Mass (1963) found that for strands up to 0.5 in., live end transfer lengths averaged 20% longer than dead end transfer lengths, while 0.6 in. diameter strands showed a 30% increase from dead to live ends. For uncoated strands, Cousins et al. (1990) found that transfer lengths at live ends for 0.5 in. and 0.6 in. diameter strands averaged 8% higher than dead ends, while 0.375 in. diameter strands actually had live end transfer lengths 6% shorter than the dead ends. Additionally, Russell and Burns (1997) reported live end transfer lengths to be 34% longer than dead end transfer lengths.

In the last few decades, self-consolidating concrete has become increasingly popular due to its high workability. Several studies have looked at different types of self-consolidating concretes and how the transfer and development length is impacted by the concrete composition required. In 2007, Larson et al. looked at transfer and development length of 0.5 in. strands in self-consolidating concrete for prestressed bridge girders. The girders had concrete compressive strengths near 5000 psi at release. During this experiment, the researchers found that the transfer lengths observed were in general accordance with the ACI and AASHTO estimates. Staton et al. (2009) also looked at self-consolidating concrete, but with 0.6 in. strands in prismatic beams. These beams had high concrete compressive strengths in the 7000 to 8500 psi range at release and exhibited shorter than predicted values. According to the researchers, the measured transfer lengths were 60% and 56% shorter than the values predicted by ACI and AASHTO, respectively. Transfer and development length in high-strength, normal and self-consolidating concrete were studied by Floyd et al. (2011). The self-consolidating concrete specimens exhibited compressive strengths at release in the 7000 to 8500 psi range and the conventional high-strength specimens were in the 8500 to 10,000 psi range. The researchers found that the self-consolidating concrete specimens had slightly shorter transfer lengths than the conventional high-strength specimens, and that the ACI and AASHTO equations overestimated the development length of all beams by more than 60%. Lightweight self-consolidating concrete was studied with 0.6 in. prestressing strands by Floyd et al. (2015). This mix used lightweight aggregate for minimized dead load and had concrete strengths at release in the range of 3500 to 7000

psi. Overall, it was found that the ACI and AASHTO predictions overestimated the transfer length for the lightweight self-consolidating concrete members.

Current codes do not directly define an equation for transfer length other than simplified versions used for shear capacity analysis. Using the equation for development length from ACI 318 Building Code Requirements for Structural Concrete and AASHTO LRFD Bridge Design Specifications however, the transfer length can be determined by

$$l_t = \frac{f_{se}}{3} d_b$$

where f_{se} is the effective prestress (ksi), accounting for all prestress losses and d_b is the diameter of the prestressing strand (in.). The equations used in shear capacity calculations in ACI 318 and AASHTO LRFD are $50d_b$ and $60d_b$, respectively.

Transfer length can also be measured experimentally using strand draw-in and concrete surface strain. Strand draw-in defines the transfer length of the specimens from the following equation (Thatcher, et al., 2002; Russell & Burns, 1996; Fédération International de la Précontrainte (FIP), 1982; Balázs, 1993)

$$L_t = \frac{\alpha \Delta_d}{\varepsilon_{si}}$$

where Δ_d is the measured draw-in (in.), ε_{si} is the initial strain in the strand due to prestress, and α corresponds to the bond stress variation. An α value of 2 corresponds to a linear bond stress variation, while an α value of 3 corresponds to a parabolic bond stress variation. There is some disagreement among researchers as to the exact value of α, but they all tend to agree that it is between 2 and 3 (Thatcher, et al., 2002; Russell & Burns, 1996; Fédération International de la Précontrainte (FIP), 1982; Balázs, 1993).

Concrete surface strain measurements can be used to determine transfer length by directly identifying where a constant strain, and therefore constant stress, begins (Russell & Burns, 1996; Girgis & Tuan, 2005; Hegger et al., 2007).

The mixture composition of CSA cement concrete has the potential to affect the transfer length. Additionally, the rapid strengthening of the concrete may also have an effect on the transfer length of the strands as studies have shown that high strength concrete can produce shorter transfer lengths. Since limited research has been done on the material in prestressed applications, further investigation into prestress transfer behavior within CSA specimens is necessary.

Development length is affected by the same factors as transfer length. To predict development length, ACI 318 uses the equation

$$L_d = \left(\frac{f_{se}}{3}\right) d_b + (f_{ps} - f_{se}) d_b$$

where f_{se} is the effective prestress in the strand after all losses are accounted for (ksi), d_b is the nominal diameter of the prestressing strand (in.), and f_{ps} is the stress in the steel at nominal flexural strength (ksi). The equation is essentially the same in the AASHTO LRFD Specifications, just in a slightly different form.

In an experiment performed by Floyd and Ramseyer (2016), their preliminary analysis determined that the American Concrete Institute (ACI) and American Association of State Highway and Transportation Officials (AASHTO) estimates of transfer and development length for ordinary portland cement concrete prestressed beams were reasonably accurate when used for CSA cement concrete prestressed beams with 0.5 in. special strands. The scope of the project however, focused on concentrically prestressed specimens. Further testing of eccentrically prestressed

specimens and larger strand diameters is required to determine the adequacy of the ACI and AASHTO estimates for development length in CSA cement concrete prestressed beams. In addition, examination of the effects of prestress release times on development length in the beams can help aid in a better understanding of CSA cement concrete prestressed beams as a structural element going forward.

Chapter 3: Objectives

This experiment builds on the initial research on transfer and development length conducted by Floyd and Ramseyer (2016) in an attempt to more precisely define the role that CSA cement and prestress release time plays in the performance of the beams. The objectives of the study include the following:

1. Study the effects of citric acid retarder on strength gain in CSA cement concrete
2. Conduct quantitative and qualitative investigation on the effect of CSA cement concrete on transfer and development length of 0.6 in. prestressing strands in eccentrically prestressed beams
3. Determine the effect of prestress release time on transfer and development length of 0.6 in. prestressing strands in eccentrically prestressed, CSA cement concrete beams
4. Investigate the prestress losses in eccentrically prestressed, CSA cement concrete beams over time using Vibrating Wire Strain Gages (VWSG)

The results garnered from this study were expected to show that the transfer and development length of 0.6 in. prestressing strands in CSA cement concrete falls within the typical bounds specified by ACI and AASHTO. Additionally, the transfer and development lengths were expected to be larger for the specimens with an early release

due to the lower compressive strengths (Janney, 1954; Nilson, 1987; Staton et al., 2009; Hanson and Kaar, 1959).

Chapter 4: Methodology

4.1 Beam Specimens

Overall, twelve 6.5 in. by 12 in. by 18-ft-long beam specimens were constructed at the Donald G. Fears Structural Engineering Laboratory at the University of Oklahoma for testing and analysis. These dimensions are based on those used in previous research on transfer and development length (Logan 1997, Rose and Russell 1997, Peterman et al. 2000, Larson et al. 2007, Ramirez and Russell 2008, Staton et al. 2009, Ward et al. 2009, Floyd et al. 2011, and Floyd 2015) to produce comparable data. The specimens were eccentrically prestressed with two 0.6 in., Grade 270 prestressing strands at 2 in. from the bottom of the beams. These strands were prestressed to 75 percent of the available tensile strength of the strands. In order to overcome the large tensile stresses present at prestress release at the top of the specimens, two Grade 60, No. 6 bars were positioned 2.5 in. from the top of the specimens. The nominal flexural moment capacity of each section was calculated using strain compatibility. Shear reinforcement of the specimens consisted of 60 ksi tensile strength, W4 welded wire reinforcement (WWR) designed to ensure that a tension controlled bending failure would occur during testing. All of the vertical components of the WWR were spaced at 6 in. on center throughout the length of each beam. The shear steel was designed using the ACI detailed method for shear that is outlined in the ACI Code for prestressed concrete (ACI 2011). Figure 1 presents a detailed diagram of the reinforcement used for each of the specimens.

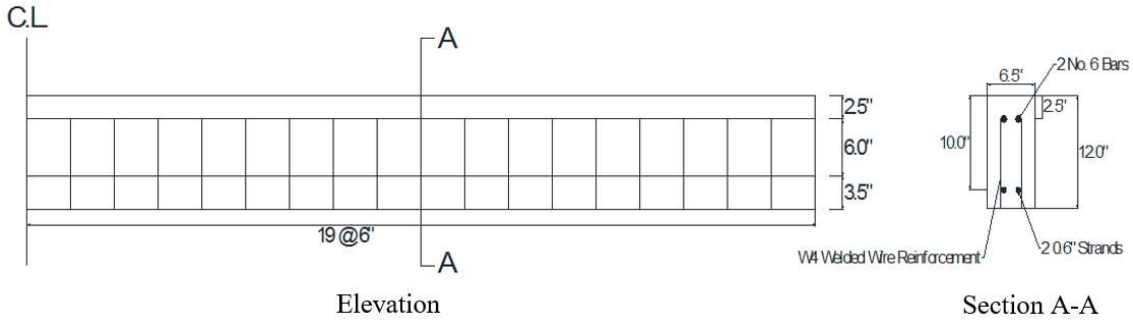

Figure 1: Beam Reinforcing Detail

The twelve specimens were split into three distinct groups with identification tags RS, 24RS, and PC. Each group of four beams was constructed with a specific cement type and prestress release time of interest. For this experiment, calcium sulfoaluminate – belite cement produced by CTS Cement Manufacturing Corporation under the trade name Rapid Set® was used. Table 1 summarizes the three specimen groups.

Table 1: Specimen Groups

Group	Cement Type	Prestress Release Time (hr)	Number of Beams	Identification
1	CSA	2	4	RS
2	CSA	24	4	24RS
3	Portland	24	4	PC

4.2 Mix Design

4.2.1 CSA Cement Concrete

The mix design (Table 2) used for the CSA specimen groups was an adapted version of the one used on the research done by Floyd and Ramseyer (2016). The original w/c was increased and the HRWR dosage was decreased to limit the impact of the HRWR in the experiment and trial batches TB1-TB24 were carried out to determine the final mix design for the CSA specimens. The trial batches, which are all summarized in Appendix B, started with small, 1 ft^3 mixes, then moved up to 3 ft^3 mixes, before finally doing large, 13 ft^3 mixes. The trial batches focused on practicing

with CSA concrete and defining the citric acid retarder dosage necessary to extend working time, while still meeting the following criteria:

1. A concrete strength of 3500 psi must be reached at prestress release for Group 1
2. The fresh concrete must allow 20 to 40 minutes of workability to fill the forms easily and perform appropriate tests
3. The water-cement ratio (w/c) must fall between 0.40 and 0.60, based on Winnefeld & Lothenbach (2010), Juenger et al. (2011), and recommendations by CTS Cement Manufacturing Corporation

Additionally, trial batches TB9-TB18 were used for a small study to simulate the effect of various citric acid retarder dosages on set time for 70 and 80-degree days. The results of this study can be found in Section 5.1.

Table 2: Final Mix Design for CSA Specimens

Material	CSA
Cement (lb/yd^3)	658
Coarse Agg. (lb/yd^3)	1560
Fine Agg. (lb/yd^3)	1188
Water (lb/yd^3)	329
w/c	0.50
HRWR (oz/cwt)	6.0
Citric Acid (lb/lb cement)	0.001

4.2.2 Portland Cement Concrete

The mix design for the portland cement specimens was used on several past projects at the University of Oklahoma including work by Mayhorn (2016), Sadhasivam (2014), and Wendling (2014). It was designed to produce a 9 to 11 in. slump for maximum workability and a 24-hour strength of 4000 psi. A low w/c was utilized for increased strength and superplasticizer was added to provide the required workability of the fresh concrete. The mix design in shown in Table 3. It is important to note that while this mix design was easy to work with, it was essentially designed to be a self-

consolidating concrete (SCC) mix with a high percentage of sand, which may have affected the transfer and development lengths of the control group, PC.

Table 3: Mix Design for PC Specimens

Material	PC Control
Cement (lb/yd^3)	851
Coarse Agg. (lb/yd^3)	1372
Fine Agg. (lb/yd^3)	1459
Water (lb/yd^3)	315
w/c	0.37
HRWR (oz/cwt)	6.5

This PC mix design allowed for the PC and RS groups to have similar concrete compressive strengths at prestress release, while the 24RS group had higher strength at release. The measured compressive strengths for each specimen at prestress release can be found in Chapter 5.

4.3 Beam Construction

4.3.1 Overview

All beam construction took place at the Donald G. Fears Structural Engineering Laboratory at the University of Oklahoma using the approximately 58-ft-long prestressing bed. The bed is long enough to allow two beams to be constructed at once with ample space in between the formwork. The formwork was placed on the bed in between the two prestressing abutments and the prestressing strands and mild steel reinforcement were placed at the necessary locations within the formwork. Once the strands were tensioned, concrete was poured into the formwork where it was allowed to cure until the appropriate prestress release time for each set of specimens. Prior to prestress release for each set of specimens, the formwork was removed and the beams were fitted with detachable mechanical (DEMEC) targets to measure surface strain of the concrete and clamps to measure strand end slip. After the prestress was released,

the specimens were moved to storage where they were allowed to cure for a minimum of 28 days.

4.3.2 Prestressing Strands

As mentioned in Section 4.1, the prestressing strands used in this experiment were 0.6 in. in diameter and Grade 270. The Standard Test for Strand Bond (ASTM 1081), previously the North American Strand Producers (NASP) strand bond test, was carried out by Sadhasivam (2014) for the prestressing strands used in this project. She determined that the 0.6 in. strands were well above the minimum threshold for bonding quality and were therefore qualified for research purposes. The strands were carefully stored at Fears lab between projects to prevent exposure to moisture or dust that could affect the bonding quality of the strand.

4.3.3 Formwork

Formwork was built using ¾ in. plywood attached to a supporting frame made of 2 in. by 4 in. dimension lumber. To mitigate any water absorption into the plywood, oil-based polyurethane was applied to the face of the plywood and at the seams between the plywood and supporting frame. The formwork on each side of a beam was connected with plywood at the ends and steel straps at the top. Each endplate had holes to allow for the strands to feed through. Special steel strips were inserted into the face of the plywood to aid in the installation of DEMEC targets for strain measurements. Further discussion regarding measurements and arrangement of the targets can be found in Section 4.3.6 Instrumentation.

4.3.4 Reinforcement

In the days leading up to the construction of each set of beams, the reinforcement was assembled to match the geometry of Figure 1. Two No. 6 bars were hung from steel tubes at the top of the formwork using bailing wire. The WWR was

placed on either side of the prestressing strands and tied to the compression steel at the top and prestressing strands at the bottom. The ties between the WWR and the prestressing strands were tied loosely to accommodate movement of the strands during tensioning. The ties were checked following strand tensioning to ensure that they had not pulled the WWR reinforcement or compression bars out of position.

4.3.5 Strand Tensioning

Tensioning of the strands was done using the approximately 58-ft-long prestressing bed at Fears Lab. The bed is composed of wood tables topped with smooth formwork in between two steel abutments attached to the Fears Lab strong floor. The abutment located on the south side of the bed, known as the dead end of the bed (Figure 2), holds the prestressing strands in place with frictional chucks while the northern abutment (Figure 3), or live end, applies the tension to the strands.

Figure 2: Steel Abutment at Dead End of Prestressing Bed

Figure 3: Steel Abutment at Live End of Prestressing Bed

The tensioning apparatus on the live end of the prestressing bed shown in Figure 3 consists primarily of two, 100 ton hydraulic rams (1) and a stiffened, steel plate (2). Once the prestressing strands were fed through the appropriate holes in the steel plate, frictional chucks (3) were used to hold the strand in place. The rams moved the steel plate outwards, which in turn tensioned the prestressing strands simultaneously. A 50-kip load cell was located between the chucks and the plate on the live end to monitor the load being applied to the strands (Figure 4). The strands were then tensioned to slightly above 75 percent of their tensile strength (Approximately 205 ksi) to account for seating losses and the nuts on the inside face of the steel plate were tightened to hold the plate in place. This maintained the tension in the strands until prestress release.

Figure 4: 50-kip Load Cell

4.3.6 Concrete Mixing and Placement

Materials were gathered the day before each set of beams was made. Rock, sand, and cement were weighed out in 5 gallon buckets and covered with lids to ensure that the moisture content of the materials did not change drastically overnight. The volume of concrete needed for each set of beams exceeded the capacity of the transfer bucket. In order to avoid leaving any fresh concrete in the mixer during transfer to the formwork, a separate batch of concrete was needed for each beam so as not to risk the CSA cement concrete setting up in the mixer. The materials were labeled and

organized into two distinct batches. On the mornings of beam construction, water, superplasticizer, and citric acid retarder, if necessary, were measured out for each batch immediately prior to mixing all of the materials. Half of the superplasticizer was added to the water buckets before mixing and the remaining half was added directly into the concrete after all of the other elements had been added. The citric acid retarder used in the CSA batches was mixed into the second half of water prior to being placed in the mixer. The materials were poured into a running 24 ft^3 rotary mixer in the following order: the rock, the sand, half of the water, the cement, the remaining half of the water, and the remaining superplasticizer that was not added to the water buckets. The elements were allowed to mix until the desired consistency of the concrete was achieved, typically only 3-4 minutes due to the rapid setting nature of the CSA cement concrete.

Once mixing was completed, a portion of the fresh concrete was discharged from the mixer into a 13.5 ft^3 hopper that was used to transport the concrete to the prestressing bed where it was poured into the formwork. The PC specimens were consolidated by striking the sides of the formwork with a rubber mallet since the batches were highly flowable. Originally the 24RS and RS specimens were to be consolidated in the same fashion to avoid any unnecessary heat from a vibrator, but the poor consolidation in 24RS1 and 24RS2, mentioned in Chapter 5, proved the need for a vibrator. The tops of the beams were finished with steel trowels and steel lifting hooks were inserted so the specimens could be transported easily in the future. The rest of the concrete in the mixer was released into a wheelbarrow so that slump and temperature of the fresh concrete could be measured and cylinders could be made for the future

compression tests. In total, 12-15 cylinders were made from each batch. This allowed for three cylinders to be tested at 2 hours (RS and 24RS), 24 hours (all groups), 7 days (PC and RS), 28 days (all groups), and at time of testing (all groups). All tests were completed and cylinders cast following the procedures and specifications outlined by ASTM International (Table 4). The companion cylinders were stored alongside their respective specimens to subject them to similar curing conditions.

Table 4: ASTM Standards

Procedure	ASTM Standard
Temperature	ASTM C1064/C1064M-12
Slump	ASTM C143/C143M-15a
Cylinders	ASTM C192/C192M-16a
Compression Tests	ASTM C39/C39M-16

4.3.7 Transfer Length Measurements

The formwork was removed 1-2 hours prior to the required prestress release time to ensure the beams could be instrumented and preliminary measurements could be taken. Steel blocks were attached to the strands protruding from each specimen. These blocks were fabricated so that the distance between the block and the face of the beam could be measured with a depth micrometer (Figure 5). Rectangular pieces of Plexiglas were epoxied on the beam face immediately above the prestressing strands (Figure 6) to provide a level surface for the end of the micrometer to press against when taking measurements. The distance between the block and face of the beam on each strand was measured using the micrometer to analyze how much the strands slipped into the beams over time. These measurements were used to compare behavior and calculate the transfer lengths of the specimens using the equation mentioned in section 2.3.

Figure 5: Depth Micrometer to Measure End Slip

Figure 6: Plexiglas and Steel Clamps for End Slip

DEMEC targets were placed at a 100 mm spacing on the eastern side of the beams to measure the surface strain of the concrete. Measurements were taken using the 200 mm British Cement Association gage in Figure 7. Measurements were taken over the measurement period to determine strain distribution along the length of each beam. The difference between the initial surface strain measurements and subsequent measurements were used to plot strain along the length of each beam. The 95% Average Maximum Strain method used by previous researchers (Russell and Burns, 1996) was used to determine the transfer length using this value. This method consists of averaging the maximum strain values following the strain plateau, taking 95% of that average value, and finding the corresponding point on the strain profile. The location of the corresponding point is taken to be the transfer length (Figure 8). A three-point

moving average was used in plotting the surface strains to smooth out some of the inherent variability in the measurements.

Figure 7: British Cement Association Gage for DEMEC Measurements

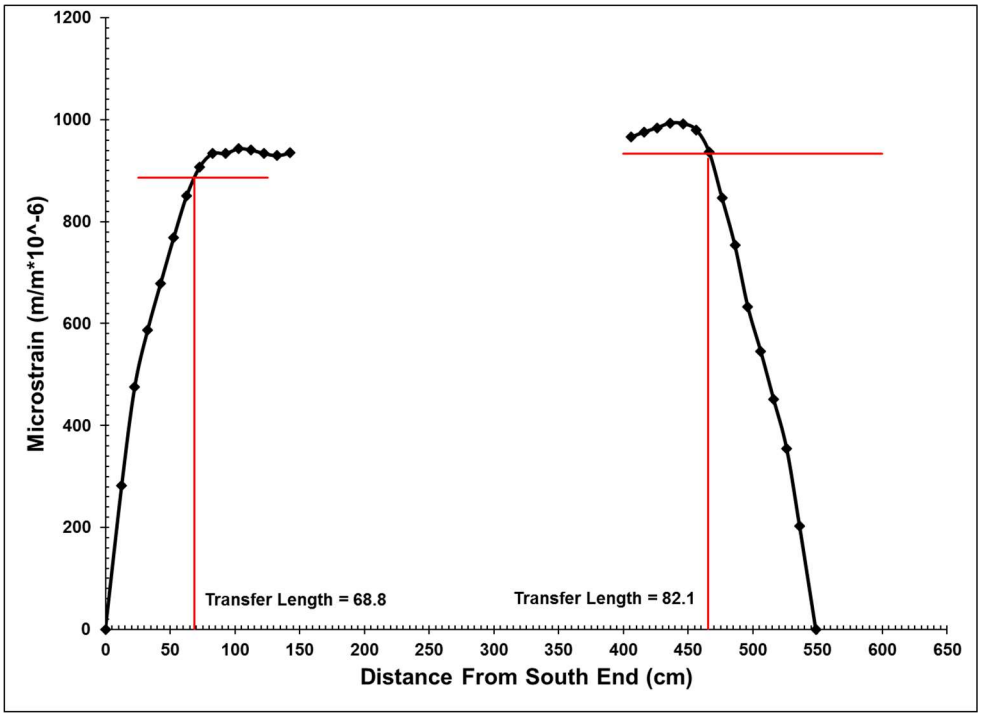

Figure 8: 95% Average Maximum Strain Method

The DEMEC targets were fitted to the specimens during the construction process using the following procedure, which is similar to previous research (Bodapati et al., 2016):

1) Prior to casting, brass inserts (Figure 9) were secured to the formwork using a special steel plate with holes drilled at the 100 mm spacing. A ½ in. long hex-

head screw was fit through the back of the formwork and steel plate and threaded into each of the brass inserts so that the collars of the inserts were flush with the formwork (Figure 10). The inserts were cast in the concrete in this arrangement to maintain precise location and orientation. The threads on the inserts provided proper anchorage in the concrete. Figure 11 shows the configuration of the inserts for each specimen. There were 16 inserts on each end which were labelled 1-32 beginning from the south end and moving to the north end. The inserts were located at the same height as the strands and spanned 122 in. from the ends, well past the ACI and AASHTO estimated transfer lengths of 30 in. and 36 in., respectively.

Figure 9: Brass Inserts used for DEMEC Points

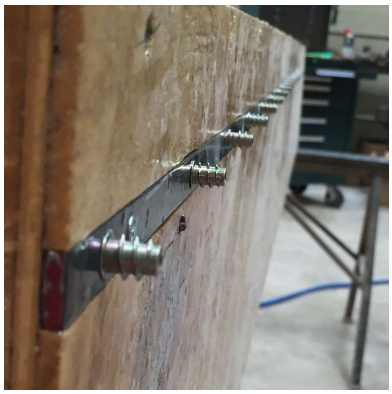

Figure 10: Special Formwork for Brass Insert Installation

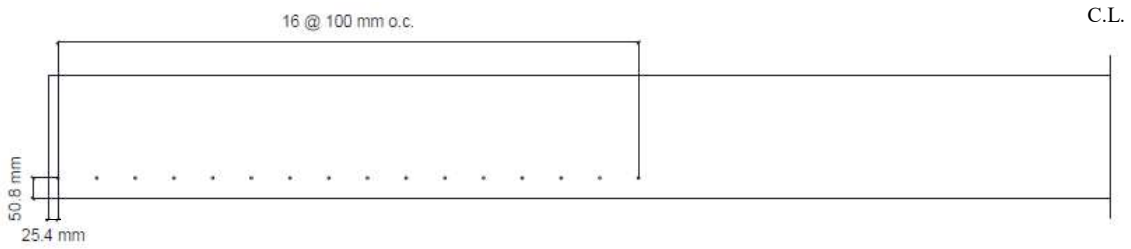

Figure 11: DEMEC Point Layout

2) Before prestress transfer, the screws threading into the inserts were removed so the formwork could be detached from the beams.

3) DEMEC targets were made out of ¼ in. long hex-head screws. Each screw had a 1.0 mm dimple drilled into the center of its head to match the prongs on the gage. The targets were threaded into the brass inserts (Figure 12).

Figure 12: DEMEC Point

4.3.8 Prestress Loss Measurements

Prestress losses were also monitored in select specimens. VWSGs were embedded in specimens 24RS3, 24RS4, RS3, and RS4. The VWSGs were placed at the level of the prestressing strands at the center of the beam (Figure 13). VWSG measurements were taken daily for approximately 28 days after casting the beams using a hand held reader. The difference between measurements taken before prestress release and at each increment provided change in strain which could be used to determine change in stress using the modulus of elasticity of the prestressing strands.

Figure 13: VWSG Attachment to Strands

4.4 Beam Testing

All beams were tested in flexure after reaching 28 days of age to evaluate development length. After approximating the development length of each beam using the ACI equation for development length (Appendix A), an embedment length of 71 in. was chosen. This embedment length was at the bottom of the range of the calculated development lengths for all of the specimens and would therefore apply to all of the specimens. For each beam, this length was measured from the beam end that was closest to an abutment during prestressing. Supports consisting of steel rollers were placed 6 in. from the ends of the beams creating a 17 ft span length.

The load was applied to each specimen using a hydraulic ram extending into a spreader beam, all mounted to a steel reaction frame above the specimen. Spacers, a cylindrical loading head, a loading plate, and sand were used to ensure the load was applied vertically. A 50-kip load cell was placed on top of the spreader beam so that the applied load could be monitored throughout the test using a data acquisition system. The full load application set-up is shown in Figure 14. The load was applied using 2 kip increments until the first crack appeared, followed by 1 kip increments until failure. Cracks were marked and manual deflection measurements were taken with a laser level and a ruler between load increments. Deflection was measured at the load point with

wire potentiometers (Figure 15). Lastly, strand slip during testing was measured with linear variable differential transformers (LVDTs) mounted on each of the prestressing strands (Figure 16).

Figure 14: Load Application Set-up

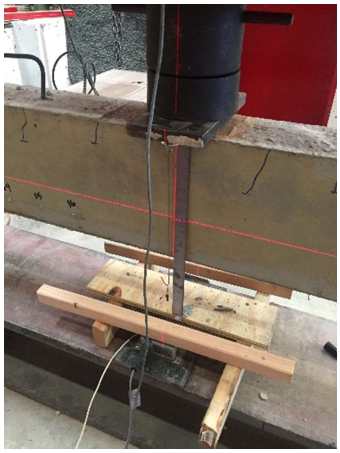

Figure 15: Wire Pot Set-up at Load Point

Figure 16: LVDTs Mounted on Strands

After testing, qualitative and quantitative analyses were performed to determine whether the failure occurred due to flexure or due to the strand bond. Beams considered to exhibit flexural failures reached their nominal flexural capacity, crushed at the top, and exhibited no strand slip. Beams considered to exhibit bond failures did not reach their nominal flexural capacity and exhibited strand slip. If a flexural failure occurred, the embedment length was considered greater than the development length. If a bond failure was observed the embedment length was considered to be less than the development length. This analysis helped determine if the full capacity of the beam was reached during testing at the approximate ACI specified development length or if the development length was farther from the end of the beam.

Chapter 5: Beam Concrete Results

5.1 CSA Trial Batches

The results of all trial batches are presented in Appendix B. The specific goal for trial batches TB9-TB18 was to better understand the effect of citric acid dosage and temperature on the set time of the fresh concrete. A small study was done to simulate the effect of various citric acid retarder dosages on set time for 70 and 80-degree days.

Aggregates and cement were temperature controlled in an environmental chamber, water was heated to the controlled temperature, and the mixer was heated as much as possible to match the air temperature. The measured material temperatures for the simulated 70-degree day are shown in Table 5.

Table 5: Temperatures on a 70-Degree Day

Batch	**TB9**	**TB10**	**TB11**	**TB12**	**TB13**
Slump (in.)	8.5	8.75	8.5	8.25	3.5
Rock Temp (ºF)	73.4	74.8	74	74	74
Sand Temp (ºF)	66	66	68	68	68
Mixer Temp (ºF)	68	65	65	62	63
Water Temp (ºF)	70	67	68	69	66
Air Temp (ºF)	65	65	65	65	66
Concrete Temp (ºF)	71	70	70	70	70
Citric Acid Dosage (lb/lb cement)	0.0025	0.0020	0.0015	0.0010	0

All of the components of the mixes as well as the air and mixer were relatively close to the 70ºF target and in the end the fresh concrete temperatures were all within 1ºF of 70ºF. Compressive strength cylinders were made for each batch and the approximate strength gain over time is illustrated in Figure 17.

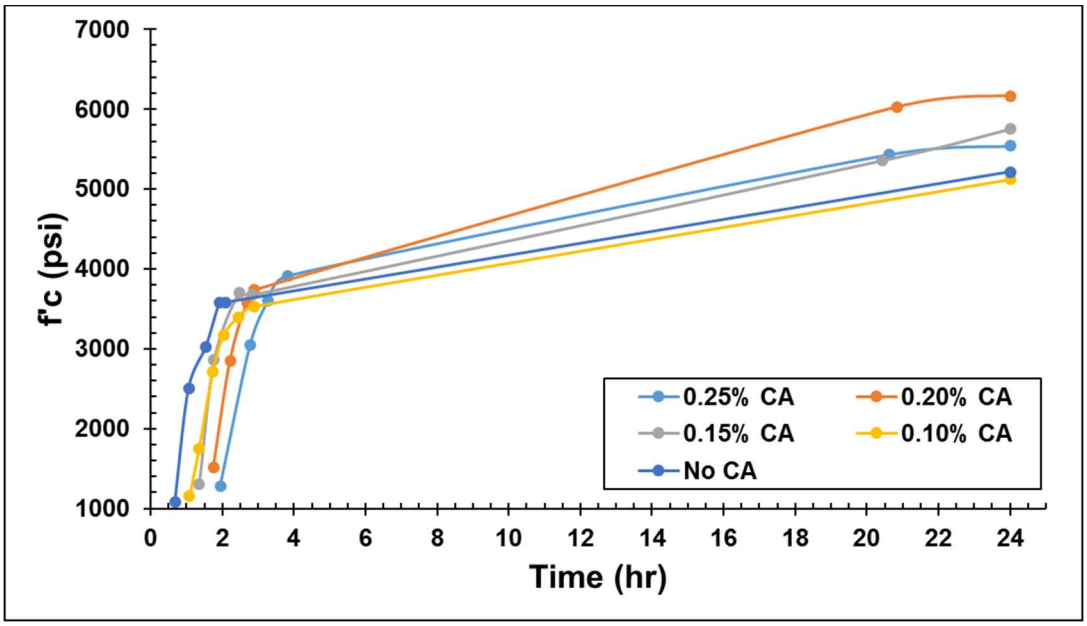

Figure 17: Strength Gain vs. Time on a 70-Degree Day

All of the batches reached the 3500 psi compressive strength target at around 2 hours, although batch TB13 with no citric acid retarder produced a slump of only 3.5 in. and was difficult to work with. All of the other batches produced slumps in the 8.5 to 9 in. range and were very workable.

The measured temperatures for the simulated 80-degree day are shown in Table 6. All of the components of the mixes as well as the air and mixer were relatively close to the 80ºF target and in the end the fresh concrete temperatures were all within 2ºF of 80ºF. Compressive cylinders were made for each batch and the approximate strength gain over time is illustrated in Figure 18.

Table 6: Temperatures on an 80-Degree Day

Batch	**TB14**	**TB15**	**TB16**	**TB17**	**TB18**
Slump (in.)	7	7.75	8	6	1.25
Rock Temp (ºF)	74	74	74	74	74
Sand Temp (ºF)	74	74	72	74	72
Mixer Temp (ºF)	80	71	71	71	71
Water Temp (ºF)	83	82	84	82	81
Air Temp (ºF)	77	77	79	79	80
Concrete Temp (ºF)	80	78	79	79	80
Citric Acid Dosage (lb/lb cement)	0.0025	0.0020	0.0015	0.0010	0

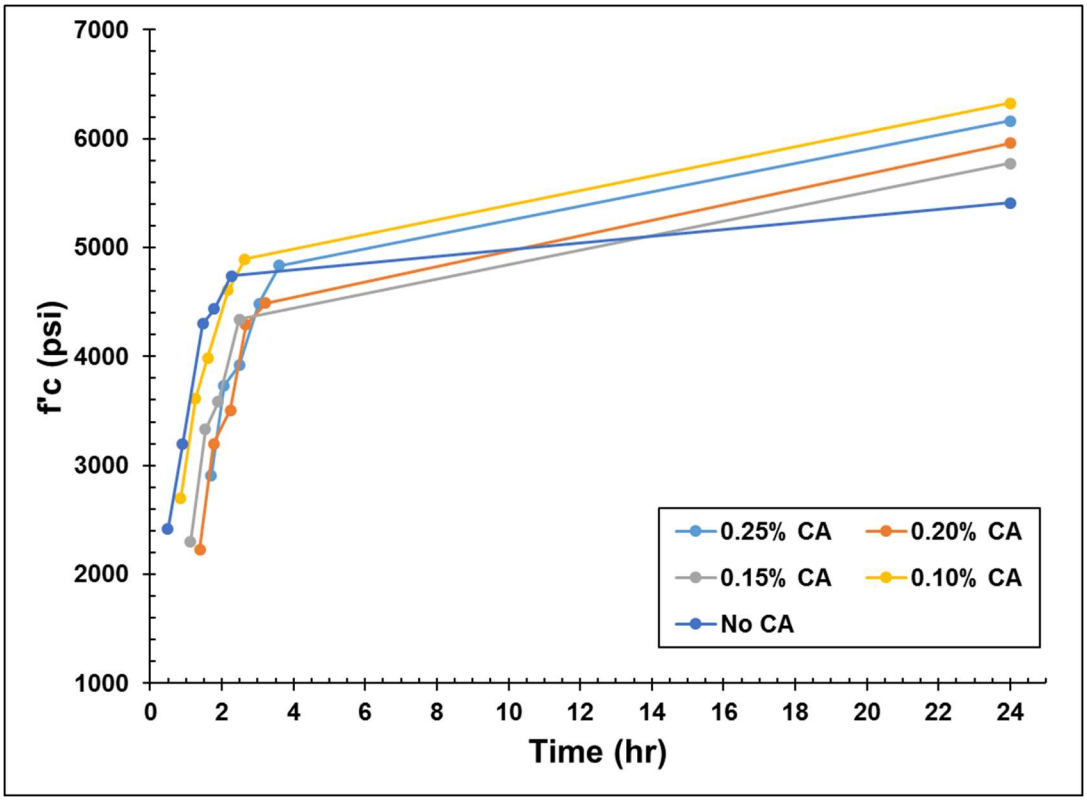

Figure 18: Strength Gain vs. Time on an 80-Degree Day

All of the batches reached the 3500 psi compressive strength target at around 2 hours, although the TB17 and TB18 batches with 0.10% and no citric acid retarder produced slumps of only 6 and 1.25 in. and were difficult to work with. All of the other batches produced slumps in the 7.5 to 8 in. range and were very workable.

Based on the high compressive strengths measured on an 80-degree day, which was the approximate expected temperature during beam construction, the 24RS and RS specimens were made with a citric acid dosage of 0.1%. A higher HRWR dosage was added to the final mix design to improve workability and the final mix design can be found in Section 4.2.

5.2 Portland Cement (PC) Beams

Table 7 presents the concrete properties of each of the PC batches. The slump of each batch fell within the desired 9 in. to 11 in. range and the compressive strength of all four batches were above the required 3500 psi compressive strength at prestress release (f'_{ci}). At the time of testing, only PC1 fell below the design compressive strength (f'_c) of 6000 psi which may be due in part to segregation. The compressive strength gain in the companion cylinders for each PC specimen can be found in Appendix C.

Table 7: Concrete Properties of PC Batches:

Beam	Slump (in.)	Temperature (°F)	f'_{ci} (psi)	f'_c (psi)
PC1	10.75	80	4180	5950
PC2	10.5	82	4760	7010
PC3	9.5	84	4860	6990
PC4	10.25	83	5110	7010

All four PC beams experienced some loss of paste in areas at the bottom of the beams due to a small gap between the formwork and the table (Figure 19). The companion compression cylinders for PC1 and PC2 also exhibited signs of segregation upon examination, which may have been due to an error in determining the moisture content of the aggregates prior to batching. Figure 20 shows the difference in the distribution of coarse aggregate between the top and bottom of one of the cylinders.

Figure 19: Loss of Paste at Bottom of Specimen

Figure 20: (Left) Bottom of Cylinder. (Right) Top of Cylinder

5.3 24-Hour Release CSA (24RS) Beams

Table 8 summarizes the concrete properties of the 24RS batches. All batches reached the minimum 3500 psi compressive strength at prestress release and exhibited compressive strengths higher than the PC batches at the time of beam testing. Each batch was adequately workable. The sample taken for 24RS1 had a large, unmixed mass in it, which may have resulted in a low slump. The compressive strength gain in the companion cylinders for each 24RS specimen can be found in Appendix C.

Table 8: Concrete Properties of 24RS Batches

Beam	Slump (in.)	Temperature (ºF)	f'_{ci} (psi)	f'_c (psi)
24RS1	5	80	4800	8270
24RS2	9.75	75	4570	8160
24RS3	10.5	70	4360	7730
24RS4	10.5	68	3990	6560

Specimens 24RS1 and 24RS2 exhibited small bug holes due to poor consolidation (Figure 21). The largest consolidation concern occurred in 24RS1 near the top on the northeast side of the beam (Figure 22). The approximately 5 in. long gap exposed compression and shear steel. Additionally, a bug hole occurred at DEMEC point 31 near the north end on 24RS1 that rendered the brass insert useless (Figure 23). The consolidation issues were due to the original plan to not use a vibrator as mentioned in Section 4.3.5. Specimens 24RS3 and 24RS4 exhibited excellent consolidation, but experienced the same loss of paste as PC1, PC2, PC3, and PC4 due to the gap between the formwork and the table.

Figure 21: Bugholes in Specimen 24RS1

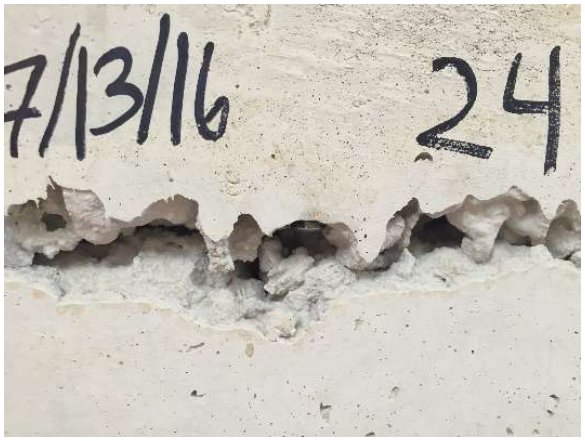

Figure 22: Large Bughole in 24RS1

Figure 23: Unusable Brass Insert on 24RS1

5.4 2-Hour Release CSA (RS) Beams

Table 9 presents the concrete properties for the RS batches. All batches besides RS4 achieved the 3500 psi target compressive strength at prestress release. Although RS4 did not reach 3500 psi, an engineering decision was made that it was close enough for prestress release since it was within 3% of the target value and the companion specimen RS3 had achieved the target compressive strength. The average compressive strengths of the RS specimens at release were approximately 20% less than the 24RS specimens and approximately 33% less than the PC specimens. At the time of beam

testing, the average compressive strengths of the RS specimens were approximately the same as the PC specimens and 10% lower than the 24RS specimens. All four RS beams exhibited excellent consolidation and had the same issues with loss of paste due to the gap between the formwork and the table. The compressive strength gain in the companion cylinders for each RS specimen can be found in Appendix C.

Table 9: Concrete Properties of RS Batches

Beam	Slump (in.)	Temperature (°F)	f'_{ci} (psi)	f'_c (psi)
RS1	10.25	70	3960	6340
RS2	11	70	3670	6970
RS3	10.5	65	3610	7130
RS4	10.5	65	3400	7050

Chapter 6: Transfer Length Results

6.1 Introduction

The primary objective of this study was to examine how the bond behavior of 0.6 in. prestressing strands cast in CSA cement concrete differs from strands cast in conventional concrete. One feature of interest is the transfer length of the prestressing strands. This chapter summarizes the results of the transfer lengths measured for the 12 beams described in Chapter 4 and how those values compare to the values estimated by the ACI and AASHTO equations for transfer length. It is important to note that the odd numbered beams were cast on the south (dead) end of the prestressing bed and the even numbered beams were cast on the north (live) end of the prestressing bed.

6.2 DEMEC Transfer Lengths

6.2.1 Introduction

DEMEC measurements were taken using the methods described in Section 4.3.6. Transfer lengths for each end of the specimens were calculated using the 95% Average Maximum Strain (AMS) described in Section 4.3.6. Most specimens presented somewhat erratic and unclear surface strain plateaus and were difficult to interpret accurately. These indistinct strain plateaus could have been due to the moving average method with which the strains were determined. If one point presented incorrect data, it would have had an effect on the points around it. It is also possible that some of the DEMEC points were machined differently, resulting in minor inconsistencies in the measurements. The 28-day and 36-day strain profiles illustrated in this chapter are shown in SI units since the British Cement Association Gage (Section 4.3.6) presents data in SI units. There is some subjectivity involved in taking measurements with the gage, so some error is inherent in the results. To minimize this error, measurements were taken by typically taken by two people and averaged. Additionally, a few of the embedded DEMEC points began to loosen over the course of the measurement time frame which may have had an influence on the results. DEMEC strain profiles over the entire measurement period can be found in Appendix D.

6.2.2 Portland Cement (PC) Beams

The DEMEC transfer lengths for the PC beams over time are summarized in Table 10. All of the DEMEC points for the PC specimens were usable and none of the points loosened over the 28 days measurements were taken. Overall, the transfer length of each of the PC specimens stayed relatively constant over the 28 days measurements

were taken. There did not appear to be a trend in the difference between the north and the south ends of the beams.

Table 10: DEMEC Transfer Lengths over Time for PC Specimens

End	South End (in.)				North End (in.)			
Specimen	**PC1**	**PC2**	**PC3**	**PC4**	**PC1**	**PC2**	**PC3**	**PC4**
Release	32.2	34.1	19.4	24.3	27.5	32.9	27.7	20.7
7-Day	31.7	36.0	25.5	23.6	29.8	30.2	27.9	23.2
14-Day	31.8	35.6	20.4	23.3	29.7	29.7	28.4	23.2
21-Day	31.8	35.6	20.8	23.4	27.8	30.5	28.6	24.1
28-Day	31.6	35.6	21.2	23.6	29.4	30.1	29.1	23.6

Figure 24 shows the 28-day strain profiles for the PC specimens. The plateaus for many of the specimens were irregular and not entirely clear. In some cases, these irregularities made it difficult to determine which points to use for calculating the AMS. In the end, all of the points after the first plateau were used to determine the AMS. The maximum strains at 28 days were all within a range of approximately 200 microstrains and the slopes of the strains prior to the plateau are similar for all of the specimens.

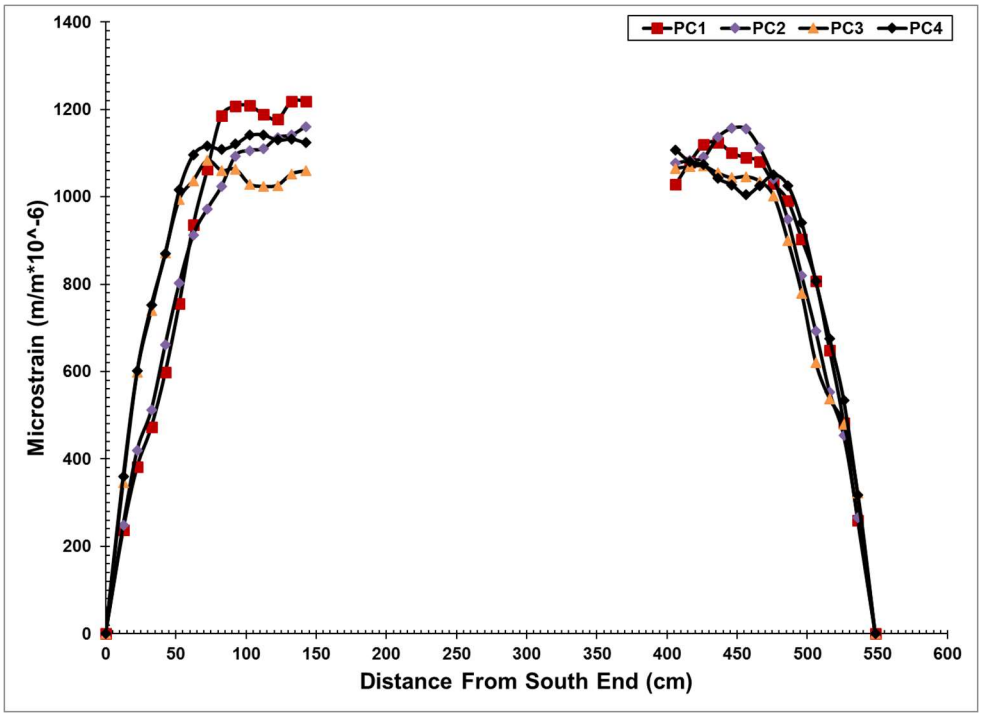

Figure 24:DEMEC Strain Profiles at 28 Days for PC Specimens

The PC transfer length values using the DEMEC system at 28 days along with the ACI and AASHTO predicted values are shown in Figure 25. The transfer length of the south end of PC2 ranges from 4 in. to 14.4 in. higher than the rest of the PC ends. PC3 and PC4 displayed lower transfer lengths at 28 days than PC1 and PC2. One explanation for this difference may be the segregation that occurred in PC1 and PC2 during the batching process. The segregation could have played a role in the weaker bond in PC1 and PC2, thereby increasing the transfer length. The ACI approximated transfer length of 30 in. was close to the average transfer length for the four PC specimens while the AASHTO approximated value of 36 in. was greater than all of the measured transfer lengths.

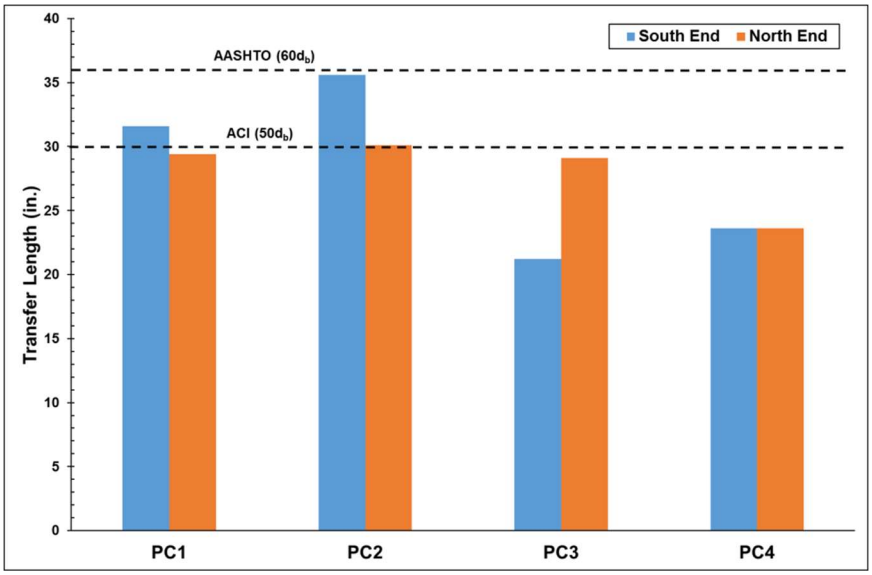

Figure 25: Comparison of Transfer Lengths for PC Specimens at 28 Days

6.2.3 24-hr Release CSA (24RS) Beams

The DEMEC transfer lengths for the 24RS beams over time are summarized in Table 11. Unfortunately, the beams were unavailable for measurement at 28 days and were instead measured at 36 days due to problems with the Fears Lab overhead crane. Overall, the transfer length of each of the 24RS specimens stayed relatively constant over the 36 days measurements were taken. There did not appear to be a trend in the difference between the north and the south ends of the beams.

Table 11: DEMEC Transfer Lengths Over Time for 24RS Specimens

End	**South End (in.)**				**North End (in.)**			
Specimen	**24RS1**	**24RS2**	**24RS3**	**24RS4**	**24RS1**	**24RS2**	**24RS3**	**24RS4**
Release	24.0	31.7	26.7	26.5	24.5	29.2	26.0	24.4
7-Day	24.8	31.1	24.7	27.0	25.1	26.6	24.9	24.0
14-Day	26.0	32.2	25.9	28.7	26.3	26.5	27.9	25.4
21-Day	27.4	30.4	27.0	31.4	26.6	27.0	28.1	24.8
36-Day	26.8	32.4	27.3	27.7	24.1	27.2	27.7	23.5

As mentioned in Section 5.3, the second DEMEC target from the north end of 24RS1 was lost during the construction of the beam and was not usable for measurements. Since the point likely fell within the transfer length, the missing measurement should not have had a significant influence on the transfer length calculations. The 36-day strain profiles for the 24RS specimens are presented in Figure 26. The plateaus for some of the specimens were irregular and not entirely clear. These irregularities made it difficult to determine which points to use for calculating the AMS. In the end, all of the points after the first plateau were used to determine the AMS. The maximum strains on the south and north ends of the beams were all within a range of approximately 200 microstrains and the slopes of the strains prior to the plateau are similar for all of the specimens. On average, the maximum strains at 36 days for the 24RS specimens were nearly 400 microstrains less than those measured for the PC specimens at 28 days due to reduced creep, shrinkage, and elastic shortening. Since the maximum strains for the 24RS specimens were only approximately 125 microstrains less than the PC specimens at release, and the 24RS specimens were measured at a later age, the majority of the difference in strain came from reduced creep and shrinkage.

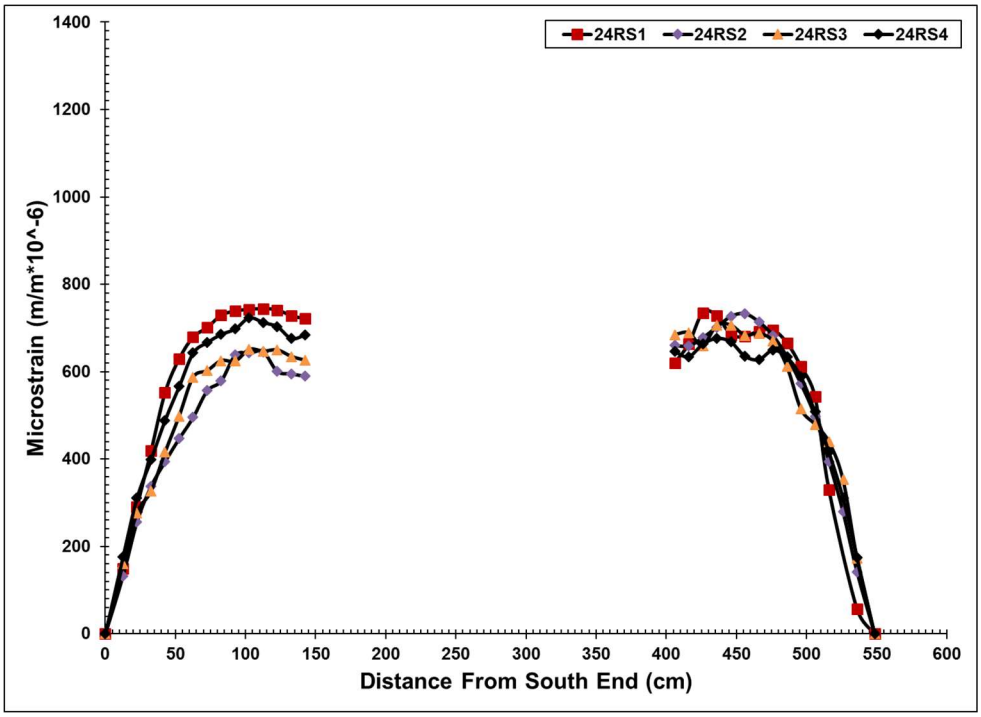

Figure 26: DEMEC Strain Profile at 36 Days for 24RS Specimens

The 24RS transfer length values at 36 days along with the ACI and AASHTO predicted values are shown in Figure 27. Although the transfer lengths do not differ considerably from beam to beam, the transfer length at the south end of 24RS2 is significantly larger than all of the other 24RS ends. The larger transfer length for 24RS2 may be due to the poor consolidation discussed in Section 5.3. The ACI approximated transfer length of 30 in. was greater than the average transfer length for the four 24RS specimens and greater than the individual transfer lengths besides the south end of 24RS2. The AASHTO approximated value of 36 in. was higher than all of the measured transfer lengths.

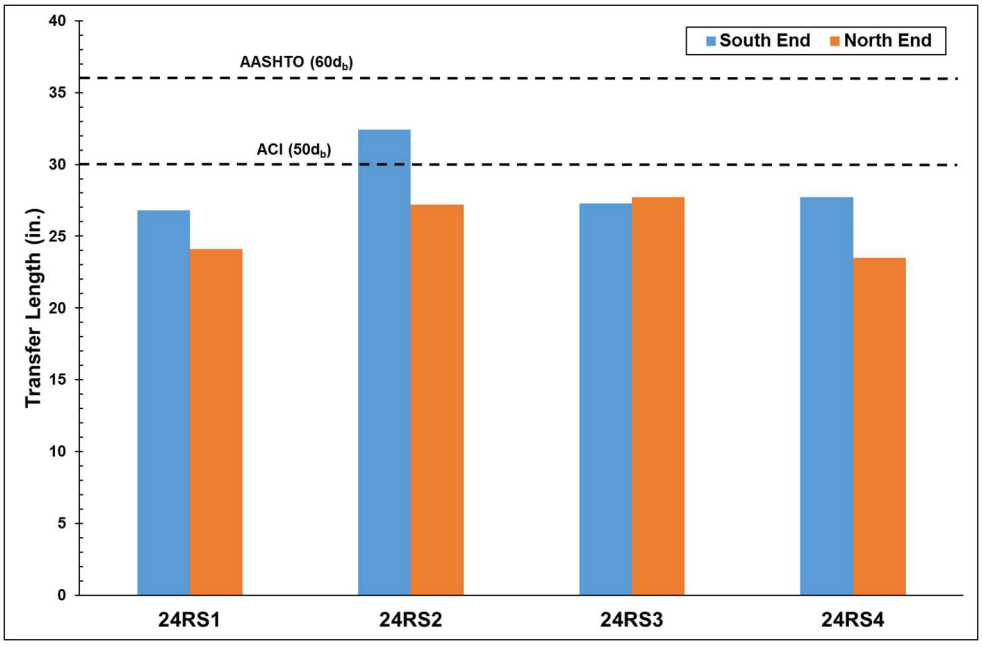

Figure 27: Comparison of Transfer Lengths for 24RS Specimens at 36 Days

6.2.4 2-hr Release CSA (RS) Beams

The DEMEC transfer lengths for the RS beams over time are summarized in Table 12. All of the DEMEC points for the RS specimens were usable and none of the points loosened over the 28 days. Unfortunately, RS3 and RS4 were unavailable for measurement at 14 days and RS1 and RS2 were unavailable for measurement at 21 days due to a malfunction of the fears lab overhead crane. Measurements were taken at 36 days in order to compare data with the 24RS measurements. Overall, the transfer length of each of the RS specimens stayed relatively constant over the 36 days measurements were taken. There did not appear to be a trend in the difference between the north and the south ends of the beams.

Table 12: DEMEC Transfer Lengths Over Time for RS Specimens

End	South End (in.)				North End (in.)			
Specimen	**RS1**	**RS2**	**RS3**	**RS4**	**RS1**	**RS2**	**RS3**	**RS4**
Release	27.8	34.7	35.7	31.9	34.7	27.8	28.6	25.2
7-Day	26.1	28.3	35.4	31.0	33.6	27.2	28.0	25.5
14-Day	28.9	28.0	-	-	32.7	27.2	-	-
21-Day	-	-	34.0	32.1	-	-	28.3	25.6
28-Day	27.0	28.5	37.5	30.5	33.3	27.2	28.5	25.7
36-Day	27.5	35.2	36.2	31.7	32.8	27.2	28.6	24.8

The 36-day strain profiles for the RS specimens are presented in Figure 28. The plateaus for some of the specimens besides RS1 were irregular and not entirely clear. These irregularities made it difficult to determine which points to use for calculating the AMS. In the end, all of the points after the first plateau were used to determine the AMS. The maximum strains on the south and north ends of the beams were all within a range of approximately 200-300 microstrains and the slopes of the strains prior to the plateau are similar for all of the specimens. On average, the maximum strains for the 24RS specimens were nearly 200 microstrains less than those measured for the PC specimens which could be due in part to the decreased creep, shrinkage, and elastic shortening. Since the maximum strains for the RS specimens were approximately 25 microstrains higher than the PC specimens at release, the difference in strain came from reduced creep and shrinkage.

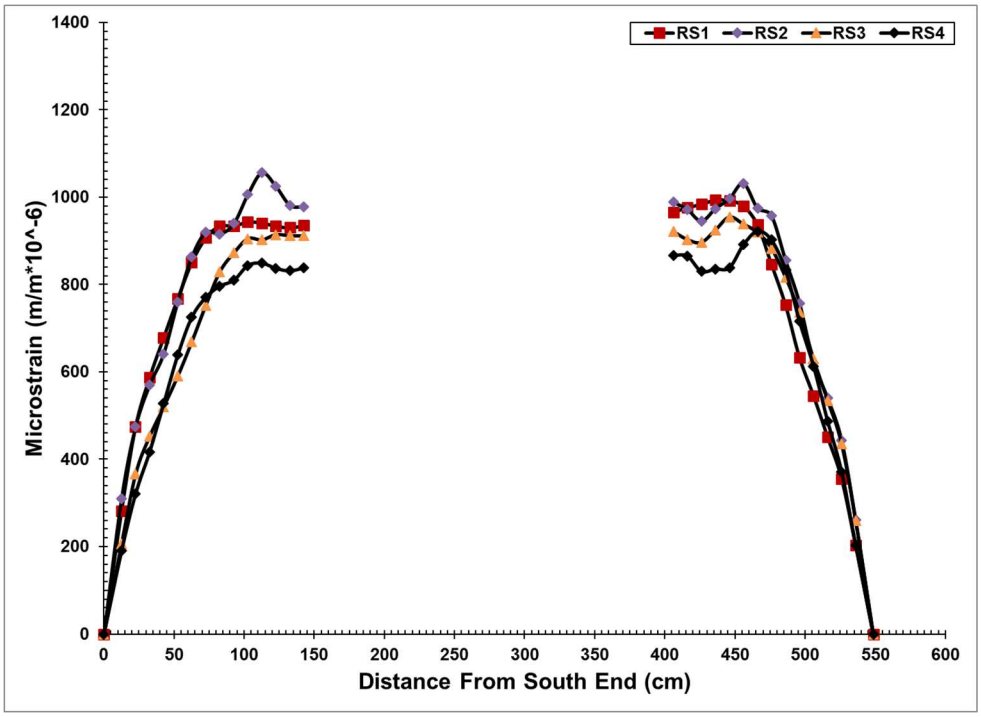

Figure 28: DEMEC Strain Profile at 36 Days for RS Specimens

The RS transfer length values at 36 days along with the ACI and AASHTO predicted values are shown in Figure 29. Overall the four RS specimens were relatively similar to one another in their transfer length measurements. The ACI approximated transfer length of 30 in. was nearly the same as the average transfer length for the four RS specimens. The AASHTO approximated value of 36 in. was higher than all of the measured transfer lengths besides the south end of RS3.

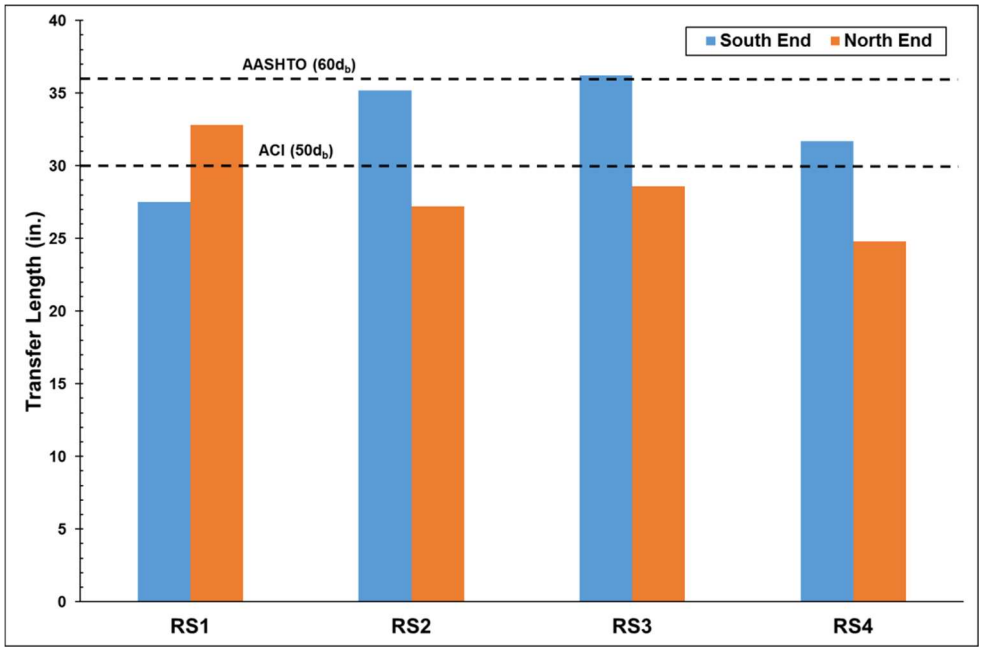

Figure 29: Comparison of Transfer Lengths at 36 Days for RS Specimens

Figures 30-32 show all of the DEMEC transfer lengths for each of the specimens over time.

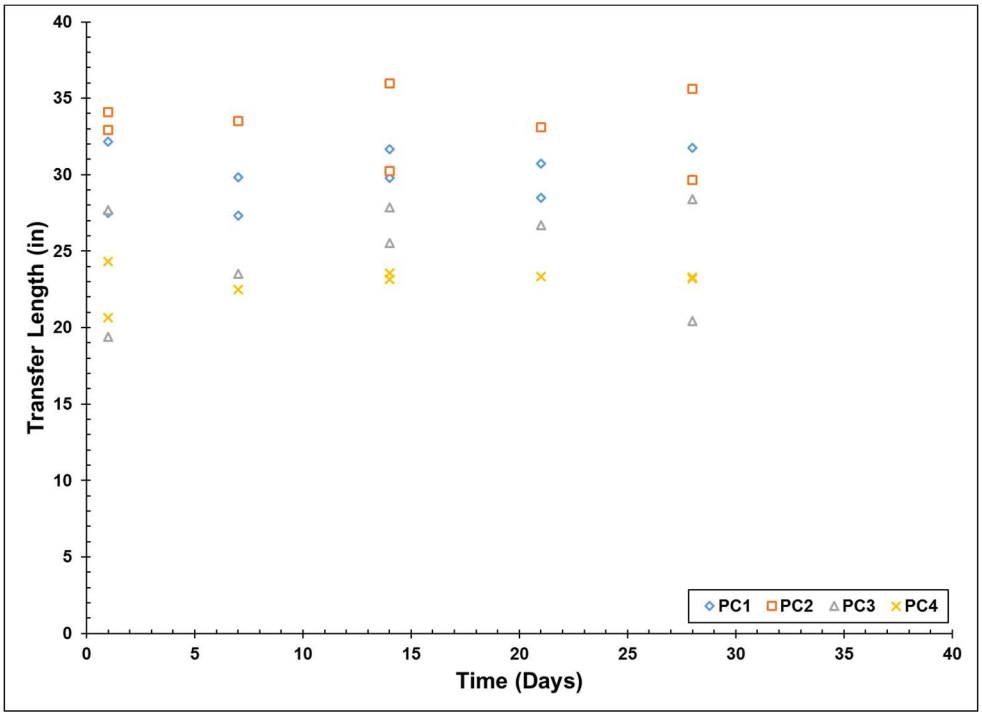

Figure 30: DEMEC Transfer Lengths Over Time for the PC Group

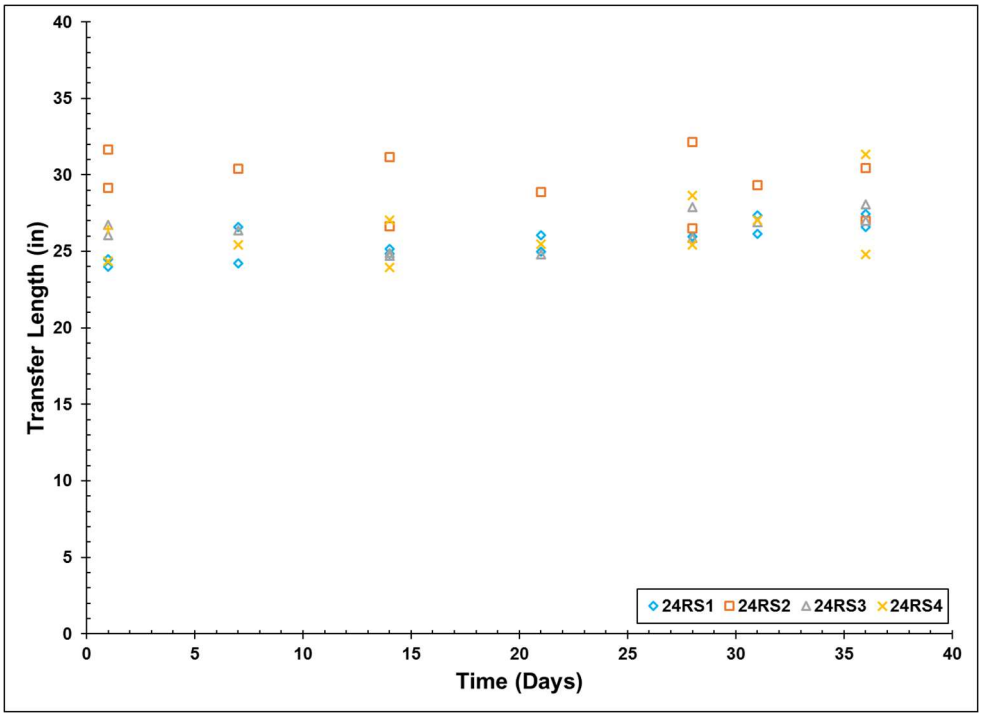

Figure 31: DEMEC Transfer Lengths Over Time for the 24RS Group

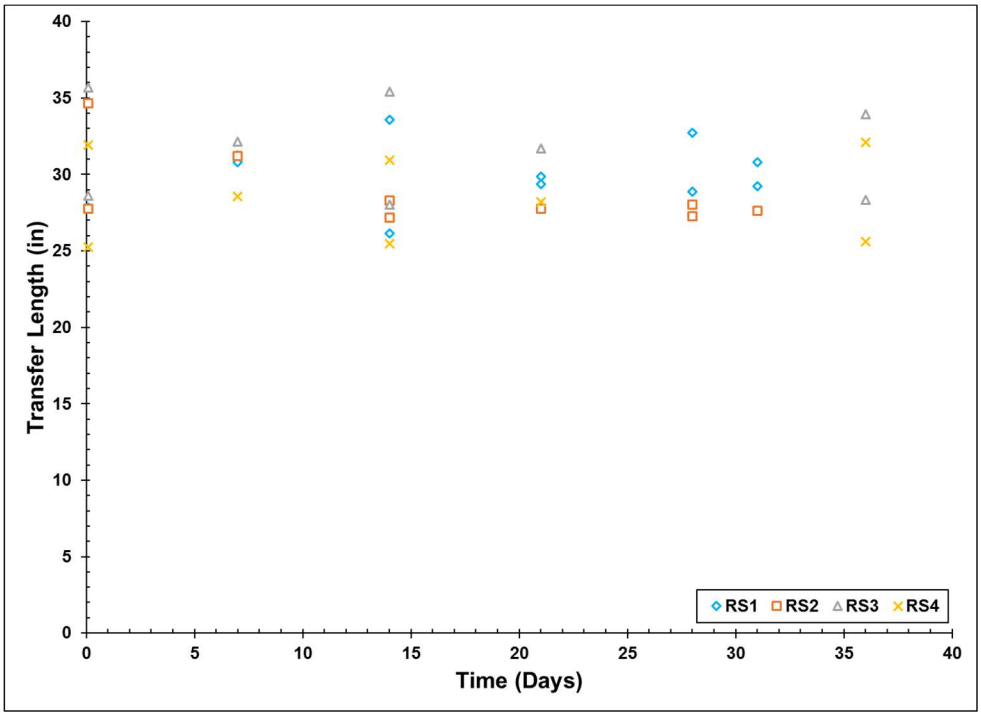

Figure 32: DEMEC Transfer Lengths Over Time for the RS Group

6.3 End Slip Transfer Lengths

6.3.1 Introduction

End slip measurements were taken using the process outlined in Section 4.3.6 to calculate the transfer lengths of the specimens. Due to the uncertainty surrounding the value of the constant, α, transfer lengths were analyzed using α=2 and α=3. This section summarizes the end slip transfer lengths, how they compare to the ACI and AASHTO estimates, and how they compare to the DEMEC transfer lengths described in Section 6.2.

6.3.2 Portland Cement (PC) Beams

The average transfer lengths calculated using end slip for the PC specimens are illustrated in Figure 33. On average, the transfer length of the specimens remained relatively constant over the 28 days. The DEMEC transfer lengths for the PC specimens tend to correspond to an α value of approximately 2.42.

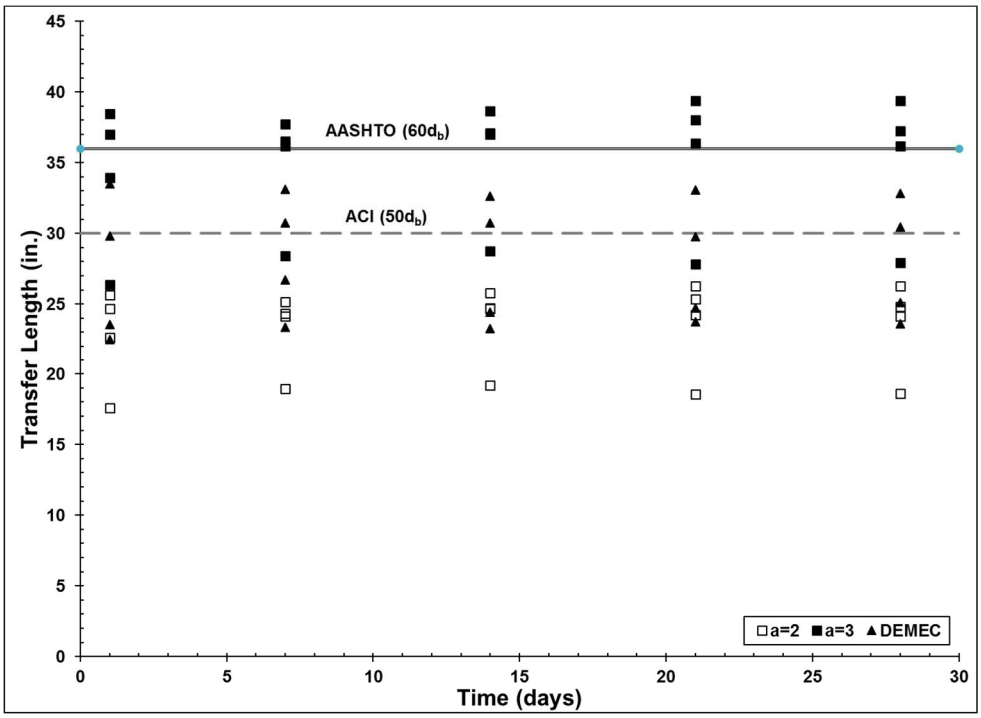

Figure 33: Transfer Lengths of PC Specimens from End Slip and DEMEC

6.3.3 24-hr Release CSA (24RS) Beams

The average transfer lengths calculated using end slip for the 24RS specimens are illustrated in Figure 34. All 24RS specimens were unavailable for measurement at 28 days so the last measurement was taken at 36 days. Additionally, 24RS3 and 24RS4 were measured at 31 days. On average, the end slip transfer lengths of the specimens remained relatively constant over the 36 days. All of the end slip transfer lengths fall below the AASHTO estimate while the ACI estimate falls in between the α=2 and α=3 ranges. The DEMEC transfer lengths for the 24RS specimens tend to correspond to an α value of approximately 2.48. The transfer length calculations for 24RS3 most likely do not reflect the actual transfer lengths since the Plexiglas on the south end of 24RS3 began to pull away from the beam over the 36 days.

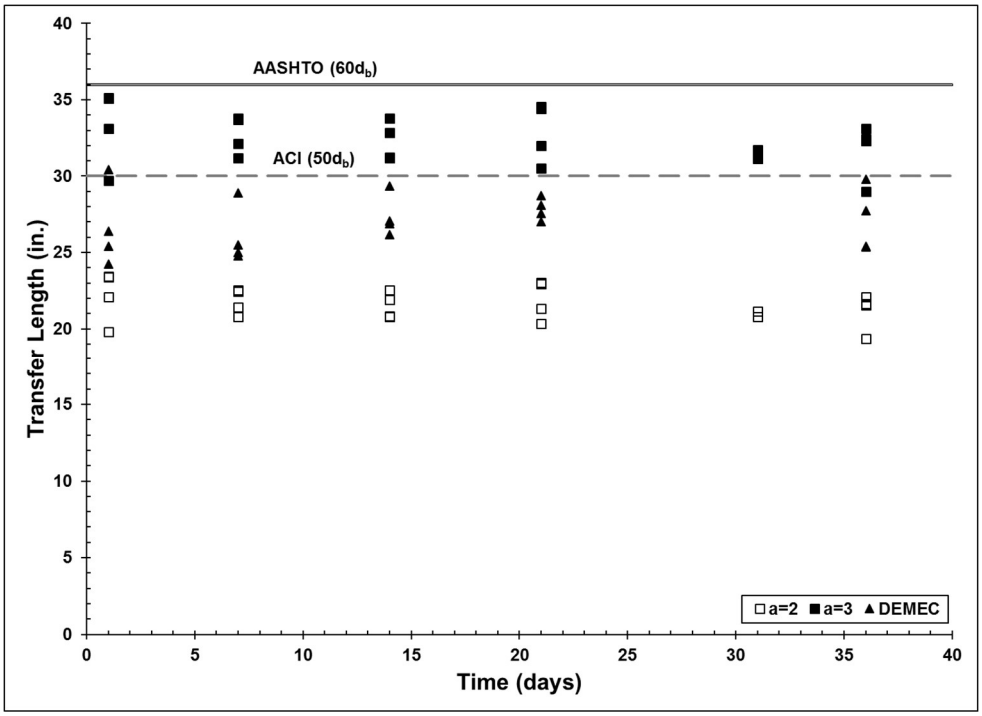

Figure 34: Transfer Lengths of 24RS Specimens from End Slip and DEMEC

6.3.4 2-hr Release CSA (RS) Beams

The average transfer lengths calculated using end slip for the RS specimens are illustrated in Figure 35. RS1 and RS2 were unavailable for measurements at 21 days

and RS4 was unavailable for measurements at 14 days. Measurements were also taken at 36 days to compare to 24RS. The end slip of the RS specimens was difficult to measure due to issues with the Plexiglas pieces. Since the prestress in the RS specimens was released at two hours, the surface of the beams was still warm and damp when the Plexiglas attachments were epoxied to the beams. These conditions decreased the effectiveness of the epoxy and many of the Plexiglas pieces fell off or were falling off for ensuing end slip measurements. The transfer lengths calculated by end slip measurements therefore, may not be representative of the actual transfer lengths. The transfer lengths for RS3 are left out of Figure 32 because end slip measurements for RS3 were unsuccessful. On average, the end slip transfer lengths of the RS specimens stayed relatively constant over the 36 days. The ACI estimate for transfer length is near the top of the range of α=2 values and the AASHTO estimate is within the α=3 range. Some α=3 transfer lengths are well above the AASHTO estimate. The DEMEC transfer lengths for the RS specimens tend to correspond to an α value of approximately 2.3.

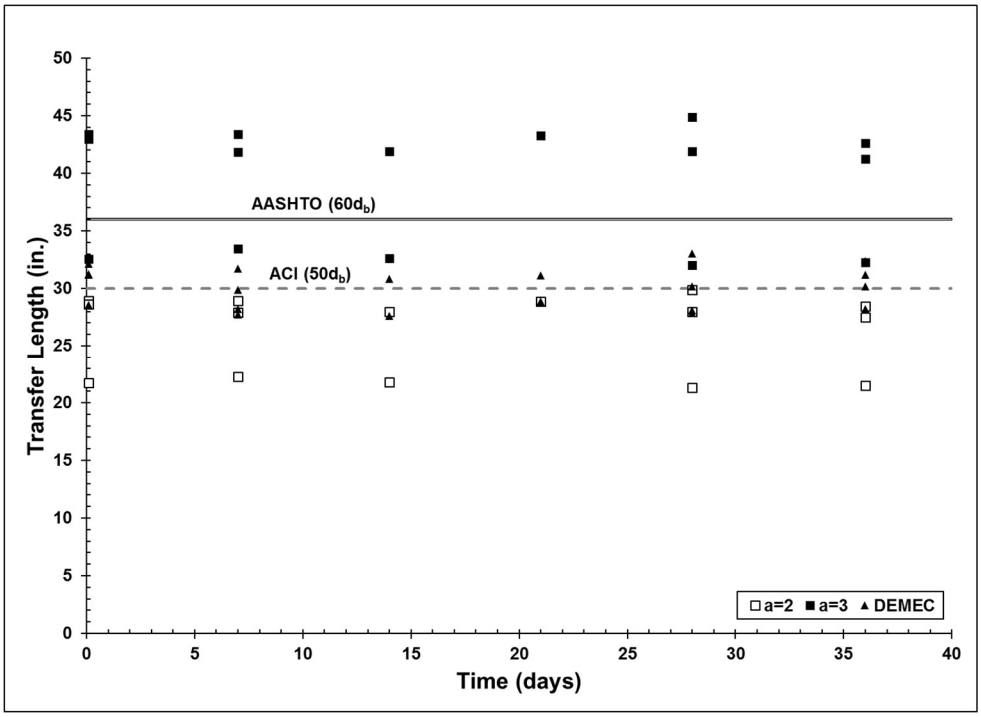

Figure 35: Transfer Lengths of RS Specimens from End Slip and DEMEC

6.4 Summary and Discussion

The average transfer lengths calculated with the DEMEC procedure are shown in Figure 36 for all of the specimens over time compared to the ACI and AASHTO estimates. All of the specimens exhibited transfer lengths lower than the AASHTO estimate while the ACI estimate fell near the top of the range of transfer lengths. Overall, the transfer lengths for each group remained rather constant over time and each group had a widespread range of values, possibly due to the different concrete compressive strength at release for each specimen. The RS specimens produced transfer lengths higher than the PC and 24RS specimens, meaning that the 2-hour release time may have had an effect on the transfer length. To better compare the three groups, Figure 37 shows the average transfer lengths for each specimen over time when normalized using the square root of the concrete compressive strength. Figure 38 shows the average transfer length at 28 days (PC) and 36 days (24RS and RS) when

normalized using the square root of the concrete compressive strength. Despite the incorporation of the differing concrete compressive strengths at prestress transfer, the specimens still had a relatively widespread range (Figure 37) and the RS specimens still exhibited longer transfer lengths than the other two beam groups (Figure 38).

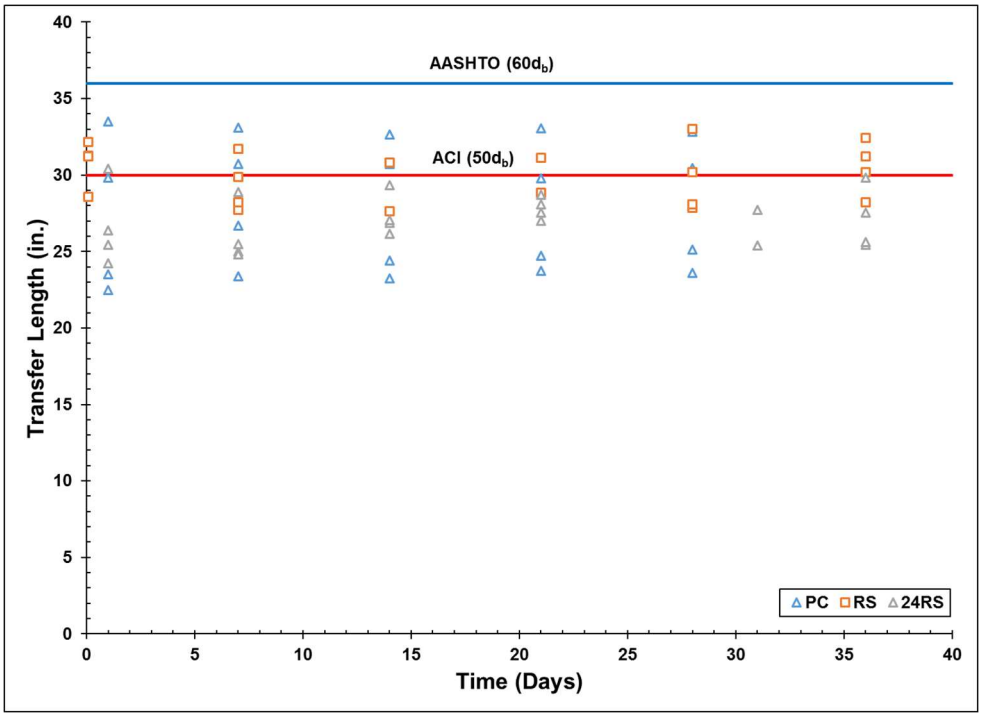

Figure 36: Average DEMEC Transfer Lengths of Specimens Over Time

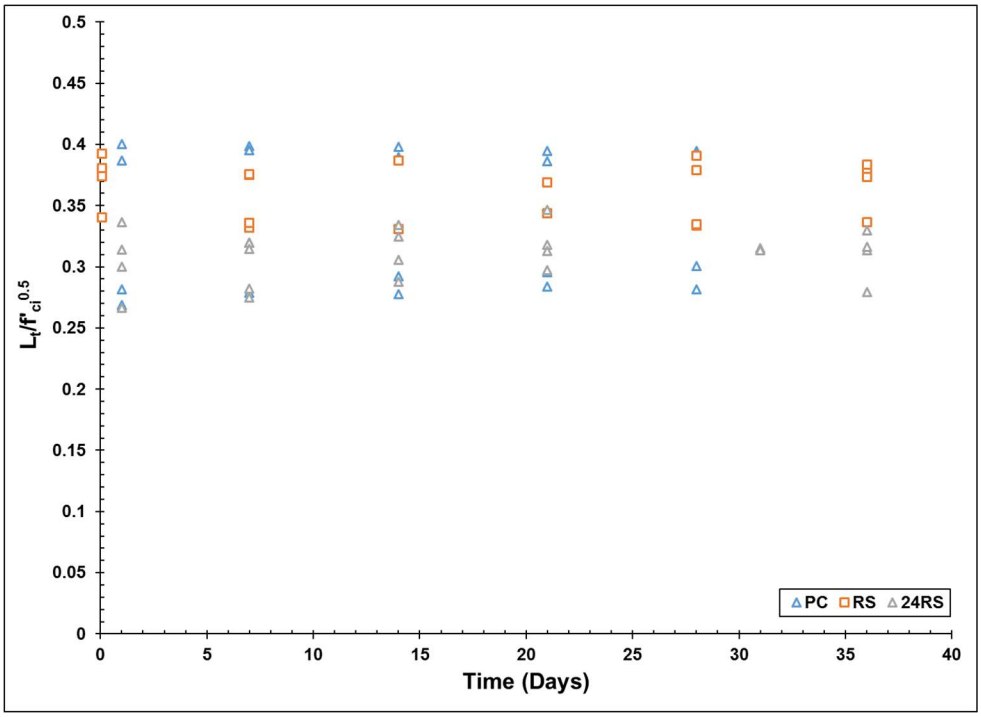

Figure 37: Average Normalized DEMEC Transfer Lengths of Specimens Over Time

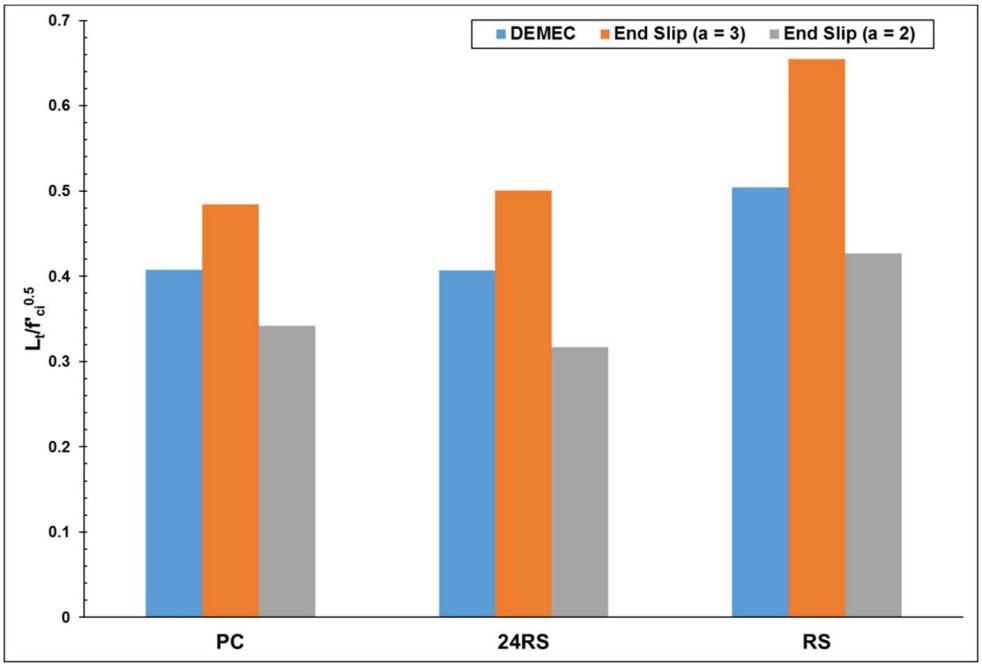

Figure 38: Average Normalized Transfer Lengths for Each Group

Figure 39 shows the raw average transfer lengths of each group at 28 days (PC) and 36 days (24RS and RS) that were calculated with the DEMEC and end slip measurements compared to the ACI and AASHTO estimates. It also includes the error

bars for average values per ASTM E2655-14. Since the transfer lengths showed little change over time, the 28 day measurements for the PC specimens and the 36 day measurements for the RS and 24RS specimens should be comparable. The transfer lengths of the PC and 24RS groups are similar, while the RS specimens produced transfer lengths longer than the other two groups.

The ACI estimate appears to be adequate for the transfer lengths calculated by the DEMEC procedure and end slip measurements with α=2, but when the transfer lengths are calculated with α=3, they are several inches longer than the estimate. Calculating transfer length with an α=3 is meant to be a more conservative estimate so it would make sense for these values to be higher. For comparison, some α values that have been determined for conventional concrete experimentally are 2.61, 2.86, and 2.44 by Dang (2016), Federation International de la Precontrainte (1982), and Marti-Vargas et al. (2007), respectively. These values from previous research are consistent with the values of 2.42, 2.48, and 2.30 calculated from the DEMEC transfer lengths for the PC, 24RS, and RS specimens, respectively, which further indicate that α=3 is a conservative estimate.

The average RS transfer length calculated with α=3 was nearly 10 in. higher than the ACI estimate. The AASHTO estimate appears adequate for the PC and 24RS groups, but was also below the average RS transfer length calculated with α=3. The troubles with the plexiglas pieces on the RS specimens could be an explanation for why the average transfer length with α=3 is much higher, however there is also an increase in the DEMEC calculated transfer length for RS when compared to 24RS and PC. Further exploration into transfer length of CSA specimens with prestress release at 2

hours may be needed to fully assess the ramifications of the early release time on transfer length.

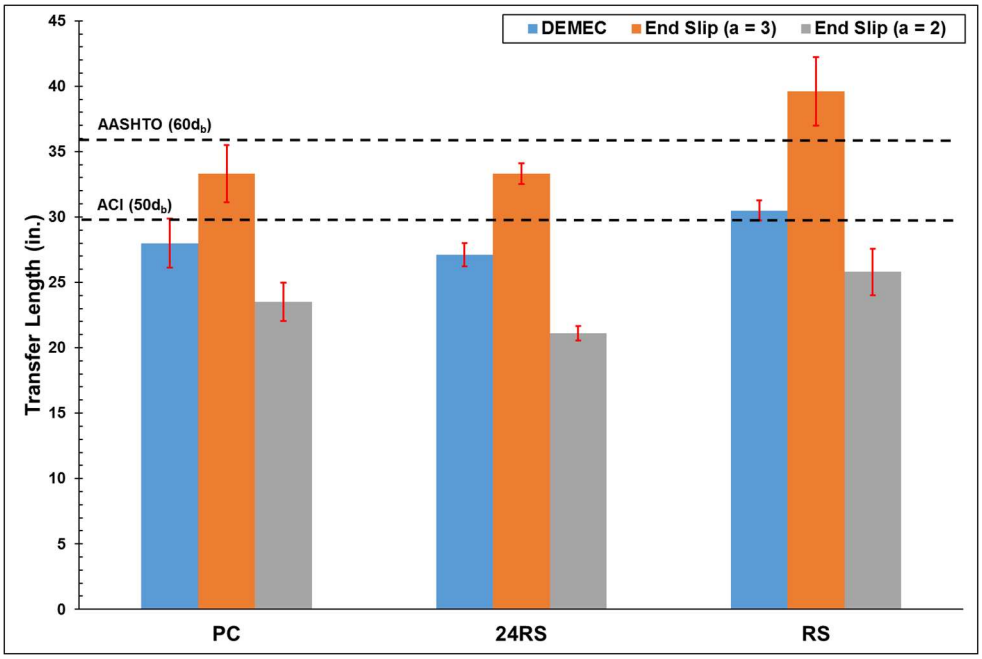

Figure 39: Raw Average Transfer Lengths of Each Group with Error Bars

Figure 40 illustrates how the specimens from this study compared to some previous research that has been done on 0.6 in. prestressing strands with other types of specialty concrete. According to this comparison, the transfer lengths in this study were significantly higher than the other studies. This may be due partly to the high concrete compressive strengths that were present in the other studies, and in the case of Larson (2007) smaller strand diameter, as mentioned in Section 2.3.

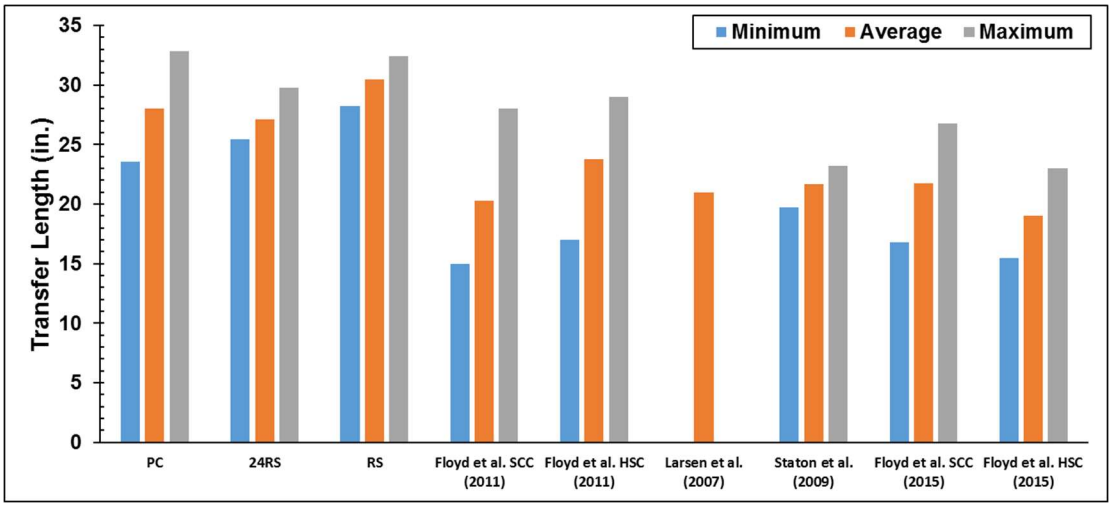

Figure 40: Comparison to Previous Research

Chapter 7: Development Length Results

7.1 Introduction

This section summarizes the results of the flexural tests that were done on each beam to evaluate the development length of each of the specimens. The specimens were loaded approximately at the code predicted development length to analyze whether the nominal flexural capacities could be reached, as well as whether or not the strands slipped into the beams. The full testing and instrumentation set-up is explained in Section 4.4. The cracking and crushing patterns for each specimen after failure is presented in Appendix E.

7.2 Portland Cement (PC) Beams

The measured load vs. deflection curves for each of the PC specimens are shown in Figure 41. It is important to note that the specimens were loaded after their ultimate load to better show the crushing and cracking and the point when loading was stopped was not always consistent. This explains some of the differences in maximum deflection among specimens.

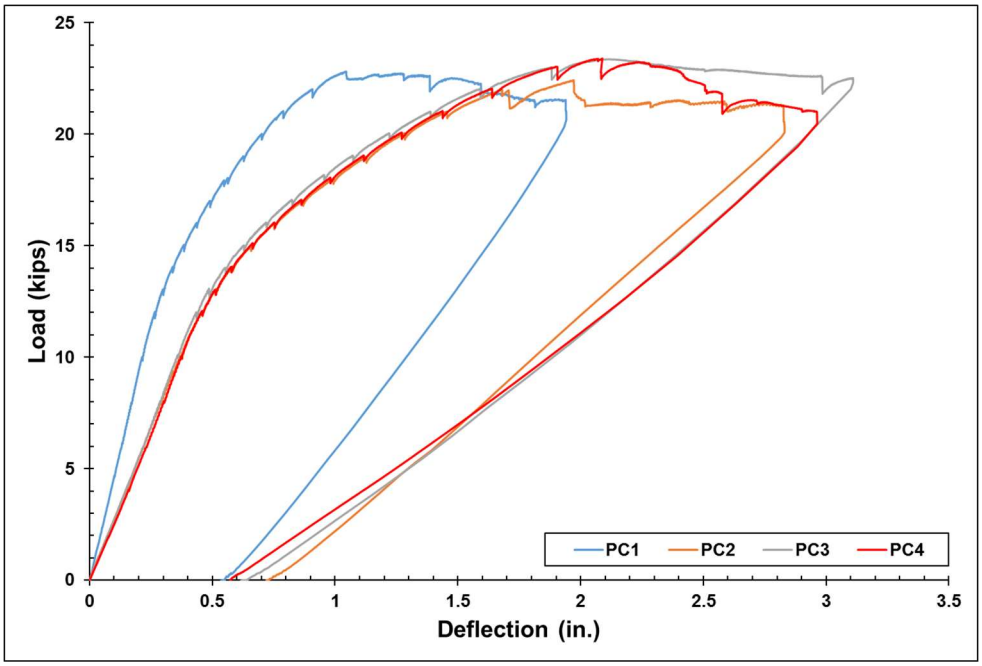

Figure 41: Load vs. Deflection Curves for PC Specimens

The performance of each of the specimens is summarized in Table 13. The cracking load was determined by finding the point where the slope changed on the load vs. deflection curve. The maximum load and maximum deflection for each specimen was simply the maximum y-value and x-value, respectively on each curve. Strand slip was measured with LVDTs as mentioned in Section 4.4. The load corresponding to the nominal flexural capacity (P_n) of each beam was determined using the strain compatibility method. Cracking loads and maximum deflections were verified manually while testing.

Table 13: Flexural Testing Results of PC Specimens

Specimen	**PC1**	**PC2**	**PC3**	**PC4**
P_{cr} (kips)	12	12	12	12
P_{max} (kips)	22.8	22.4	23.4	23.4
Δ_{max} (in.)	1.94	2.83	3.10	2.96
Max Strand Slip (SW) (in.)	0.16	0.25	None	None
Max Strand Slip (SE) (in.)	0.33	0.24	None	None
Failure Type	Flex Bond	Flex Bond	Flexural	Flexural
P_{max}/P_n	1.14	1.10	1.15	1.15

All of the PC specimens exceeded their nominal flexural capacities and had similar cracking and maximum loads. No strand slip was observed on the non-testing (north) ends of the specimens. All specimens displayed crushing at the top at the load point as well as a wide distribution of flexural and flexural-shear cracks surrounding the load point (Figure 42). PC1 and PC2 did exhibit some large cracks longitudinally at the height of the strands due to strand slip (Figure 43). PC1 and PC2 exhibited significant strand slip (plotted in Figure 44 and Figure 45, resulting in slightly more brittle failures than PC3 and PC4. This is evidenced in the load vs. deflection plots for PC1 and PC2. Since the nominal flexural capacities of PC1 and PC2 were reached prior to the strands slipping, a failure type of "Flexural Bond" was assessed to those specimens, while PC3 and PC4 failed only in flexure. One explanation for the strand slip in PC1 and PC2 could be the segregation that occurred during casting discussed in Section 5.2. This segregation could have affected the strand bond and resulted in this type of behavior.

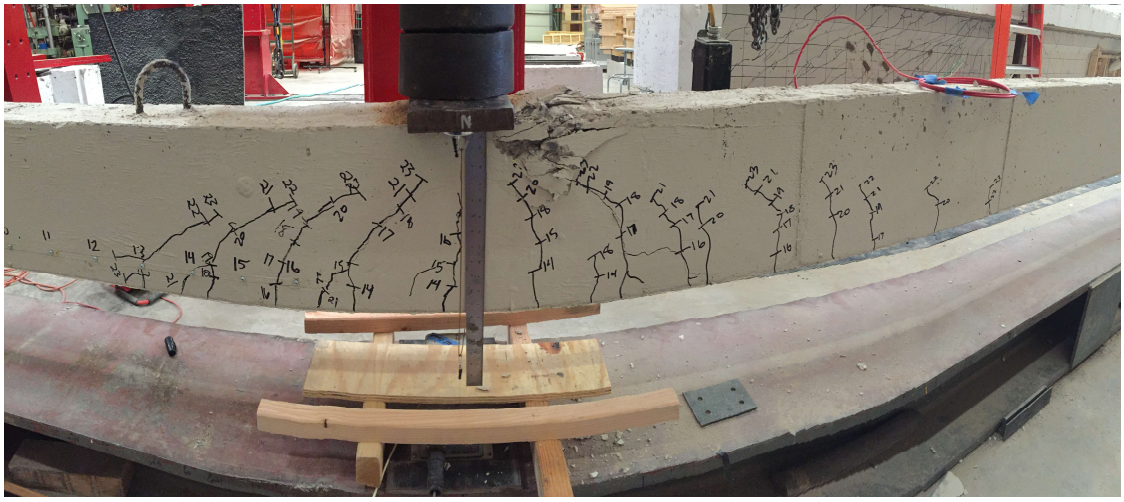

Figure 42: Typical Crushing and Crack Distribution for Flexural Failure

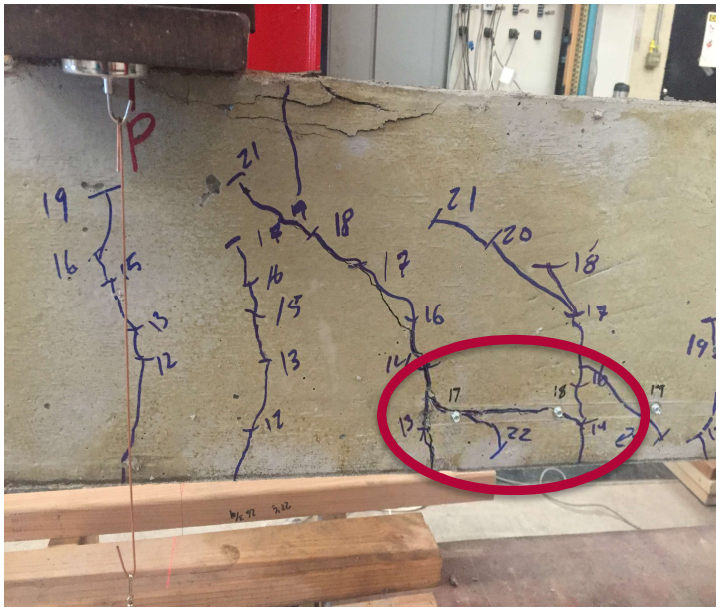

Figure 43: Longitudinal Cracks Appear when Strands Slip

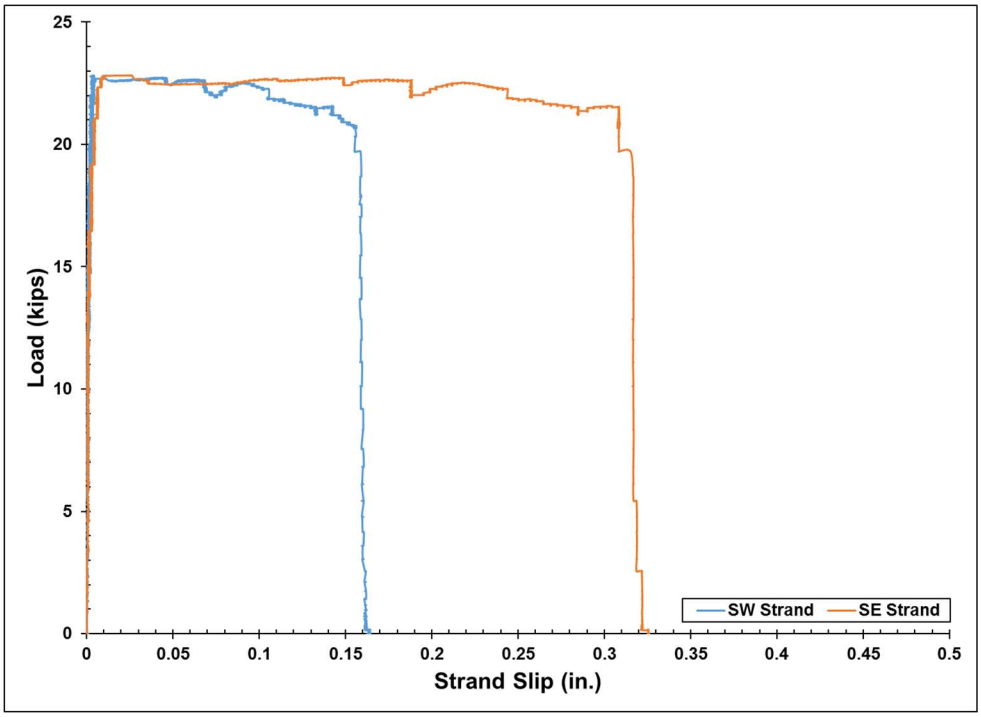

Figure 44: Load vs. Strand Slip Plot for South PC1 Strands

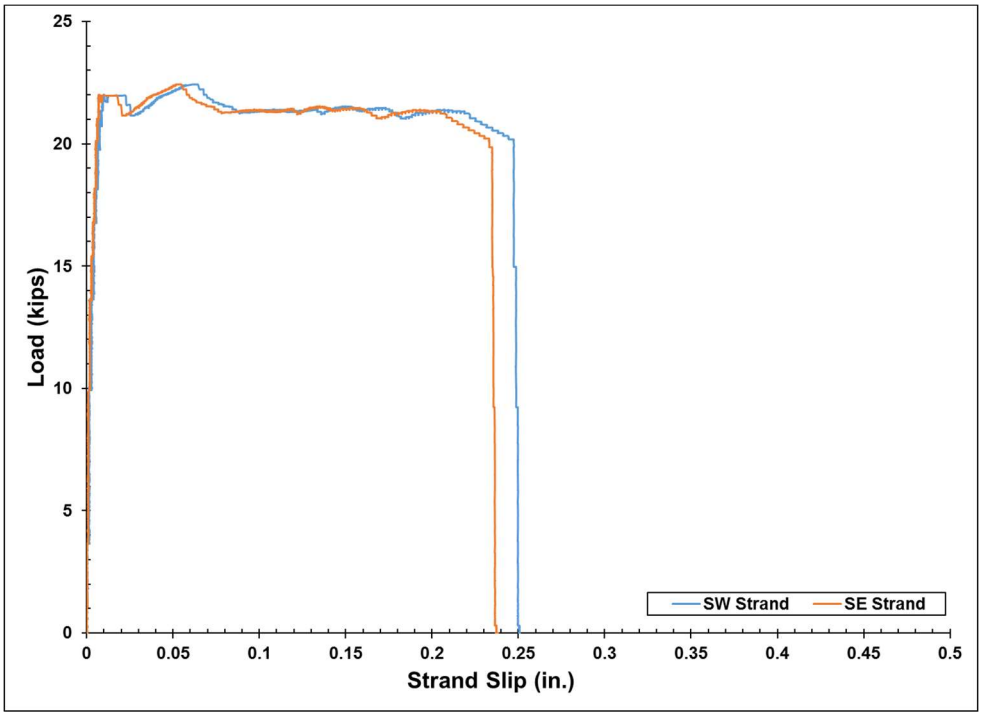

Figure 45: Load vs. Strand Slip Plot for South PC2 Strands

7.3 24-hr Release CSA (24RS) Beams

The measured load vs. deflection curves for each of the 24RS specimens are shown in Figure 46 and a summary of the results of the tests is presented in Table 14.

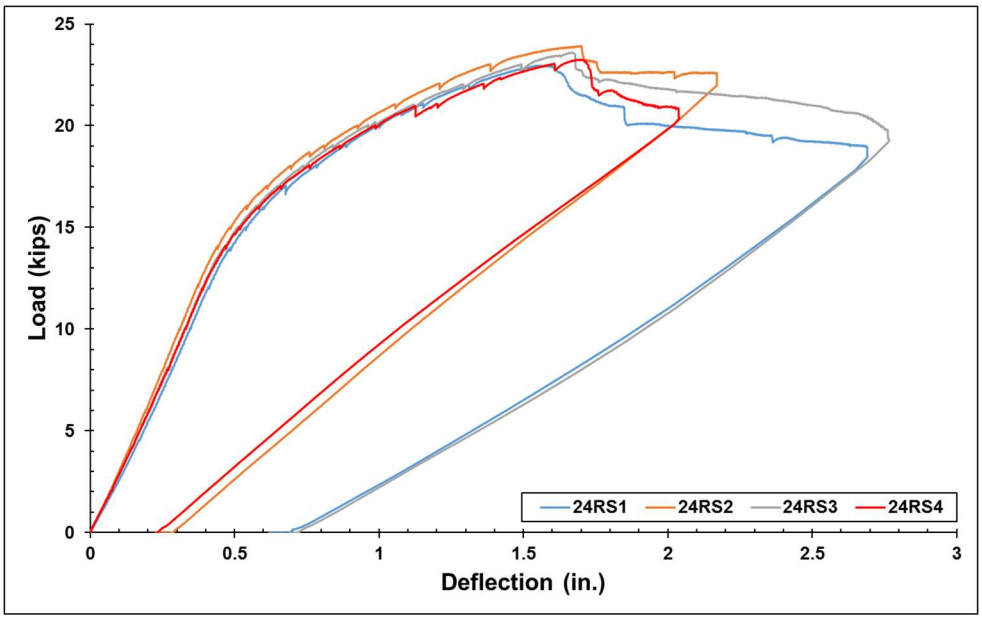

Figure 46: Load vs. Deflection Curves for 24RS Specimens

Table 14: Results of Flexural Tests for 24RS Specimens

Specimen	**24RS1**	**24RS2**	**24RS3**	**24RS4**
P_{cr} (kips)	14	14	14	14
P_{max} (kips)	23.0	23.9	23.6	23.3
Δ_{max} (in.)	2.69	2.17	2.77	2.04
Max Strand Slip (SW) (in.)	None	None	None	None
Max Strand Slip (SE) (in.)	None	None	None	None
Failure Type	Flexural	Flexural	Flexural	Flexural
P_{max}/P_n	1.10	1.15	1.14	1.14

The load vs. deflection curves present similar profiles for each of the specimens, meaning they all behaved consistently. All of the 24RS specimens exceeded their nominal flexural capacities and had similar cracking and maximum loads. None of the 24RS specimens exhibited strand slip. All specimens displayed crushing at the top at the load point as well as a wide distribution of flexural and flexural-shear cracks surrounding the load point (Figure 42).

7.4 2-hr Release CSA (RS) Beams

The measured load vs. deflection curves for each of the RS specimens are shown in Figure 47 and a summary of the results of the tests is presented in Table 15.

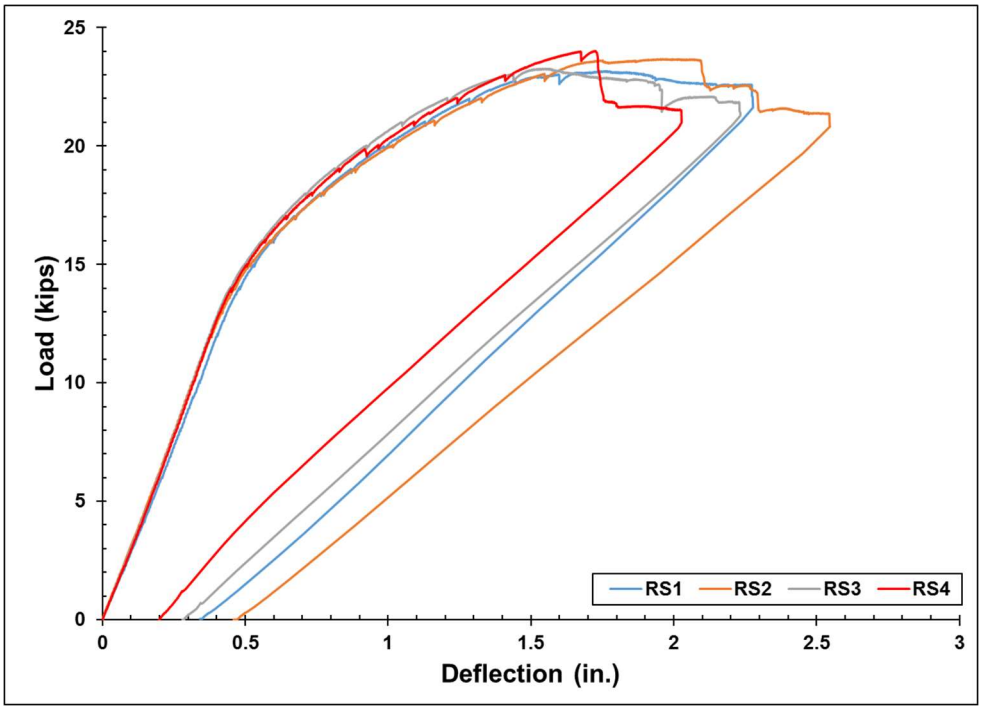

Figure 47: Load vs. Deflection Curves for RS Specimens

Table 15: Results of Flexural Tests for RS Specimens

Specimen	**RS1**	**RS2**	**RS3**	**RS4**
P_{cr} (kips)	14	14	14	14
P_{max} (kips)	23.2	23.7	23.3	24.0
Δ_{max}(in.)	2.28	2.55	2.23	2.03
Max Strand Slip (SW) (in.)	None	None	None	None
Max Strand Slip (SE) (in.)	None	None	None	None
Failure Type	Flexural	Flexural	Flexural	Flexural
P_{max}/P_n	1.14	1.16	1.15	1.18

The load vs. deflection curves present similar profiles for each of the specimens, meaning they all behaved consistently. All of the RS specimens exceeded their nominal flexural capacities and had similar cracking and maximum loads. None of the RS specimens exhibited strand slip. All specimens displayed crushing at the top at the load point as well as a wide distribution of flexural and flexural-shear cracks surrounding the load point (Figure 42).

7.5 Summary and Discussion

Although an embedment length was taken from the bottom of the range of calculated development lengths, all specimens reached their nominal flexural capacities, meaning that the embedment length was greater than the required development length. Despite the occurrence of strand slip in specimens PC1 and PC2, those specimens were also able to reach the nominal flexural capacity, and exceeded it by at least 10%, which supports the prediction being sufficient to achieve the full strength of the member. All

of the CSA specimens exhibited flexural failures and showed no issues with strand slip meaning they actually performed better in this experiment than the PC specimens. Overall, the results of the flexural tests suggest that the code predicted values for development length are reasonable for CSA specimens with 2-hour and 24-hour prestress release.

Chapter 8: Prestress Losses

In addition to studying the bond behavior of the prestressing strands in the CSA specimens, prestress losses were monitored for over 28 days in specimens 24RS3, 24RS4, RS3, and RS4 using the VWSGs described in Section 4.3.6. The prestress after release is shown in Figure 48 and Figure 49 for the 24RS and RS specimens, respectively. The prestress in specimens 24RS3, 24RS4, RS3, and RS4 decreased in total by 18.9, 19.2, 18.5, and 19.5 ksi, respectively. A steep decrease in prestress occurred over the first few days for unknown reasons, followed by a gradual decrease over the next several weeks. It is important to note that due to a measuring error, specimens 24RS3 and 24RS4 were not corrected for temperature.

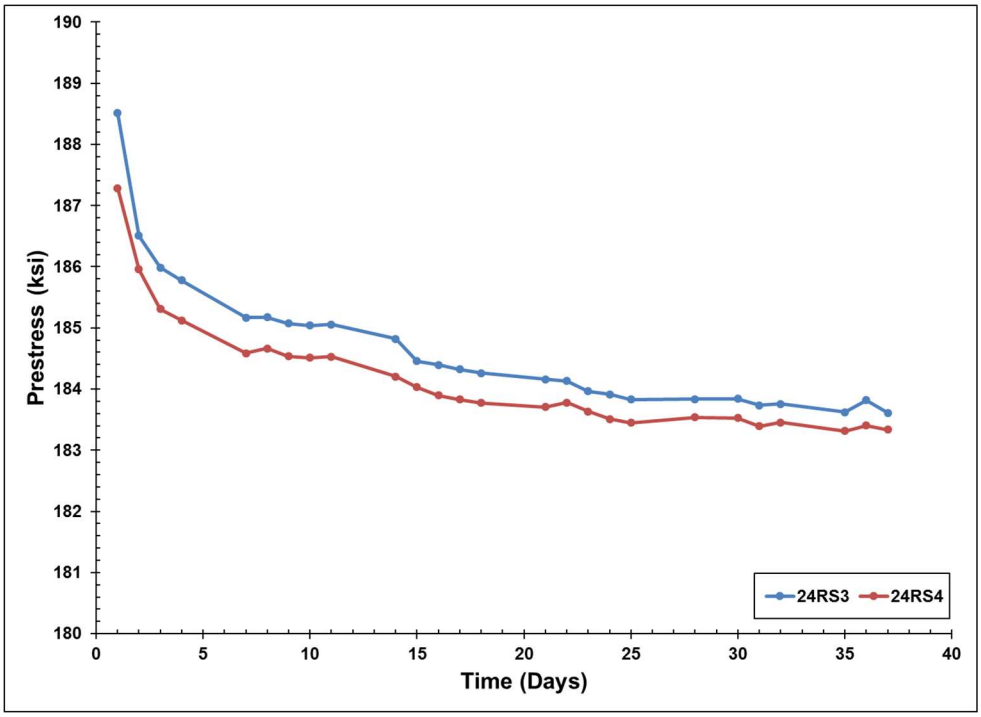

Figure 48: Prestress in Strands vs. Time for 24RS3 and 24RS4

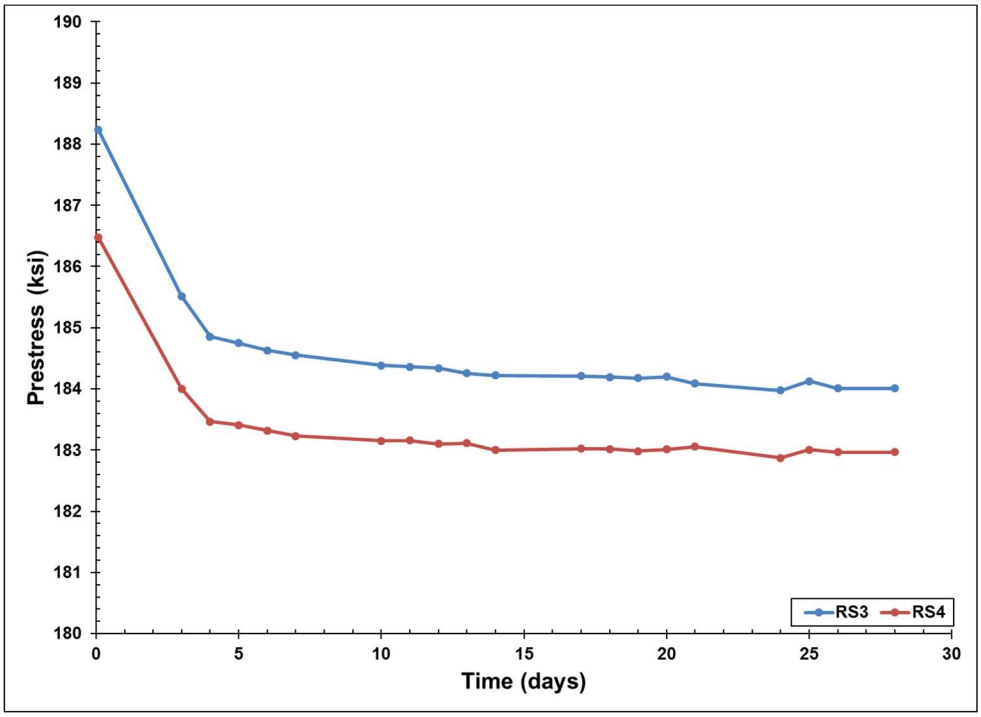

Figure 49: Prestress in Strands vs. Time for RS3 and RS4

Table 16 displays the measured prestress in the beams at 28 days compared to the predicted f_{se} values using the Zia et al. method and the AASHTO Refined Method. These predicted values are based on an initial prestress of 202.5 ksi.

Table 16: Measure Prestress Compared to Estimated Prestress after 28 Days

Specimen	**Measured Prestress at 28 days (ksi)**	**AASHTO Refined (ksi)**	**Zia et al. (ksi)**
24RS3	183.6	166.8	151.9
24RS4	183.3	166.8	150.5
RS3	184.0	166.8	150.0
RS4	183.0	166.8	150.0

The measured prestresses in the four specimens at 28 days were all within 1 ksi of each other signifying that the early prestress release in the RS specimens did not have a noteworthy, negative effect on the prestress losses in this experiment. The prestress losses predicted by the AASHTO Refined Method and Zia et al. method (Zia et al., 1979) overestimated the prestress losses by 63% in these specimens, though the AASHTO Refined Method only overestimated by nearly 50%. The Zia et al. method does not take time into account and is more conservative. The decrease in prestress loss was similar to what was observed in the research done by Floyd and Ramseyer (2016) and is mentioned in Section 2.2.

Chapter 9: Summary, Conclusions, and Recommendations

9.1 Summary

This research project focused primarily on the performance of 0.6 in. prestressing strands cast in CSA concrete. This performance was characterized chiefly by the transfer length and development length. Transfer length was calculated by taking surface strain measurements with DEMEC points and with strand end slip. Development length was assessed with flexural tests by using an embedment length

near the code predicted values for development length. The transfer lengths of the CSA specimens with prestress release at 2 hours and 24 hours were compared with the control group PC specimens as well as to the code predicted values. This section provides several conclusions and recommendations.

9.2 Conclusions

The following conclusions can be drawn for the results of the work described in this thesis and are applicable only to similar situations.

- On average, the RS group had larger transfer lengths than groups 24RS and PC, but the ACI and AASHTO estimates for transfer length appear to be adequate for all of the groups.
- Based on this experiment, the average transfer lengths calculated using the DEMEC system corresponded to an α value relating to bond stress distribution of approximately 2.48 for the 24RS specimens and 2.30 for the RS specimens.
- All of the CSA specimens in this experiment reached the nominal flexural capacity at the ACI predicted development length. This shows that code predicted values for development length are reasonable for 0.6 in. prestressing strands in precast, prestressed CSA concrete beams.
- The predictions for prestress losses by the Zia et al. method and the AASHTO Refined Method overestimate the prestress losses for 0.6 in. prestressing strands in precast, prestressed CSA concrete beams at ages of less than 36 days.
- Overall, no significant detrimental effects from using CSA concrete were observed.

9.3 Recommendations

The following are recommendations for previous research and modifications to the methods used in this study if used for future research.

- The influence of citric acid dosage on CSA cement concrete set time for various temperatures should be studied further.
- Long term prestress losses should be studied further, specifically relating to potential effects on camber predictions for CSA cement concrete.
- The variables examined in this thesis should be expanded to include effects of larger sections, other strand diameters, and different specimen shapes.
- Shorter embedment lengths should be examined to evaluate actual development length of prestressing strands in CSA cement concrete.
- Avoid use of Plexiglas for end slip measurements in CSA specimens.

References

ACI Committee 223. (1970). Expansive Cement Concretes-Present State of Knowledge. *ACI Journal*, 583-610.

ACI Committee 318. (2011). *Building Code Requirements for Structural Concrete (ACI 318-11) and Commentary (ACI 318R-11).* Farmington Hills, Michigan: American Concrete Institute .

American Association of State Highway and Transportation Officials (AASHTO). (2012). *LRFD Bridge Design Specifications. Customary U.S. Units. 6th Edition.* Washington, D.C.

ASTM International. (2012). *ASTM C1064/C1064M-12 Standard Test Method for Temperature of Freshly Mixed Hydraulic-Cement Concrete.* West Conshohocken, PA.

ASTM International. (2015). *ASTM C143/C143M-15a Standard Test Method for Slump of Hydraulic-Cement Concrete.* West Conshohocken, PA.

ASTM International. (2016). *ASTM C192/C192M-16a Standard Practice for Making and Curing Concrete Test Specimens in the Laboratory.* West Conshohocken, PA.

ASTM International. (2016). *ASTM C39/C38M-16 Standard Test Method for Compressive Strength of Cylindrical Concrete Specimens.* West Conshohocken, PA.

ASTM International. (2016). *ASTM E2655-14 Standard Guide for Reporting Uncertainty of Test Results and Use of the Term Measurement Uncertainty in ASTM Test Methods.* West Conshohocken, PA.

Balázs, G. (1993). Transfer Length of Prestressing Strand as a Function of Draw-In and Initial Prestress. *PCI Journal, 38*(2), 86-93.

Barnes, R., Burns, N., & Grove, J. (2003). Experimental Assessment of Factors Affecting Transfer Length. *ACI Structural Journal, 100*(6), 740-748.

Bescher, E., Stremfel, J., & Ramseyer, C. (Oct. 2012.). The Role of Calcium Sulfoaluminate in Concrete Sustainability. *Twelfth International Conference on Recent Advances in Concrete Technology and Sustainability Issues* . Prague, Czech Republic.

Bodapati, N. N., Peterman, R. J., Beck, B. T., Wu, C.-H. J., & Riding, K. A. (2016). Comparison of Initial and Long-Term Transfer Lengths Determined From Internal and External Concrete Strain Measurements. *PCI/NBC.*

Buckner, C. (1995). A Review of Strand Development Length of Pretensioned Concrete Members. *PCI Journal, 40*(2), 84-105.

Chen, I., Hargis, C., & Juenger, M. (2012). Understanding Expansion in Calcium Sulfoaluminate-Belite Cements. *Cement and Concrete Research, 42*, 51-60.

Cousins, T., Johnston, D., & Zia, P. (1990). Transfer Length of Epoxy-Coated Prestressing Strand. *ACI Materials Journals, 87*(3), 193-203.

Damtoft, J., Lukasik, J., Herfort, D., Sorrentino, D., & Gartner, E. (2008). Sustainable development and climate change initiatives. *Cement and Concrete Research 38*, 115-127.

Dang, C., Floyd, R., Prinz, G., & Hale, W. (2016). Determination of Bond Stress Distribution Coefficient by Maximum Likelihood Method. *ASCE Journal of Structural Engineering, 142*(5).

Federation International de la Precontrainte (FIP). (1982). *Test for the Determination of Tendon Transmission Length Under Static Conditions.* Wexham Springs, U.K.: FIP.

Floyd, R. W., & Ramseyer, C. (2016). Behavior of Precast, Prestressed Calcium Sulfoaluminate Cement Concrete Beams (In Review). *PCI Convention and National Bridge Conference.*

Floyd, R. W., Hale, W. M., & Howland, M. B. (2015). Measured Transfer Length of 0.6 in. Prestressing Strands Cast in Lightweight Self-Consolidating Concrete . *PCI Journal, 60*(3), 84-98.

Floyd, R. W., Ruiz, E. D., Do, N. H., Staton, B. W., & Hale, W. M. (2011). Development Lengths of High-Strength Self-Consolidating Concrete Beams. *PCI Journal, 56*(1), 36-53.

Floyd, R., & Sadhasivam, K. (2013). Calcium sulfoaluminate cement concrete for precast, prestressed bridge girders. *Proceedings of the PCI convention and National Bridge Conference*, *Paper No. 93.* Grapvine, TX.

Girgis, A. a. (2005). Bond Strength and Transfer Length of Pretensioned Bridge Girders Cast with Self-Consolidating Concrete. *PCI Journal, 50*(6), 72-87.

Hanson, N. a. (1959, January). Flexural Bond Tests of Pretensioned Prestressed Beams. *Journal of the American Concrete Institute, Proceedings, 55*(7), 783-802.

Hegger, J., Bulte, S., & Kommer, B. (2007). Structural Behavior of Prestressed Beams Made with Self-Consolidating Concrete. *PCI Journal, 52*(4), 34-42.

Hicks, J. K., Caldarone, M. A., & Bescher, E. (2015). Opportunities from Alternative Cementitious Materials. *Concrete International, 37*(4), 47-51.

Janney, J. (1954, May). Nature of Bond in Pretensioned Prestressed Concrete. *Journal of American Concrete Institute, Proceedings, 50*(9), 717-736.

Juenger, M., Winnefeld, J., & Ideker, J. (2011). Advances in Alternative Cementitious Binders. *Cement and Concrete Research, 41*, 1232-1243.

Kaar, P., LaFraugh, R., & Mass, M. (1963). Influence of Concrete Strength on Strand Transfer Length. *PCI Journal, 8*(5), 47-67.

Lane, S. (n.d.). *A New Development Length Equation for Pretensioned Strands in Bridge Beams and Piles.* Federal Highway Administration (FHWA), McLean, VA.

Larson, K. H., Peterman, R. J., & Esmaeily, A. (2007). Bond Characteristics of Self-consolidating Concrete for Prestressed Bridge Girders. *PCI Journal, 52*(4), 44-57.

Logan, D. R. (1997). Acceptance Criteria for Bond Quality of Strand for Pretensioned Prestressed Concrete Applications. *PCI Journal, 42*(2), 52-90.

Marti-Vargas, J. R., Arbelaez, C. A., Serna-Ros, P., & Castro-Bugallo, C. (2007). Reliability of Transfer Length Estimation from Strand End Slip. *ACI Structural Journal, 104*(4), 487-494.

Mayhorn, D. (2016). *Investigation of the Effects of End Region Deterioration in Precast, Prestressed Concrete Bridge Girders.* University of Oklahoma, Norman, OK.

Meyer, K., & Kahn, L. (2004). *Transfer and Development Length of 0.6 inch Strand in High Strength Lightweight Concrete.* High-Performance Structural Lightweight Concrete (SP-218). Farmington Hills, Michigan: American Concrete Institute.

Mitchell, D., Cook, W., Khan, A., & Tham, T. (1993). Influence of High Strength Concrete on Transfer and Development Length of Pretensioning Strand. *PCI Journal, 38*(3), 52-66.

Morcous, G., Asaad, S., & Hatami, A. (2013). *Implementation of 0.7 in. Diameter Strands in Prestressed Concrete Girders.* University of Nebraska-Lincoln, Lincoln, NE.

Nilson, A. (1987). *Design of Prestressed Concrete* (2nd ed.). New York: John Wiley & Sons.

Peterman, R. J., Ramirez, J. A., & Olek, J. (2000). Design of Semi-Lightweight Bridge Girders: Development Length Considerations. *Transportation Research Record, 1696*, 41-47.

Quillin, K. (2001). Performance of Belite-Sulfoaluminate Cements. *Cement and Concrete Research, 31*, 1341-1349.

Ramirez, J., & Russell, B. (2008). *Transfer, Development and Splice Length for Strand/Reinforcement in High-Strength Concrete.* Washington, D.C.: National Cooperative Highway Research Program, Transportation Research Board.

Ramirez-Garcia, A. T., Floyd, R. W., Marti-Vargas, J. R., & Hale, W. M. (2016). Effect of Concrete Compressive Strength on Transfer Length. *Structures, 5*, 131-140. doi:10.1016/j.istruc.2015.10.006

Ramirez-Garcia, A. T., Floyd, R. W., Marti-Vargas, J. R., & Hale, W. M. (2016). Influence of Concrete Strength on Development Length of Prestressed Concrete Members. *Journal of Building Engineering, 6*, 173-183. doi:10.1016/j.jobe.2016.03.005

Rose, D. R., & Russell, B. W. (1997). Investigation of Standardized Tests to Measure the Bond Performance of Prestressing Strand. *PCI Journal, 42*(4), 56-80.

Russell, B., & Burns, N. (1996). Measured Transfer Lengths of 0.5 and 0.6 in. Strands in Pretensioned Concrete. *PCI Journal*, 44-65.

Sadhasivam, K. (2014). *Top Strand Effect of Prestressed Concrete Members Using Ligthtweight Self-Consolidating Concrete.* Norman, OK.

Sharp, J., Lawrence, C., & Yang, R. (1999, January). Calcium Sulfoaluminate Cements--Low-Energy Cements, Special Cements of What? *Advances in Cement Research, 11*(1), 3-13.

Staton, B. N. (2009). Transfer Lengths of Prestressed Beams Cast with Self-Consolidation Concrete. *PCI Journal, 54*(2), 64-83.

Thatcher, D. B., Heffington, J. A., Kolozs, R. T., Sylva III, G. S., Breen, J. E., & Burns, N. H. (2002). *Structural Lightweight Concrete Prestressed Girders and Panels.* The University of Texas at Austin, Center for Transportation Research . Austin, TX: Texas Department of Transportation.

Ward, D. B., Floyd, R. W., & Hale, W. M. (2009). Bond of 0.5 in. Diameter Strands Cast in Lightweight SCC. *Proceedings PCI-FHWA National Bridge Conference.* San Antonio, TX.

Wendling, A. (2014). *Time Dependent Behavior or Self-Consolidating Lightweight Prestressed Members with Top-Strands.* Norman, OK.

Winnefeld, F., & Lothenbach, B. (2010). Hydration of Calcium Sulfoaluminate Cements - Experimental Findings and Thermodynamic Modelling. *Cement and Concrete Research, 40*, 1239-1247.

Zia, P., & Mostafa, T. (1977). Development Length of Prestressing Strands. *PCI Journal*, 42-59.

Zia, P., Preston, H. K., Scott, N. L., & Workman, E. B. (1979). Estimating Prestress Losses. *Concrete International, 1*(6), 32-38.

Appendix A: Beam Analysis

Nominal flexural capacities, P_n, for each specimen were calculated using the strain compatibility method using the measured concrete compressive strengths and a point load located 71 in. from a support. All of these capacities can be found in Table 17. The development lengths for each specimen were calculated using the ACI 318 equation

$$L_d = \left(\frac{f_{se}}{3}\right) d_b + (f_{ps} - f_{se}) d_b$$

where f_{se} is the effective prestress in the strand after all losses are accounted for (ksi), d_b is the nominal diameter of the prestressing strand (in.), and f_{ps} is the stress in the steel at nominal flexural strength (ksi). For the PC specimens, the f_{se} values were determined using the AASHTO Refined Method for estimating prestress losses. For the 24RS and RS specimens, the f_{se} values measured with the VWSGs were used to calculate the approximate development length. The calculated development lengths, L_d, for each specimen can be found in Table 17.

Table 17: Calculated Development Lengths and Nominal Flexural Capacities

Specimen	**L_d (in.)**	**P_n (in.)**
PC1	78.1	20.0
PC2	79.2	20.3
PC3	79.0	20.3
PC4	79.3	20.4
24RS1	73.6	20.9
24RS2	73.1	20.8
24RS3	72.9	20.7
24RS4	72.1	20.4
RS1	71.3	20.3
RS2	71.6	20.4
RS3	71.3	20.3
RS4	71.3	20.3

Appendix B: Trial Batches

Overall, 24 trial batches were done to refine batching techniques with CSA and to determine an adequate mix design as mentioned in Section 4.2. Table 18 summarizes the trial batches that were done over the course of 4 months to refine the CSA mix design.

Table 18: Summary of CSA Trial Batches

Batch	Volume (ft^3)	w/c	Slump (in.)	HRWR (fl oz./ cwt)	Citric Acid (lb/lb cement)	f'_c @ 2 hours (psi)
TB1	0.5	0.44	--	0	0	4720
TB2	1.0	0.60	5.0	0	0	2660
TB3	1.0	0.50	2.0	0	0	4005
TB4	4.0	0.55	9.5	0	0.0025	3150
TB5	4.0	0.50	8.3	0	0.0025	3050
TB6	4.0	0.50	9.5	0	0.0025	3000
TB7	2.0	0.46	7.5	0	0.0025	3150
TB8	2.0	0.50	8.5	0	0.0025	2110
TB9	2.0	0.50	8.8	0	0.0020	2800
TB10	2.0	0.50	8.5	0	0.0015	3400
TB11	2.0	0.50	8.25	0	0.0010	3200
TB12	2.0	0.50	3.5	0	0	3780
TB13	2.0	0.50	7.0	0	0.0025	3715
TB14	2.0	0.50	7.8	0	0.0020	3500
TB15	2.0	0.50	8.0	0	0.0015	3600
TB16	2.0	0.50	6.0	0	0.0010	4510
TB17	2.0	0.50	1.3	0	0	4640
TB18	2.0	0.50	8.0	0	0.0010	3688
TB19	2.0	0.50	8.0	0	0.0010	3735
TB20	2.0	0.50	8.8	1.0	0.0010	3635
TB21	2.0	0.50	9.9	5.0	0.0010	3735
TB22	2.0	0.50	11	7.5	0.0010	3657
TB23	2.0	0.50	11	7.5	0.0010	3657
TB24	19.0	0.50	8.75	5.0	0.0010	4290

Appendix C: Concrete Compressive Strengths

The strength gain for the companion compression cylinders for all of the specimens are shown in Figures 50-55. Trend lines are displayed for average strength gain for each specimen.

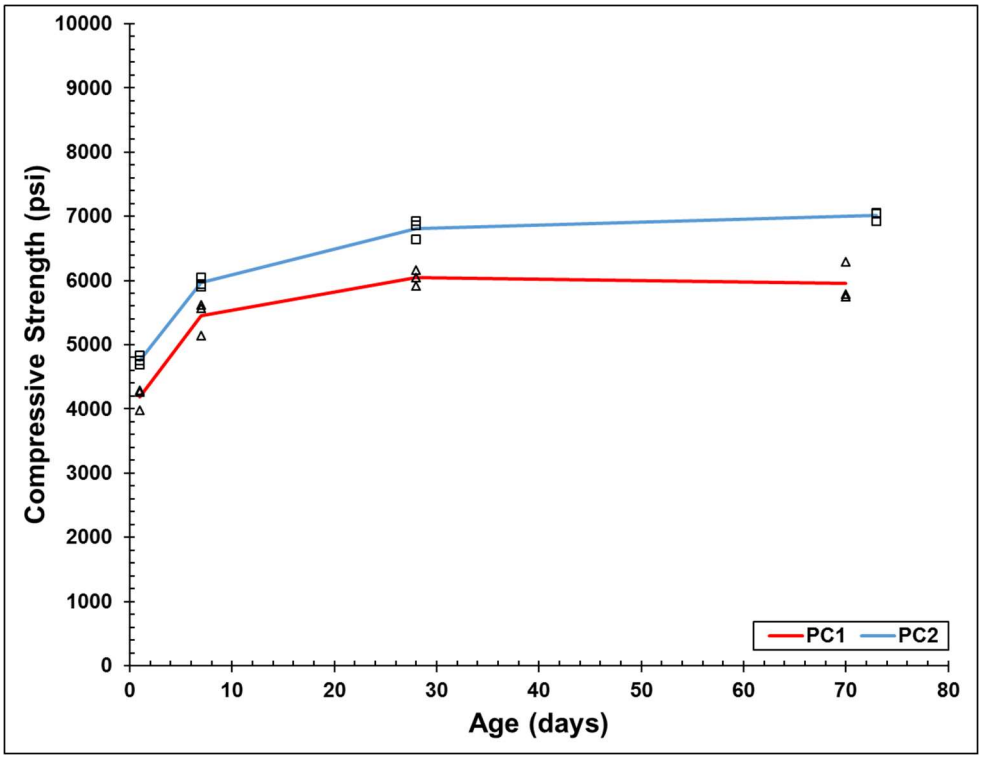

Figure 50: Strength Gain vs. Concrete Age for PC1 and PC2

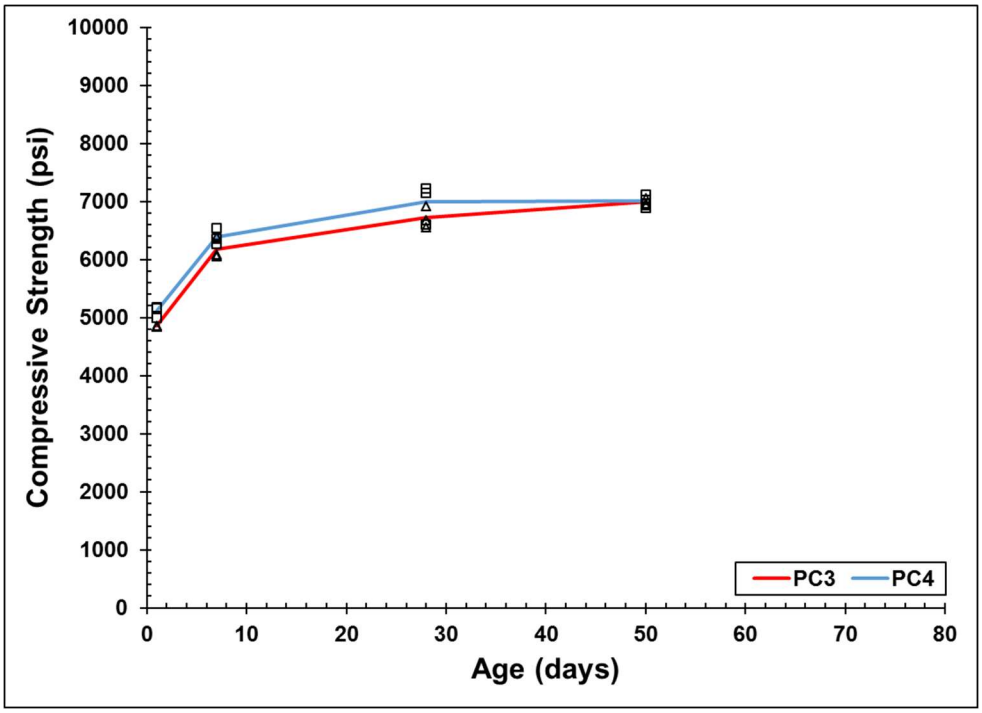

Figure 51: Strength Gain vs. Concrete Age for PC3 and PC4

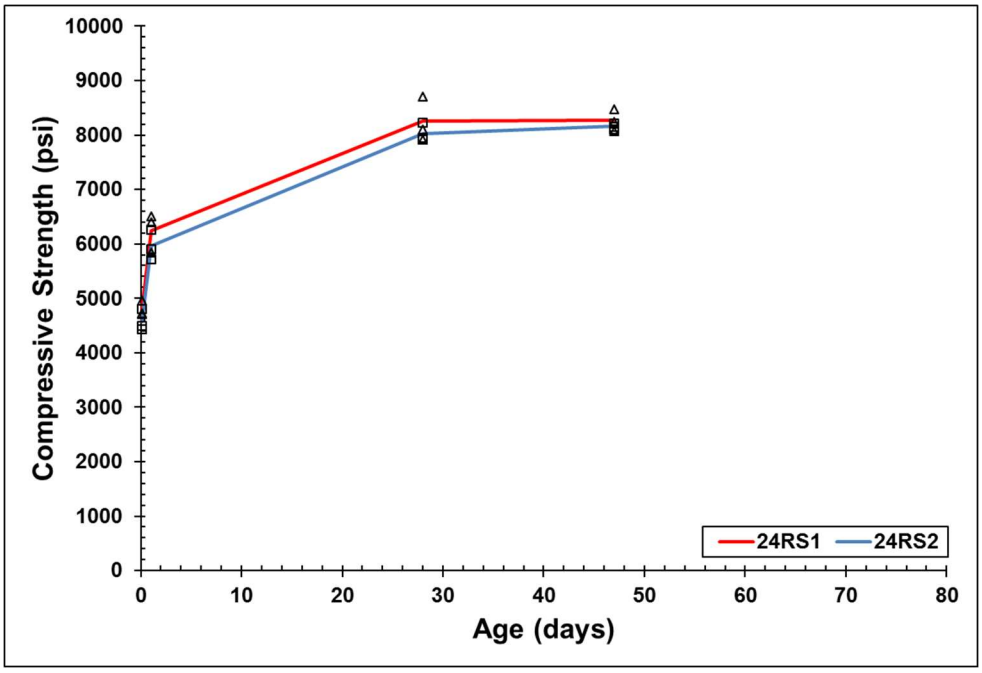

Figure 52: Strength Gain vs. Concrete Age for 24RS1 and 24RS2

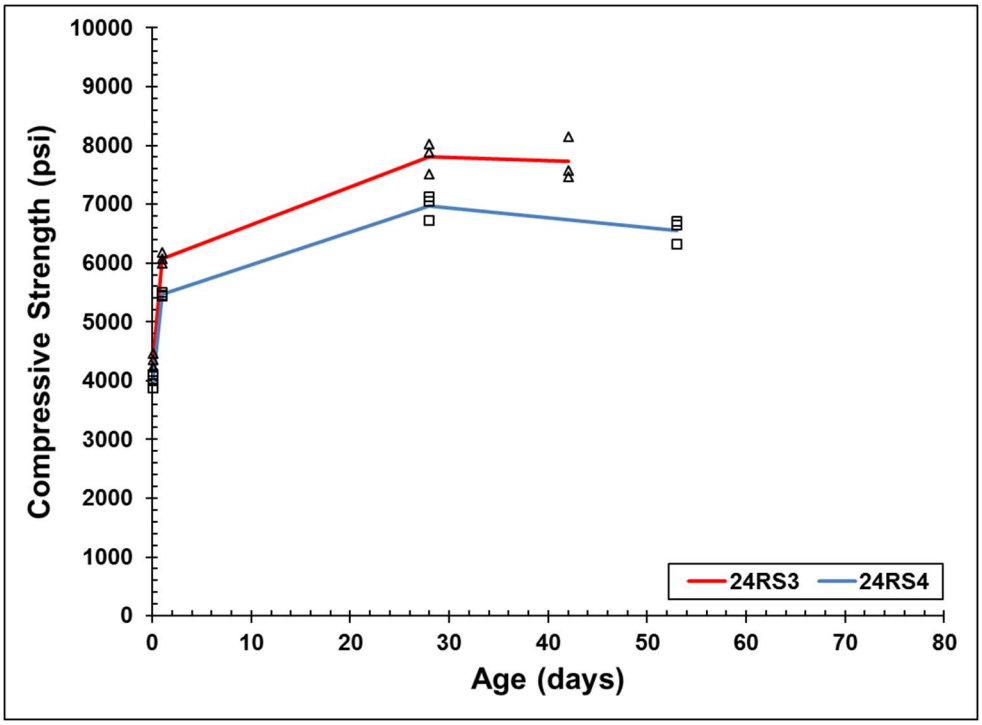

Figure 53: Strength Gain vs. Concrete Age for 24RS3 and 24RS4

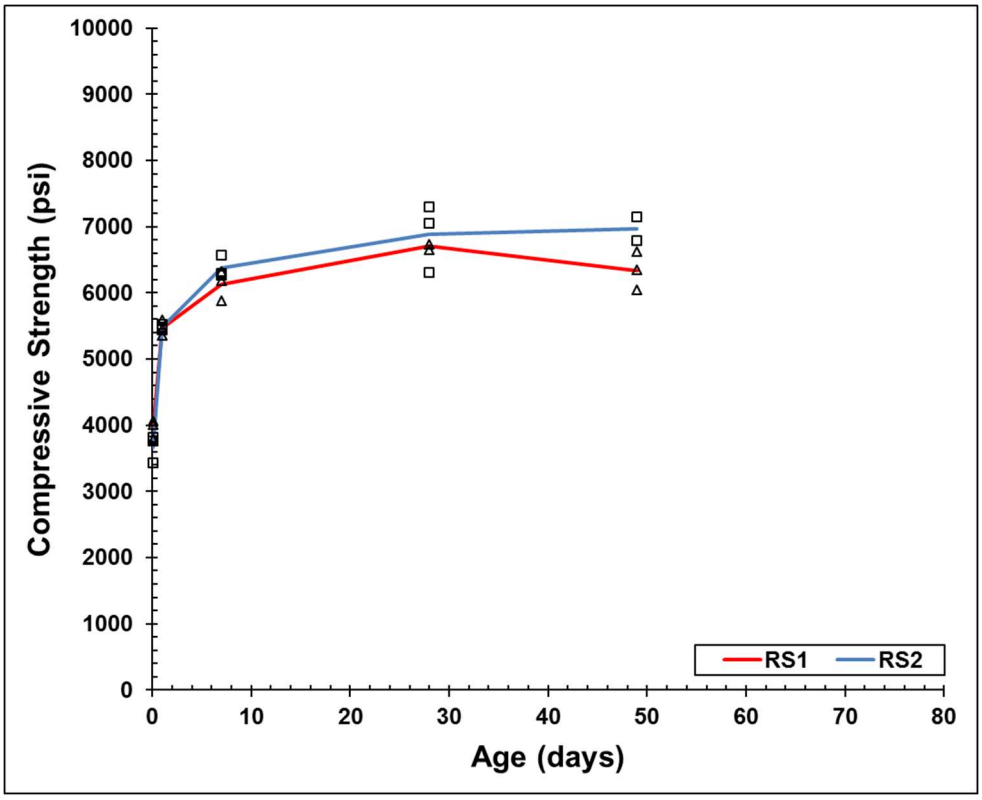

Figure 54: Strength Gain vs. Concrete Age for RS1 and RS2

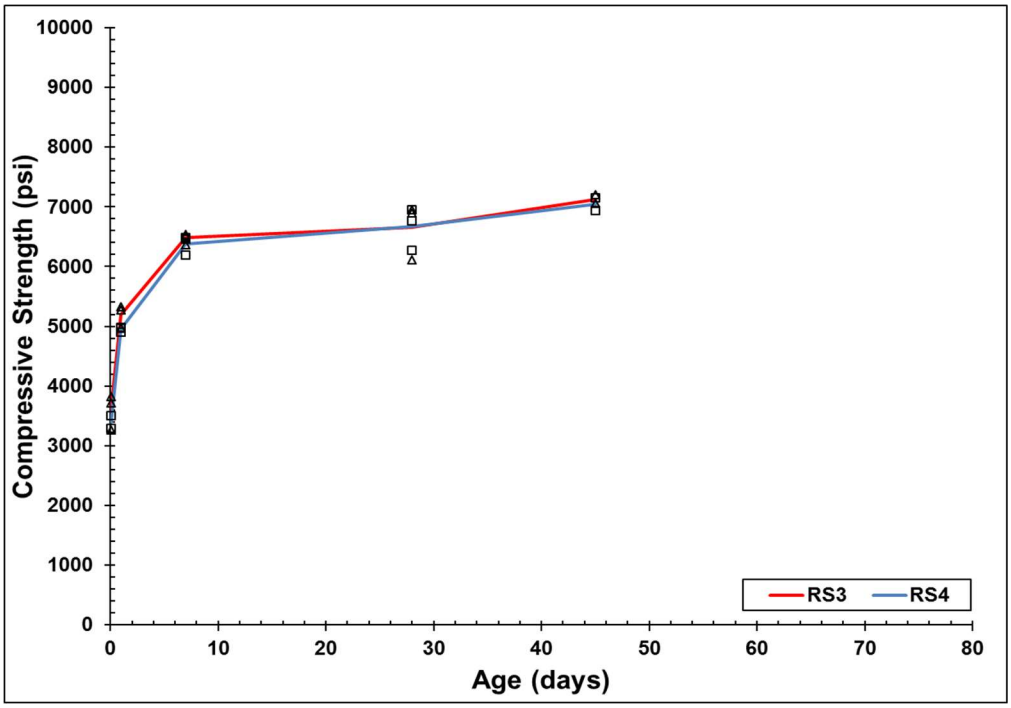

Figure 55: Strength Gain vs. Concrete Age for RS3 and RS4

Appendix D: DEMEC Strain Profiles

This Appendix presents the strain profiles for all 12 specimens over the time that they were measured. The curves on the left correspond to the south ends of the beams and the curves on the right correspond to the north ends of the beams.

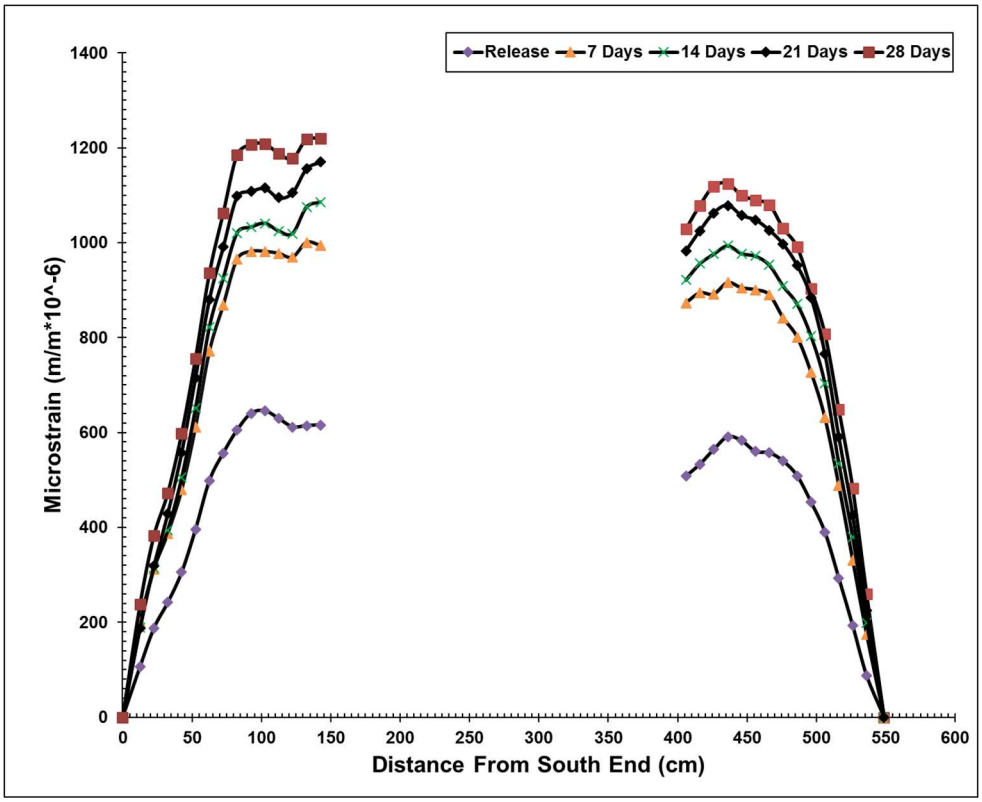

Figure 56: PC1 DEMEC Strain Profiles

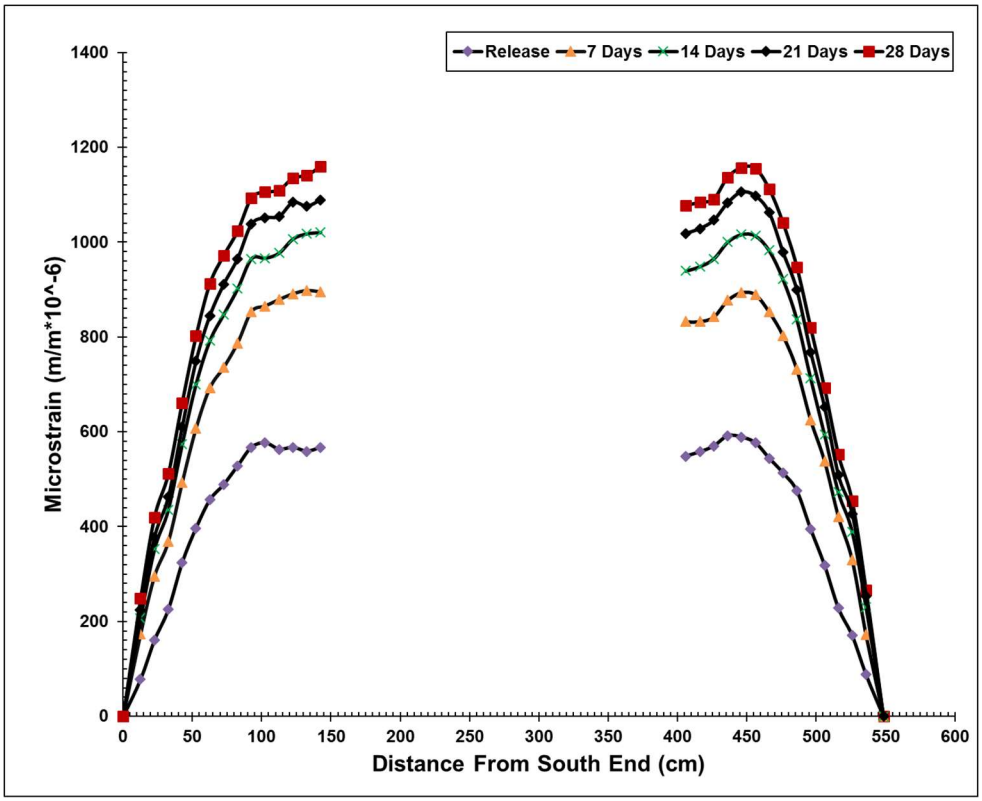

Figure 57: PC2 DEMEC Strain Profiles

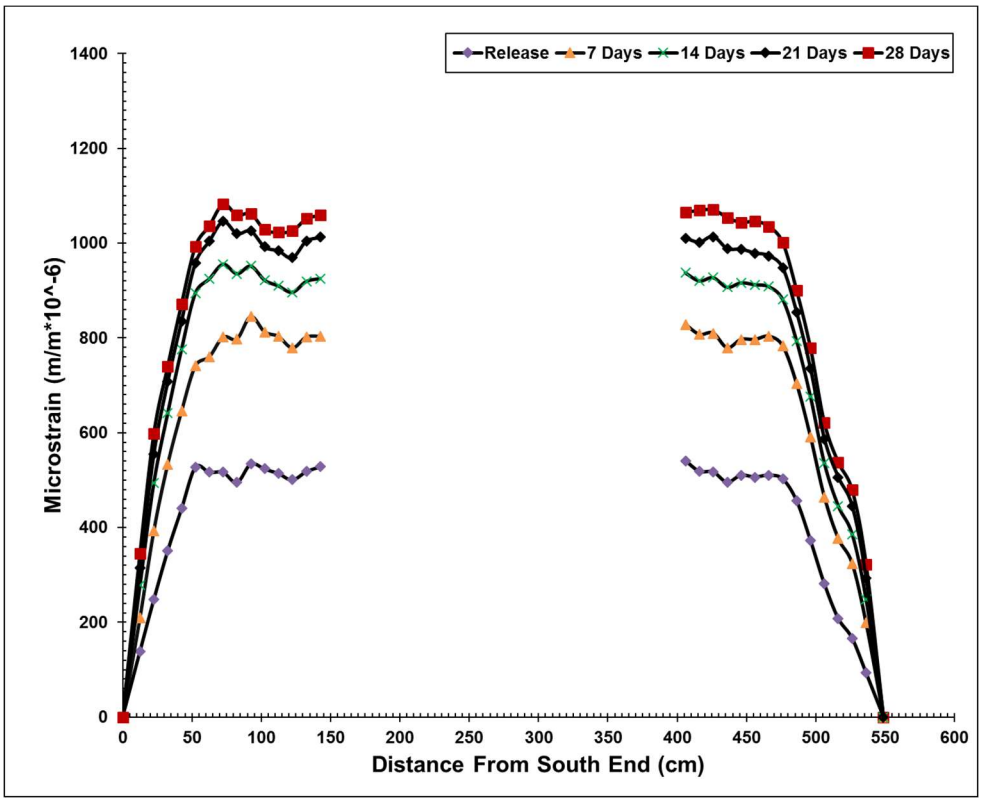

Figure 58: PC3 DEMEC Strain Profiles

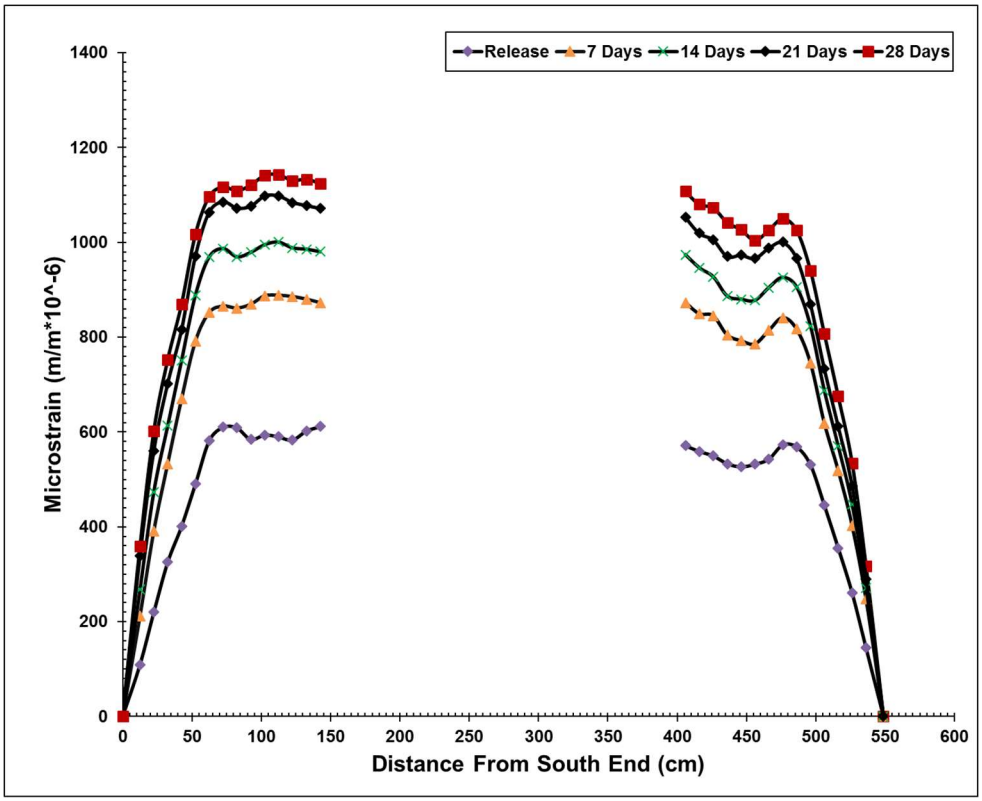

Figure 59: PC4 DEMEC Strain Profiles

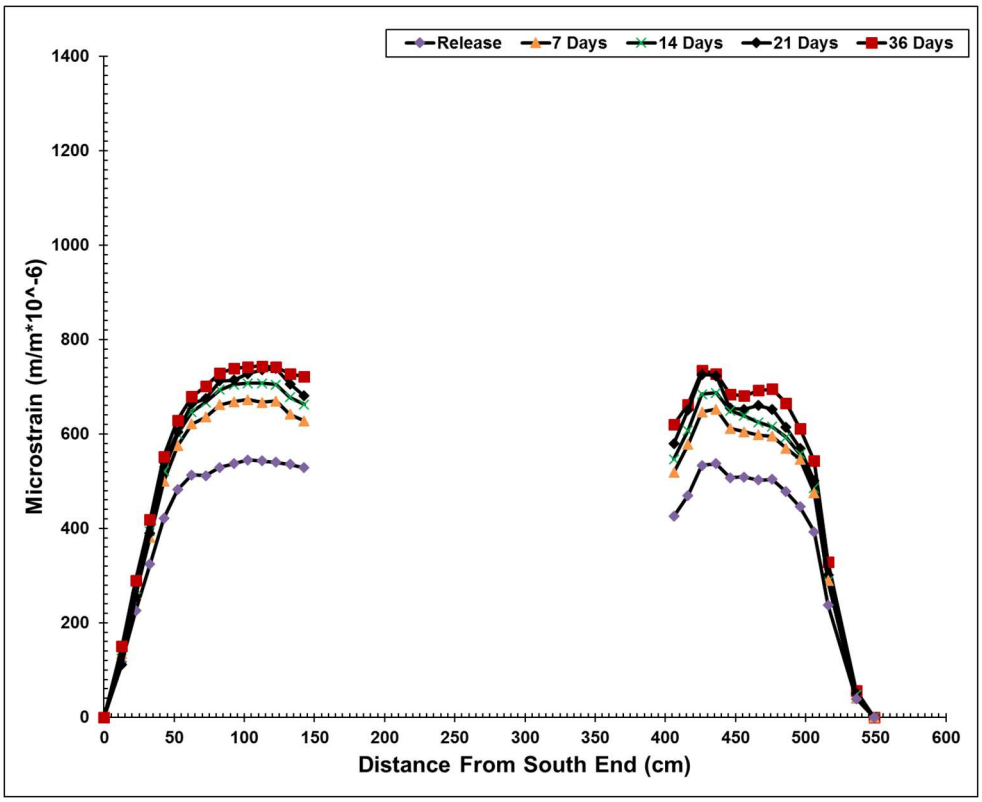

Figure 60: 24RS1 Strain Profiles

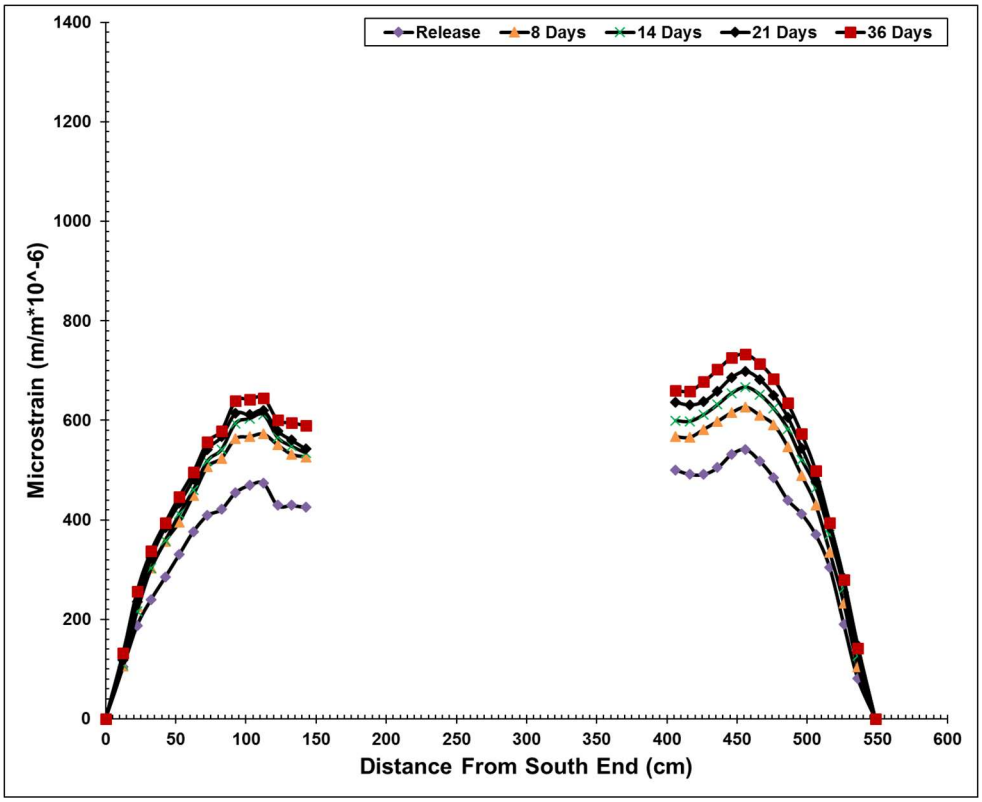

Figure 61: 24RS2 DEMEC Strain Profiles

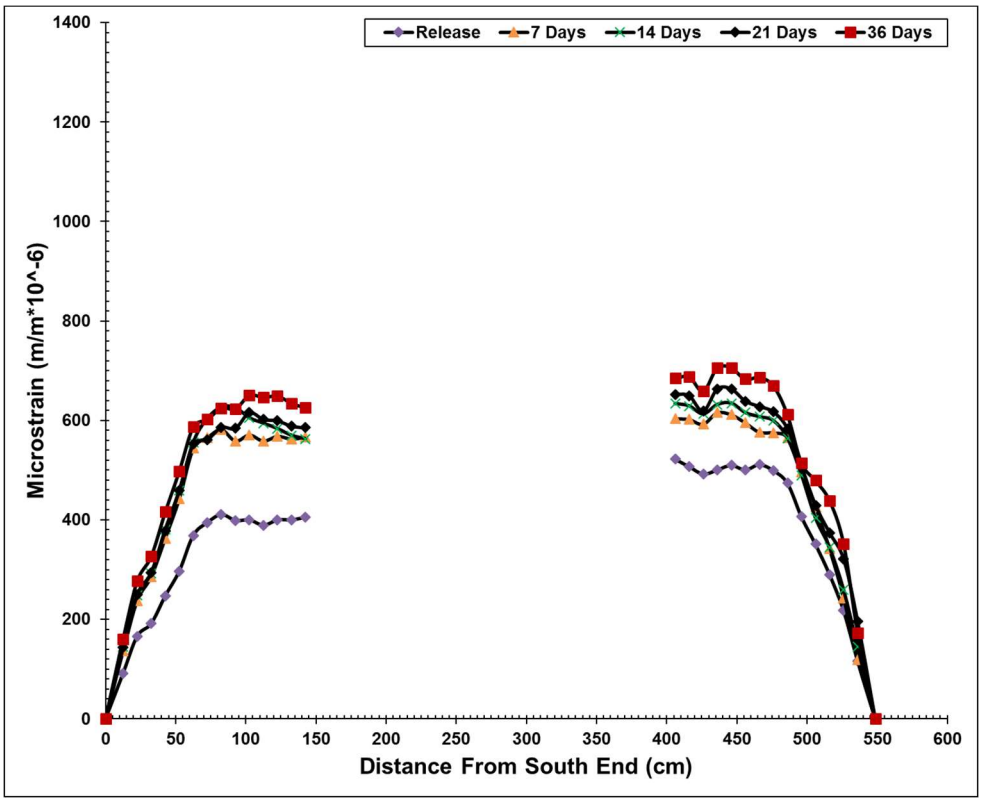

Figure 62: 24RS3 DEMEC Strain Profiles

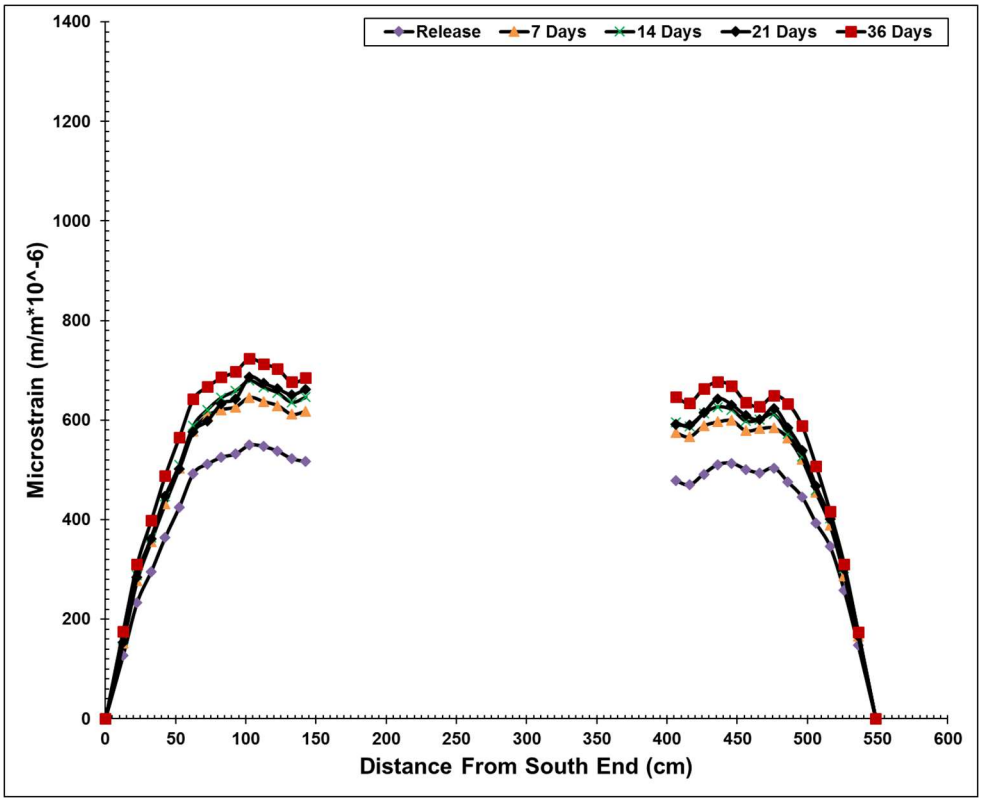

Figure 63: 24RS4 DEMEC Strain Profiles

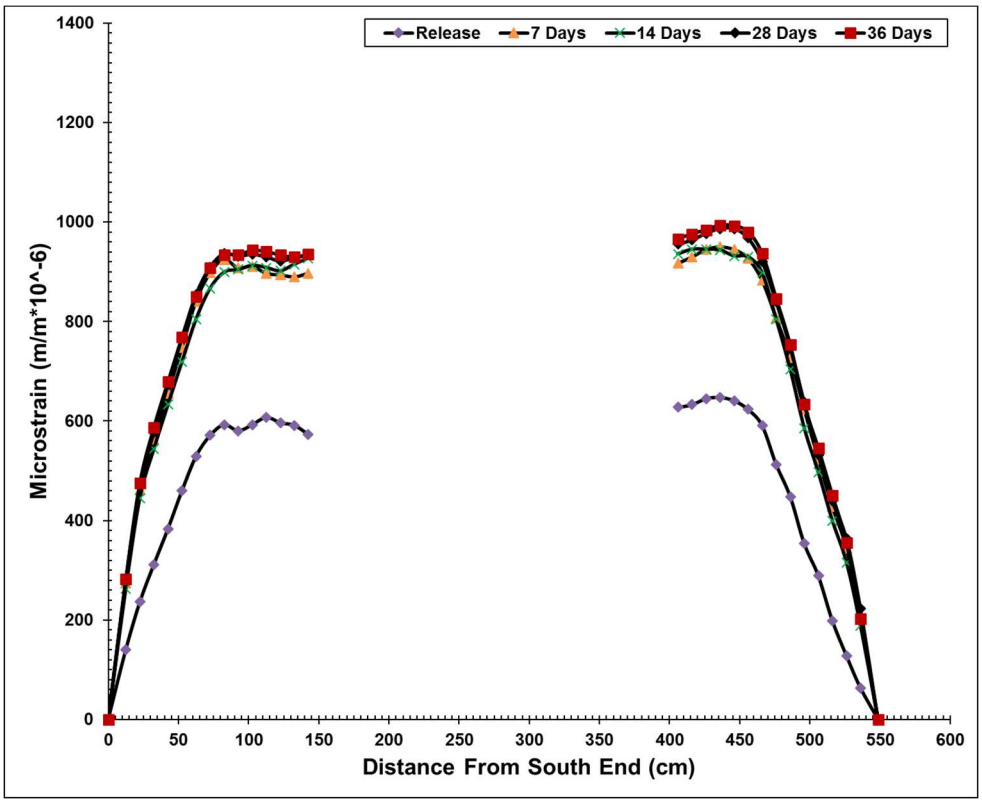

Figure 64: RS1 DEMEC Strain Profiles

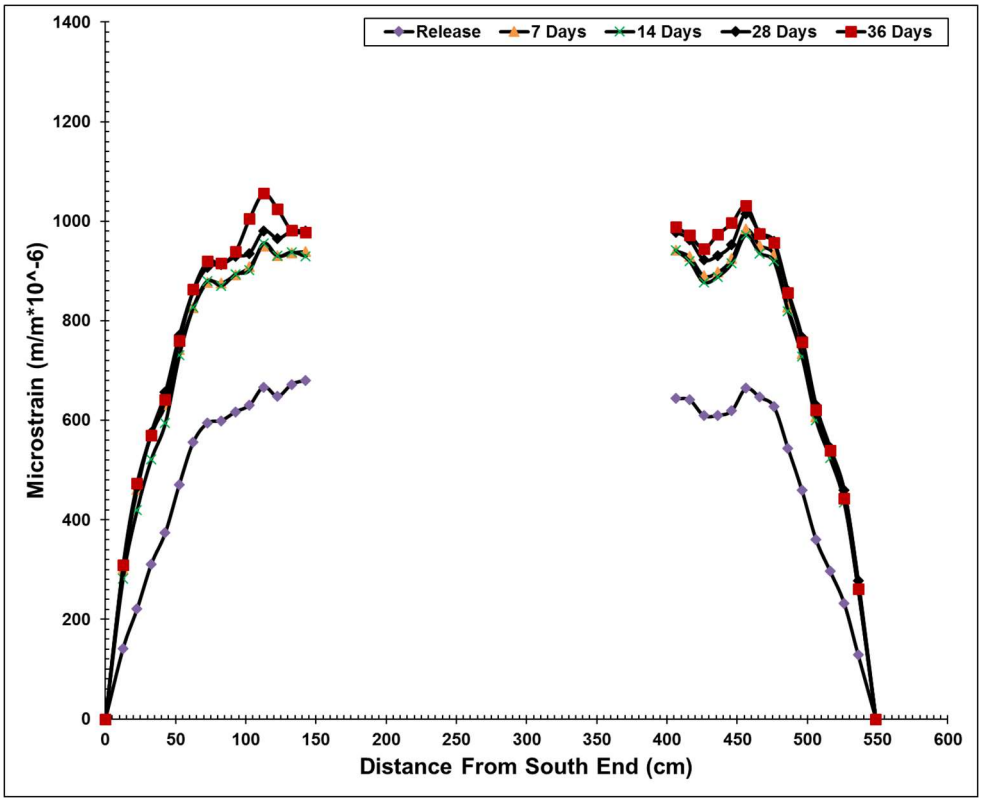

Figure 65: RS2 DEMEC Strain Profiles

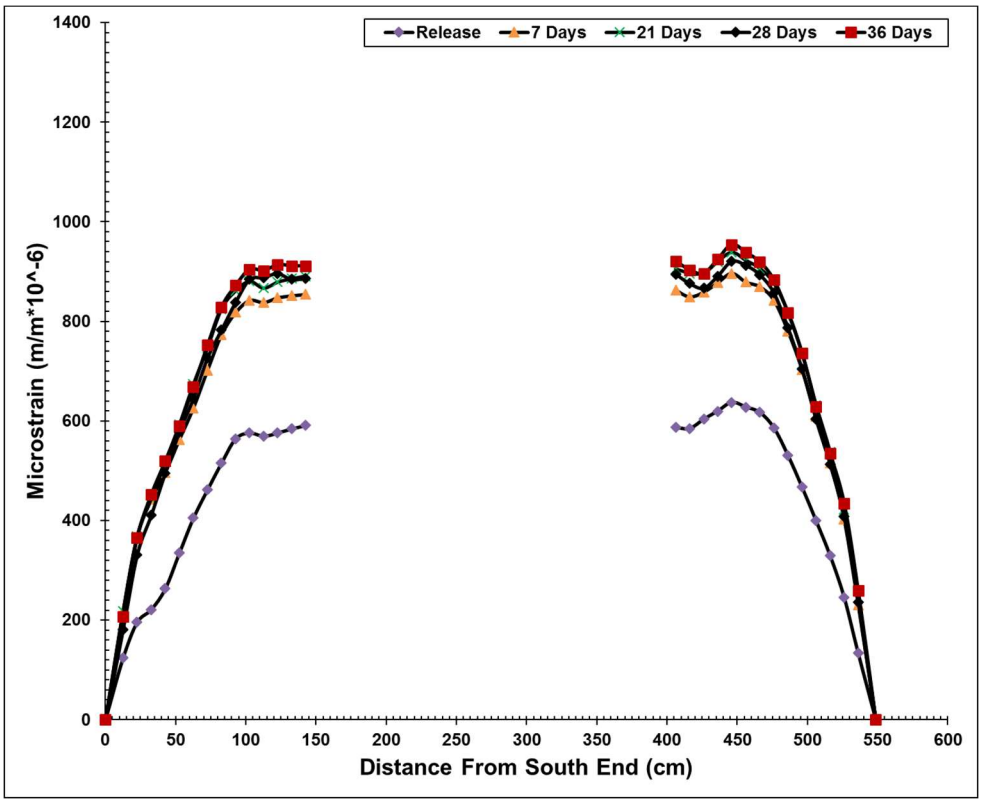

Figure 66: RS3 DEMEC Strain Profiles

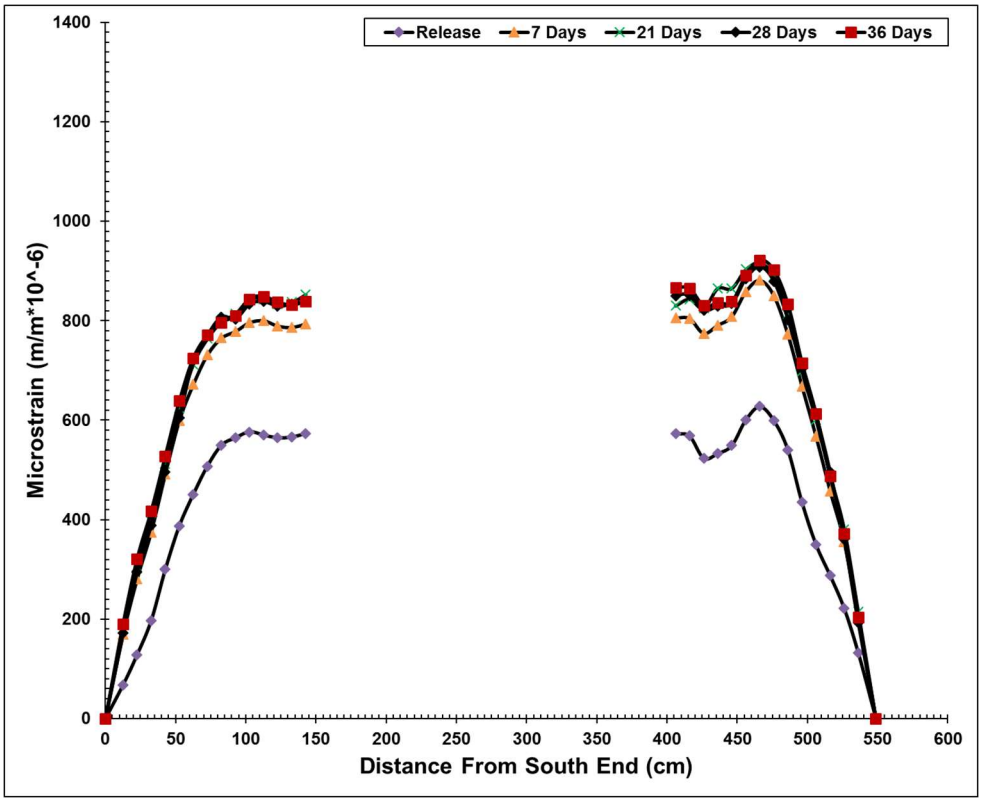

Figure 67: RS4 DEMEC Strain Profiles

Appendix E: Flexural Test Crack Patterns

This section presents the cracking patterns at failure for all 12 specimens.

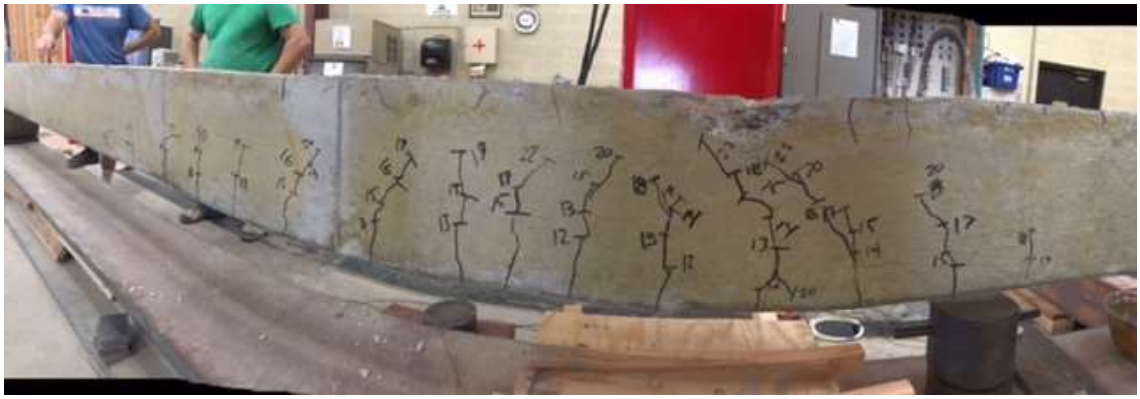

Figure 68: PC1 at Failure

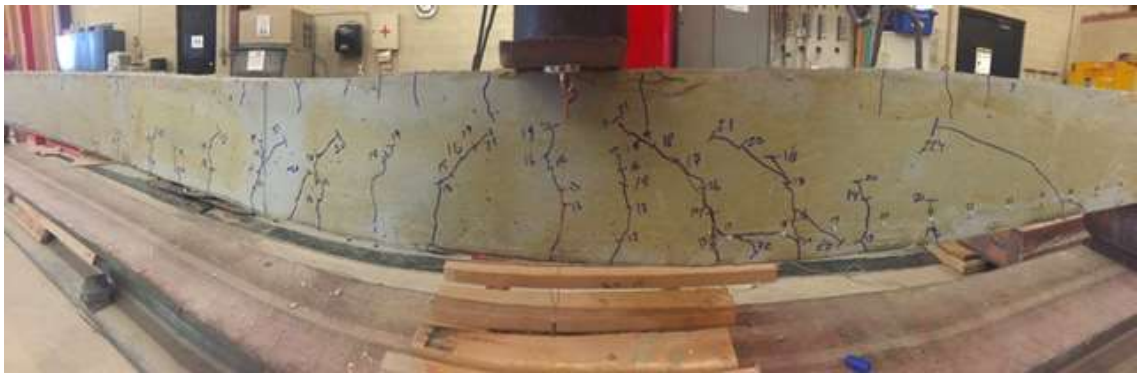

Figure 69: PC2 at Failure

Figure 70: PC3 at Failure

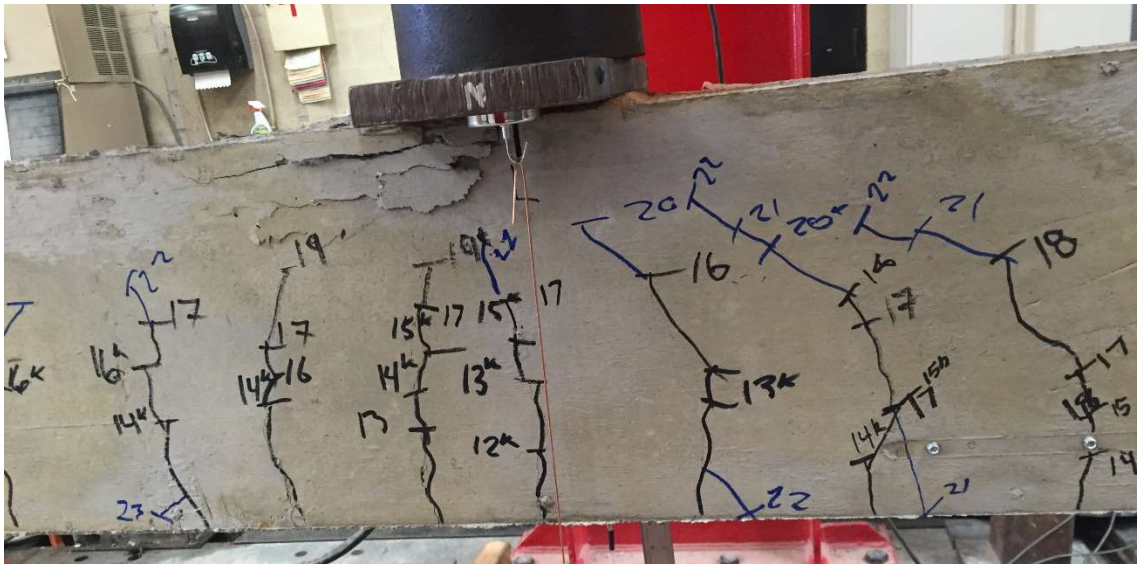

Figure 71: PC4 at Failure

Figure 72: 24RS1 at Failure

Figure 73: 24RS2 at Failure

Figure 74: 24RS3 at Failure

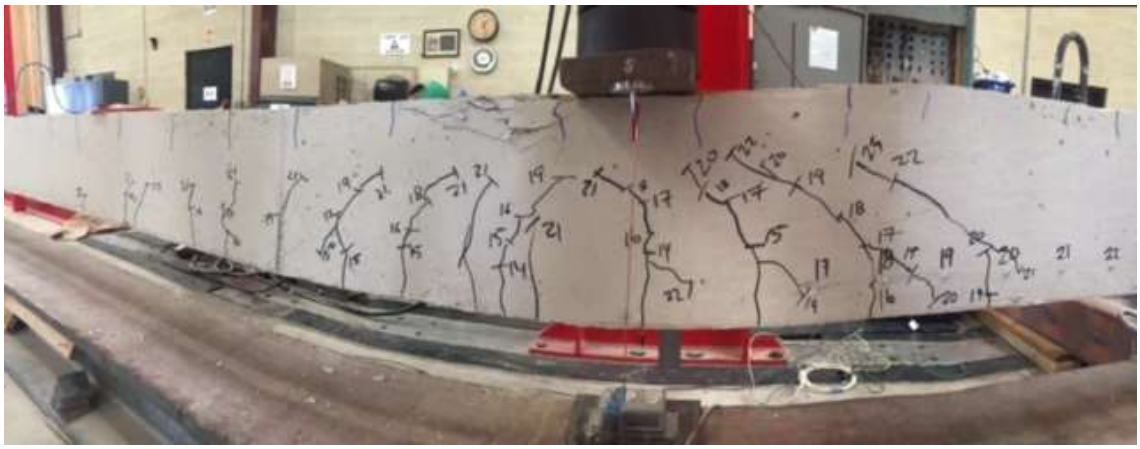

Figure 75: 24RS4 at Failure

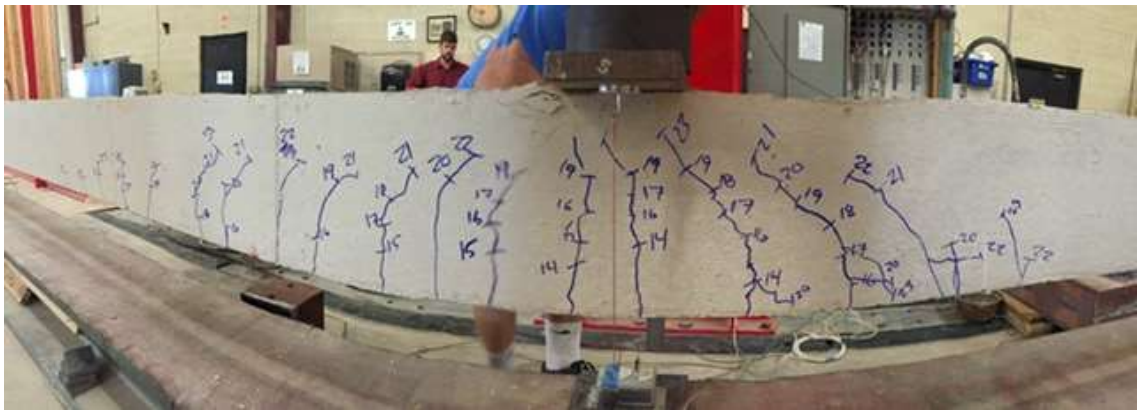

Figure 76: RS1 at Failure

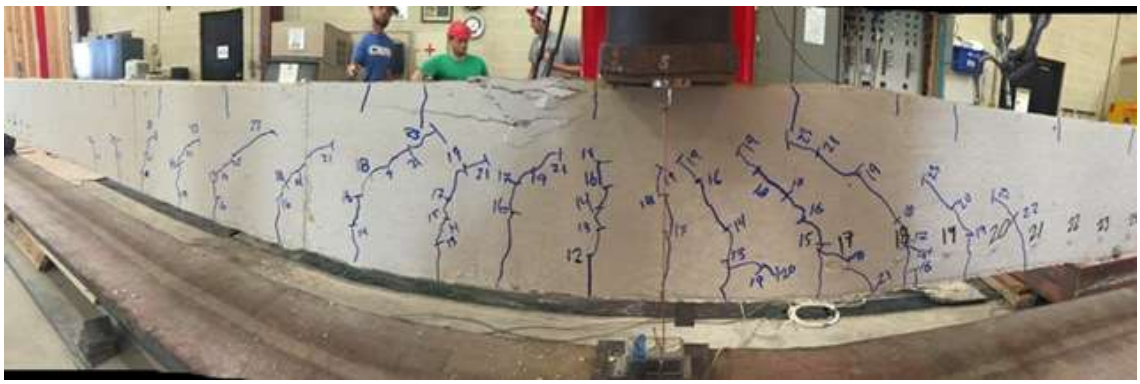

Figure 77: RS2 at Failure

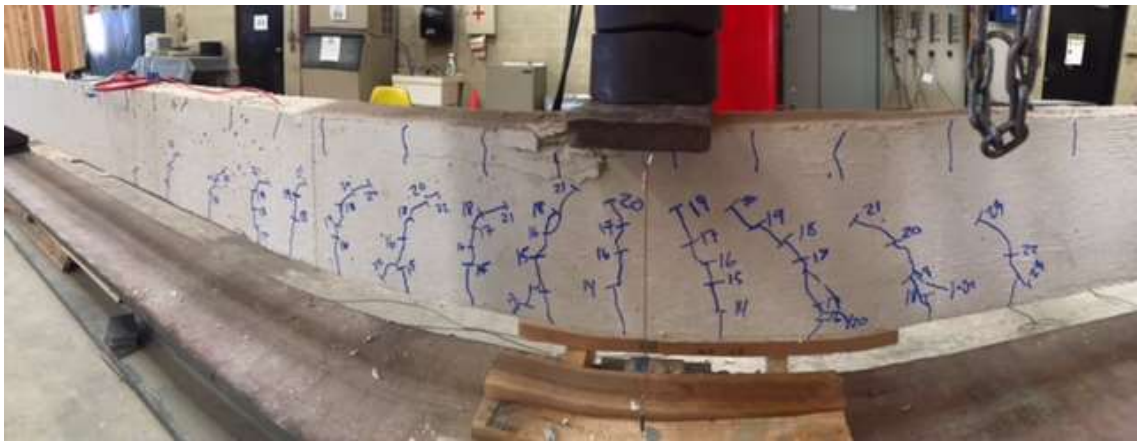

Figure 78: RS3 at Failure

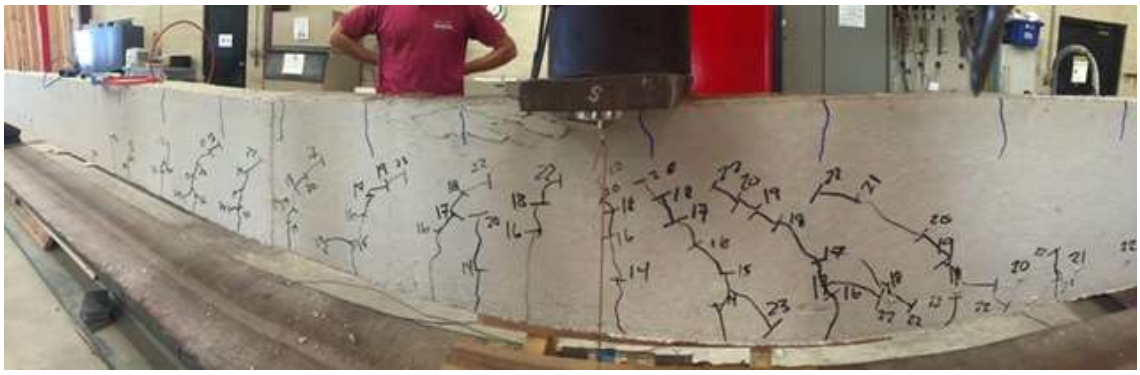

Figure 79: RS4 at Failure